Pre-clinical modeling of viral- and bacterial-induced exacerbations of chronic obstructive pulmonary disease

Dissertation

zur Erlangung des naturwissenschaftlichen Doktorgrades
der Julius-Maximilians-Universität Würzburg

Vorgelegt von: Hannes Bucher

Geburtsort: Bad Mergentheim

Würzburg, 2016

Eingereicht am: 18.10.2016

Mitglieder der Promotionskommission:

Vorsitzender: Prof. Dr. Thomas Rudel

Gutachter: Prof. Dr. Klaus Erb

Gutachter: Prof. Dr. Thomas Rudel

Tag des Promotionskolloquiums: 10.02.2017

Doktorurkunde ausgehändigt am:

To my parents and my brother

Table of contents

Aim of the study

The aim of this study was to develop and characterize pre-clinical mouse models which depict relevant aspects of viral- and bacterial-induced chronic obstructive pulmonary disease (COPD) exacerbations to test novel therapies. For this purpose, mice were exposed to cigarette smoke (CS) and additionally infected with influenza virus (H1N1), respiratory syncytial virus (RSV) or nontypeable *Haemophilus influenzae* (NTHi). As smoking causes COPD in humans, CS-exposure was used to induce pulmonary inflammation in the animals. H1N1, RSV or NTHi are well-known triggers of COPD exacerbations in patients. Therefore, infection of CS-exposed mice with these viruses/bacteria was performed to depict an exacerbated COPD phenotype. Several clinically relevant treatments were tested in the established models as benchmarks and novel drug candidates were investigated in the CS/H1N1 model.

Summary

Chronic Obstructive Pulmonary Disease (COPD) exacerbations are a considerable reason for increased morbidity and mortality in patients. Infections with influenza virus (H1N1), respiratory syncytial virus (RSV) or nontypeable *Haemophilus influenzae* (NTHi) are important triggers of exacerbations. To date, no treatments are available which can stop the progression of COPD. Novel approaches are urgently needed. Pre-clinical models of the disease are crucial for the development of novel therapeutic options.

In order to establish pre-clinical models which mimic aspects of human COPD exacerbations, mice were exposed to cigarette smoke (CS) and additionally infected with H1N1, RSV and/or NTHi. Clinically relevant treatments such as the corticosteroids Fluticasone propionate and Dexamethasone, the phosphodiesterase-4 (PDE-4) inhibitor Roflumilast and the long-acting muscarinic receptor antagonist Tiotropium were tested in the established models. Furthermore, a novel treatment approach using antibodies (Abs) directed against IL-1α, IL-1β or IL-1R1 was examined in the established CS/H1N1 model. Levels of IFN-γ, IL-1β, IL-2, IL-6, KC, TNF-α, RANTES, IL-17, MCP-1, MIP-1α and MIP-1β were measured in lung homogenate. Numbers of total cells, neutrophils and macrophages were assessed in bronchoalveolar lavage (BAL) fluid. Hematoxylin- and eosin- (H&E-) stained lung slices were analyzed to detect pathological changes. Quantitative polymerase-chain-reaction (qPCR) was used to investigate gene expression of ICAM-1 and MUC5 A/C. The viral/bacterial load was investigated in lung homogenate or BAL fluid. In addition to the *in vivo* studies, the effects of the above mentioned treatments were investigated *in vitro* in H1N1, RSV or NTHi-infected (primary) human bronchial epithelial cells using submerged or air-liquid-interface (ALI) cell culture systems.

Four pre-clinical models (CS/H1N1, CS/RSV, CS/NTHi, CS/H1N1/NTHi) were established depicting clinically relevant aspects of COPD exacerbations such as increased inflammatory cells and cytokines in the airways and impaired lung function.

In the CS/H1N1 model, Tiotropium improved lung function and was superior in reducing inflammation in comparison to Fluticasone or Roflumilast. Moreover, Fluticasone increased the loss of body-weight, levels of IL-6, KC and TNF-α and worsened lung function. In CS/RSV-exposed mice Tiotropium but not Fluticasone or Roflumilast treatment reduced neutrophil numbers and IL-6 and TNF-α levels in the lung. The viral load of H1N1 and RSV was significantly elevated in CS/virus-exposed mice and NCI-H292 cells after Fluticasone

and Dexamethasone treatment. The results from these studies demonstrate that Tiotropium has anti-inflammatory effects on CS/virus-induced inflammation and might help to explain the observed reduction of exacerbation rates in Tiotropium-treated COPD patients. Furthermore, the findings from this work indicate that treatment with Fluticasone or Dexamethasone might not be beneficial to reduce inflammation in the airways of COPD patients and supports clinical studies that link treatment with corticosteroids to an increased risk for pneumonia.

Testing of anti-IL-1α, anti-IL-1β or anti-IL-1R1 Abs in the CS/H1N1 model suggests that, in line with clinical data, antagonization of IL-1β is not sufficient to reduce pulmonary inflammation and indicates a predominant role of IL-1α in CS/virus-induced airway inflammation. In line with the *in vivo* findings, anti-IL-1α but not anti-IL-1β Abs reduced levels of TNF-α and IL-6 in H1N1-infected primary human bronchial epithelial ALI cell culture. Blocking the IL-1R1 provided significant inhibitory effects on inflammatory cells *in vivo* but was inferior compared to inhibiting both its soluble ligands IL-1α and IL-1β. Concomitant usage of Abs against IL-1α/IL-1β revealed strong effects and reduced total cells, neutrophils and macrophages. Additionally, levels of KC, IL-6, TNF-α, MCP-1, MIP-1α and MIP-1β were significantly reduced and ICAM-1 mRNA expression was attenuated. These results suggest that combined inhibition of IL-1α/IL-1β might be beneficial to reduce inflammation and exacerbations in COPD patients. Moreover, combined targeting of both IL-1α/IL-1β might be more efficient compared to inhibition of the IL-1R1.

As in the CS/virus models, corticosteroid treatment failed to reduce inflammatory cells in the CS/NTHi and CS/H1N1/NTHi models, increased the loss of body-weight and the bacterial load. Furthermore, Roflumilast administration had no significant effects on cell counts or cytokines. However, it improved compliance in the CS/NTHi model. Treatment with Azithromycin reduced the bacterial load in the CS/NTHi model and reduced numbers of total cells, neutrophils, macrophages and levels of KC and TNF-α in the CS/H1N1/NTHi model.

In conclusion, the established CS/H1N1, CS/RSV, CS/NTHi, CS/H1N1/NTHi models depict clinically relevant aspects of human COPD exacerbations in mice and provide the opportunity to investigate underlying disease mechanisms and to test novel therapies.

Zusammenfassung

Exazerbationen von Chronisch Obstruktiver Lungenerkrankung (COPD) sind ein bedeutender Grund für erhöhte Morbidität und Mortalität von Patienten. Infektionen mit Influenza Virus (H1N1), Respiratory Syncytial Virus (RSV) oder nontypeable *Haemophilus influenzae* (NTHi) gelten als wichtige Auslöser von Exazerbationen. Bis heute gibt es keine Therapien, welche die Progression von COPD verhindern können. Neue Therapieansätze werden daher dringend benötigt. Prä-klinische Modelle spielen bei der Entwicklung neuer Therapien eine entscheidende Rolle.

Um Aspekte einer humanen COPD-Exazerbation abzubilden, wurden Mäuse Zigarettenrauch (CS) ausgesetzt und zusätzlich mit H1N1, RSV und/oder NTHi infiziert. Klinisch relevante Behandlungen, z.B. die Kortikosteroide Fluticasonpropionat und Dexamethason, der Phosphodiesterase-4 (PDE-4) Inhibitor Roflumilast und der muskarinische Rezeptorantagonist Tiotropium, wurden in den etablierten Modellen getestet. Zudem wurde ein neuer therapeutischer Ansatz untersucht bei dem IL-1α, IL-1β neutralisierende bzw. IL-1R1 blockierende Antikörper (Ak) zum Einsatz kamen. Die Mengen von IFN-γ, IL-1β, IL-2, IL-6, KC, TNF-α, RANTES, IL-17, MCP-1, MIP-1α und MIP-1β wurden im Lungenhomogenat gemessen. Die Gesamtzellzahl und die Anzahl von Neutrophilen und Makrophagen wurden in bronchoalveolärer Lavage (BAL) Flüssigkeit bestimmt. Hematoxylin- und Eosin- (H&E-) gefärbte Lungenschnitte wurden analysiert, um pathologische Veränderungen zu detektieren. Quantitative Polymerase-Kettenreaktion (qPCR) wurde genutzt, um die Genexpression von ICAM-1 und MUC5 A/C zu untersuchen. Die Virus-/Bakterienlast wurde in BAL Flüssigkeit oder Lungenhomogenat gemessen. Darüber hinaus wurden die Effekte der oben genannten Behandlungen *in vitro* in H1N1, RSV oder NTHi infizierten (primären) humanen bronchialen Epithelzellen in „submerged“ oder „air-liquid-interface (ALI)“ Zellkultur-Systemen untersucht.

Vier prä-klinische Modelle (CS/H1N1, CS/RSV, CS/NTHi, CS/H1N1/NTHi) wurden etabliert, die relevante Aspekte einer Exazerbation, wie beispielsweise den Einstrom inflammatorischer Zellen, erhöhte Zytokinlevel oder verminderte Lungenfunktion abbilden.

Im CS/H1N1-Modell verbesserte Tiotropium die Lungenfunktion und zeigte stärker anti-entzündliche Effekte als Fluticason oder Roflumilast. Zudem verstärkte Fluticason den Gewichtsverlust, erhöhte die Level von IL-6 und TNF-α und verschlechterte die Lungenfunktion. Im CS/RSV-Modell reduzierte Tiotropium, aber nicht Fluticason oder

Roflumilast die Zahl der Neutrophilen sowie IL-6 und TNF-α Mengen. Die Menge von H1N1 und RSV war in den CS/Virus-Modellen sowie in NCI-H292 Zellen nach Fluticason- oder Dexamethason-Behandlung signifikant erhöht. Die Ergebnisse dieser Studien demonstrieren anti-inflammatorische Effekte von Tiotropium auf CS/Virus-induzierte Entzündung und könnten helfen, reduzierte Exazerbationshäufigkeiten in mit Tiotropium behandelten Patienten zu erklären. Zudem könnten die Resultate dieser Arbeit darauf hindeuten, dass die Behandlung mit Kortikosteroiden nicht geeignet ist, um Entzündung in COPD-Patienten zu reduzieren, und könnten dabei helfen, das in klinischen Studien festgestellte erhöhte Risiko von Pneumonien bei Behandlung mit Kortikosteroiden zu erklären.

Im Einklang mit klinischen Daten deutet die Testung von anti-IL-1α, anti-IL-1β oder anti-IL-1R1 Ak im CS/H1N1-Modell darauf hin, dass die Neutralisation von IL-1β nicht ausreicht, um die Entzündung in der Lunge zu reduzieren, und impliziert eine prädominierende Rolle von IL-1α in CS/H1N1-induzierter Atemwegsentzündung. Konform mit den *in vivo* Ergebnissen, reduzierten anti-IL-1α, aber nicht anti-IL-1β Ak, TNF-α und IL-6 in H1N1-infizierter primärer humaner bronchialer epithelialer ALI-Zellkultur. Die Blockade von IL-1R1 zeigte *in vivo* signifikante inhibitorische Effekte auf inflammatorische Zellen, die verglichen mit der Neutralisation seiner löslichen Liganden IL-1α/IL-1β allerdings unterlegen waren. Die kombinierte Neutralisation von IL-1α/IL-1β war sehr effektiv und reduzierte die Gesamtzellzahl sowie die Zahl der Neutrophilen und Makrophagen in der Lunge. Zusätzlich wurden die Level von KC, IL-6, TNF-α, MCP-1, MIP-1α und MIP-1β signifikant reduziert. Diese Ergebnisse deuten darauf hin, dass kombinierte Inhibition von IL-1α/IL-1β geeignet sein könnte, um Entzündung und Exazerbationen in COPD-Patienten zu reduzieren. Zudem könnte IL-1α/IL-1β-Neutralisation effektiver sein als IL-1R1-Blockade.

Wie in den CS/Virus-Modellen wurden inflammatorische Zellen durch Kortikosteroid-Behandlung im CS/NTHi- und CS/H1N1/NTHi-Modell nicht reduziert, verstärkten zudem den Gewichtsverlust und erhöhten die Bakterienmenge. Roflumilast zeigte keine Effekte auf Zellzahlen und Zytokine. Allerdings verbesserte die Behandlung damit die Compliance im CS/NTHi-Modell. Die Behandlung mit Azithromycin reduzierte die Bakterienmenge im CS/NTHi-Modell und reduzierte die Gesamtzellzahl und Anzahl von Neutrophilen und Makrophagen, sowie die Level von KC und TNF-α im CS/H1N1/NTHi-Modell.

Zusammenfassend bilden die etablierten CS/H1N1-, CS/RSV-, CS/NTHi-, CS/H1N1/NTHi-Modelle klinisch relevante Aspekte von humanen COPD-Exazerbationen ab und ermöglichen die Erforschung von Krankheitsmechanismen und neuen Therapieansätze.

Table of abbreviations

Ab	Antibody
ACh	Acetylcholine
AHR	Airway hyperresponsiveness
BAL	Bronchoalveolar lavage
ChAT	Choline acetyltransferase
COPD	Chronic Obstructive Pulmonary Disease
CS	Cigarette smoke
DALY	Disability-adjusted life years
DNA	Deoxyribonucleic acid
ELISA	Enzyme linked immunosorbent assay
ERK	Extracellular signal-regulated kinase
FEV_1	Forced expiratory volume in one second
FVC	Forced vital capacity
GOLD	Global Initiative for Chronic Obstructive Lung Disease
HK-NTHi	Heat-killed nontypeable *Haemophilus influenzae*
H1N1	Influenza virus A/PR/8/34
ICAM-1	Intercellular adhesion molecule-1
ICS	Inhaled corticosteroids
IFN	Interferon
IFNR	Interferon receptor
IKK	Inhibitor of nuclear factor kappa B kinase
IκB	Inhibitor of nuclear factor kappa B
IL	Interleukin
ILC	Innate lymphoid cells
IL-1R1	Interleukin type 1 receptor
IL-1RAP	Interleukin-1 receptor accessory protein
IRAK	IL-1 receptor-associated kinases
JNK	C-Jun N-terminal kinase
LOS	Lipooligosaccharides
LPS	Lipopolysaccharides
MAPK	Mitogen-activated kinase
MCh	Methacholine

MKK	MAP kinase kinase
MYD88	Myeloid differentiation primary response gene 88
NLRP3	Protein-nucleotide-binding domain and leucine-rich repeat pyrin-containing protein-3
NANS	Sialic acid synthase
NE	Neutrophil elastase
NF-κB	Nuclear factor kappa B
NTHi	Nontypeable *Haemophilus influenzae*
OMP	Outer membrane protein
PAMP	Pathogen-associated molecular pattern
PDE-4	Phosphodiesterase-4
PFA	Paraformaldehyde
PFU	Plaque forming units
P.i.	Post infection
PRR	Pattern recognition receptor
ROS	Reactive oxygen species
RSV	Respiratory Syncytial Virus
SEM	Standard error of mean
STAT	Signal transducers and activators of transcription
TAB	TAK1-binding protein
TAK	TGF-β-activated kinase
TEER	Transepithelial electrical resistance
TLR	Toll like receptor
TRAF	Tumor necrosis factor-associated factor

1 Introduction

1.1 Chronic Obstructive Pulmonary Disease

Chronic Obstructive Pulmonary Disease (COPD) is a central health and economic burden. Besides causing direct medical costs, the disease is expected to be among the ten leading causes of disability-adjusted life years (DALYs) lost and moreover the fourth leading cause of death by 2030 [1, 2]. In particular, periodically occurring periods of exacerbations of COPD account for an increased morbidity and mortality in patients [3]. Recent studies indicate that exacerbations contribute to a faster decline in lung function and therefore an accelerated disease progression [4]. Important triggers of exacerbations are viral and bacterial infections of the respiratory tract [5]. Despite the tremendous impact of COPD on human health and economic costs, the disease has often been underrecognized [6, 7]. Furthermore, as described in the BOLD study, not only the "classical" at-risk group of smokers is often affected by COPD; a substantial prevalence can also be detected among never-smokers, for example due to air pollution or genetic reasons [8, 9]. Recently initiated campaigns such as the "Learn More Breathe Better®" campaign by the United States National Heart, Lung, and Blood-Institute aim at rising the awareness of COPD. Besides rising the awareness of the disease, proper medication can help to reduce exacerbation rates, which is crucial to slow down lung function loss and mortality [3]. To date, no medication is able to stop the progression of the disease [1]. Thus, in order to help the millions of patients suffering from COPD and to disburden economies, the development of novel therapeutics is urgently needed.

1.1.1 Definition and symptoms

According to the guidelines of the Global Initiative for Chronic Obstructive Lung Disease (GOLD), COPD is defined as "a preventable and treatable disease with some significant extrapulmonary effects that may contribute to the severity in individual patients. Its pulmonary component is characterized by airflow limitation that is not fully reversible. The airflow limitation is usually progressive and associated with an abnormal inflammatory response of the lung to noxious particles or gases" [1]. The characteristic airflow limitation is expected to be caused by obstructive bronchiolitis in the small airways and emphysema (parenchymal destruction) [1]. As described above in section 1.1, patients are often not aware of COPD until they experience difficulties in breathing. However, already frequent cough or sputum hyperproduction can announce the disease [9]. The magnitude of breathlessness is the basis of the GOLD classification of disease severity, which distinguishes between four stages

of disease severity (GOLD I – GOLD IV) (**Figure 1**) [1]. Often, COPD occurs accompanied by comorbidities such as heart failures or psychiatric disorders [10, 11].

Stage	Symptoms
0: At risk	Normal spirometry Chronic symptoms (cough, sputum)
I: Mild	$FEV_1/FVC < 0.70$; $FEV_1 > 80\%$ predicted With or without symptoms (cough, sputum)
II: Moderate	$FEV_1/FVC < 0.70$; $50\% < FEV_1 < 80\%$ predicted With or without chronic symptoms (cough, sputum, dyspnoea)
III: Severe	$FEV_1/FVC < 0.70$; $30\% < FEV_1 < 50\%$ predicted With or without chronic symptoms (cough, sputum, dyspnoea)
IV: Very severe	$FEV_1/FVC < 0.70$; $FEV_1 < 30\%$ or $FEV_1 < 50\%$ predicted Chronic respiratory failure

Figure 1: GOLD classification of COPD stages (adapted from [1])
The Global Initiative for Chronic Obstructive Lung Disease (GOLD) distinguishes different stages of COPD severity based on the post-bronchodilator maximal forced expiratory volume in one second (FEV_1) and the forced vital capacity (FVC). An FEV_1/FVC ratio < 0.70 indicates persistent airflow limitation. The level of airflow obstruction is given by the FEV_1 converted to percentage of normal/predicted.

1.1.2 Risk factors

The most important risk factor for the development of COPD is smoking [9, 12]. Cigarette smoke (CS) contains numerous stimulating agents, for example lipopolysaccharides (LPS), which have the ability to induce inflammatory processes in the lungs. Furthermore, CS can modify the host response to pathogens towards a pro- and anti-inflammatory direction [13]. Previously conducted studies showed that infections with influenza virus are worse in smokers compared to non-smokers [14]. Other important destructive ingredients of CS are free radicals and their potential to react with molecules like proteins, lipids, deoxyribonucleic acid (DNA) and thereby to damage the airways. Notably, the inflammatory process in the lung continues for a long time after smoking cessation [15, 16].

Air pollution also appears to be an important cause of inflamed airways and the development of COPD, in particular in emerging countries such as China or India [17, 18]. Important pro-inflammatory pollutants include particulate matter, ozone (O_3), sulfur dioxide (SO_2), nitrogen dioxide (NO_2), carbon monoxide (CO) and lead [19]. In addition to outdoor air pollutants, also indoor air pollution, for example due to cooking or heating, may constitute a risk factor, especially in less developed countries [20, 21]. Moreover, occupational dust should not be neglected as a potential driver of inflammatory processes in the airways [22, 23].

Recently, genetic factors entered the focus of interest. They are expected to play a role in the development of COPD [24]. A well-known genetic risk factor for the development of emphysema is alpha-1-antitrypsin deficiency. Reduced levels of this anti-protease due to genetic reasons can lead to an impaired protease/anti-protease balance in the lungs. Consequently, the uncontrolled action of proteases such as neutrophil elastase (NE), which is normally inhibited by alpha-1-antitrypsin, has the ability to destroy lung tissue [25, 26]. Besides the malfunction of distinct genes also epigenetics might play a role. Important epigenetic mechanisms include DNA methylation, hydroxyl methylation and chromatin remodeling [27-29]. Epigenetic modification can affect the expression of inflammatory genes in the airways and distinct epigenetic patterns were previously linked to the health status of COPD patients [30, 31]. In particular, DNA methylation might be an important determinant for the susceptibility and severity of COPD [32]. It was shown that smoking has the ability to change methylation patterns in pulmonary alveolar macrophages [33]. As described in section 1.1.3, these cells play an important role in the orchestration of inflammation in the lungs. Therefore, methylation changes in these cells might be important in pulmonary inflammatory processes. Moreover, changes in the methylation pattern due to smoking might explain ongoing inflammatory processes in the airways even after smoking cessation [34].

All in all, a number of both inherent and external factors exist which can contribute to the development of COPD. As described, an important mode of action of all these factors is the promotion of inflammatory processes in the airways. Therefore, in order to be able to intervene in disease relevant inflammatory processes and to develop novel therapeutic strategies in the fight against the disease, a good understanding of the underlying inflammatory processes of COPD is essential.

1.1.3 Pathophysiology and molecular mechanism

Major pathologies in COPD patients include peribronchial fibrosis, mucus overproduction and emphysema [9, 35]. It is expected that an abnormal, chronic inflammation in the airways is causative for these pathologies and the development of COPD [35-37]. Distinct inflammatory cell types and cytokines/chemokines are supposed to play a predominant role in the inflammatory pattern of COPD (**Figure 2**).

Epithelial cells and alveolar macrophages are central in the orchestration of the pulmonary inflammatory process and the recruitment of neutrophils and T lymphocytes [38]. In particular, increased neutrophil numbers are found in patients and were previously linked to disease severity [39, 40]. These cells have the ability to secrete proteases such as NE, which

in turn can destroy alveolar walls and therefore contribute to the development of emphysema [41]. Besides neutrophils, also activated macrophages can release proteases, for example matrix metalloprotease-9 (MMP-9), and may contribute to the destruction of lung tissue [42, 43]. In addition to elevated numbers of neutrophils and macrophages, also CD4+ and CD8+ T lymphocytes are linked to the pathophysiology of COPD. On the one hand, these cells play a crucial role in clearing viral pathogens from lung tissue, e.g. by inducing apoptosis of infected cells. On the other hand, this mode of action might contribute to emphysema development [44-46].

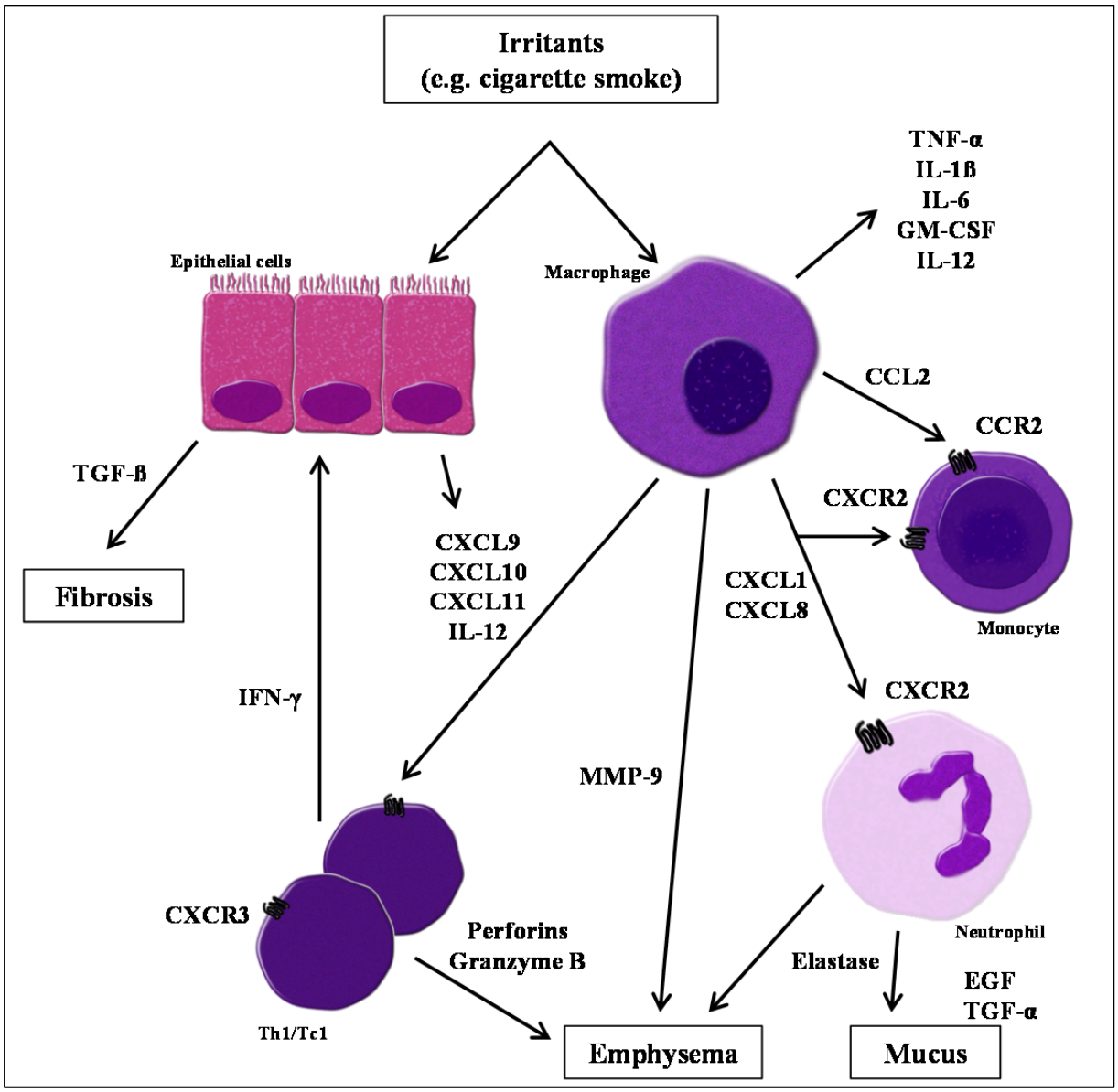

Figure 2: Model of the inflammatory process underlying COPD (adapted from [36])
Irritants such as CS induce an inflammatory cascade in the airways. Epithelial cells and macrophages are believed to orchestrate this process by the release of chemokines. Thereby they recruit monocytes, neutrophils and T lymphocytes to the site of the inflammation, which in turn release cytokines and thereby increase the inflammatory process.

In particular, type 1 helper T lymphocytes (Th1, interferon (IFN)-γ producing subclass of CD4+ T lymphocytes) and type 1 cytotoxic T lymphocytes (Tc1, IFN-γ producing subclass of CD8+ T lymphocytes) are believed to be important in the disease. However, BAL studies from patients suggest a role also for type 2 helper T lymphocytes (Th2, interleukin (IL)-4, IL-5 producing subclass of CD4+ T lymphocytes) and type 2 cytotoxic T lymphocytes (Tc2, IL-4, IL-5 producing subclass of CD8+ T lymphocytes). Occurrence of these cells might in part explain lung eosinophilia associated with exacerbations in some patients [45]. Besides the important role of macrophages, neutrophils and T lymphocytes, a distinct pattern of cytokines/chemokines is characteristic for the underlying inflammatory process of COPD [36].

Chemokines are responsible for the recruitment of macrophages, neutrophils and T lymphocytes to the lungs. Chemokine ligand 2 (CCL2, MCP-1) is released by activated macrophages, epithelial cells and smooth muscle cells and results in the recruitment of monocytes via binding to its respective chemokine receptor type 2 (CCR2). Upon IFN-γ stimulation, several cells such as macrophages, epithelial cells and fibroblasts release chemokine ligand 1 (CXCL1, KC) and chemokine ligand 8 (CXCL8, IL-8). These chemokines act through binding to chemokine receptor 2 (CXCR2) and are responsible for the recruitment and activation of neutrophils and monocytes [47, 48]. Important attractors for T lymphocytes are chemokine ligand 5 (CCL5, RANTES), chemokine ligand 9 (CXCL9), chemokine ligand 10 (CXCL10, IP-10) and chemokine ligand 11 (CXCL11, I-TAC). These chemokines act through activation of chemokine receptor type 3 (CXCR3) [49-51].

The differentiation, proliferation, activation and survival of inflammatory and structural cells is regulated by growth factors such as granulocyte-macrophage colony-stimulating factor (GM-CSF). This growth factor is released by macrophages thereby promoting the survival of neutrophils and recruitment of monocytes to the airways of patients [52]. Epidermal growth factor receptor (EGFR) is up-regulated in the airways of COPD patients. Triggering of this receptor by epidermal growth factor (EGF), transforming growth factor-α (TGF-α) or NE induces MUC5 A/C expression and subsequent mucus production [36, 53]. Moreover, the proliferation of fibroblasts is induced by transforming growth factor β (TGF-β) thereby contributing to the development of fibrosis and airway obstruction in COPD patients [54, 55].

Lymphokines are expected to have a variety of effects in the inflammatory process of COPD [56]. They are secreted by T lymphocytes. IFN-γ is a central lymphokine released by Tc1 and Th1 lymphocytes. The cytokine induces the up-regulation of chemokine receptors and

corresponding chemokines thereby enhancing inflammation through the recruitment of leukocytes [56, 57]. IL-12 is released by macrophages and epithelial cells. It is an important regulatory cytokine which promotes the differentiation and activation of Tc1/Th1 lymphocytes [58]. As described above, exacerbations in some COPD patients are linked to the appearance of eosinophils and Th2 cytokines such as IL-4, IL-5 and IL-13. Thus, these cytokines might also play a role in the pathogenesis of COPD [45]. Classically, Th2 mediators are associated with symptoms of asthma. They induce IgE production, airway hyperresponsiveness and mucus production [59, 60]. Recently, type 17 helper T lymphocytes (Th17, IL-17 producing subclass of CD4+ T lymphocytes) entered the focus of interest regarding their role in the inflammatory events of COPD. The major cytokine released by these cells is IL-17. The fact that IL-17 in turn promotes the secretion of CXCL1 and CXCL8 might be exemplary for its role in COPD pathogenesis [61]. The differentiation of Th17 lymphocytes is mediated by IL-6, IL-1β, TGF-β and IL-23 [62, 63].

Increased levels of pro-inflammatory cytokines such as IL-6 are a hallmark of the underlying inflammatory process of COPD. IL-6 is associated with the release of C-reactive protein from the liver and might be crucial for systematic symptoms observed in COPD patients, for example muscle weakness [36, 64]. A further important pro-inflammatory cytokine is tumor necrosis factor (TNF)-α, which may also contribute to COPD pathogenesis. The cytokine is secreted by several cell types including epithelial cell, macrophages, T lymphocytes and smooth muscle cells. It stimulates the release of several cytokines such as CXCL8 and GM-CSF. Moreover, TNF-α up-regulates intercellular adhesion molecule (ICAM)-1 and induces airway hyperresponsiveness (AHR) [65].

1.1.4 The role of the IL-1 pathway in COPD

Further important pro-inflammatory mediators are members of the IL-1 family such as IL-1α and IL-1β. They play a pivotal role in the context of autoimmune, infectious and degenerative diseases [66-70]. As described below, IL-1α and IL-1β are comparable in their mode of action regarding the induction of inflammatory processes via the IL type 1 receptor (IL-1R1) and co-receptor IL type1 receptor accessory protein (IL-1RAP). However, they differ with regard to their occurrence/release. IL-1α is expressed constitutively in cells such as keratinocytes, hepatocytes, fibroblasts, endothelial cells and epithelial cells and is active in its precursor as well as in its processed form [71, 72]. Upon necrosis of cells, IL-1α is released and has the ability to initiate early inflammatory processes, in particular the recruitment of neutrophils [73]. However, there is evidence that IL-1α might be also secreted in a caspase-1 dependent

manner [74]. In contrast, IL-1β is not expressed under normal conditions. The transcription, activation and release of its precursor form is triggered by bacterial components such as LPS or other "danger signals" released by injured cells such as reactive oxygen species (ROS), uric acid, ATP and IL-1α [72, 75, 76].

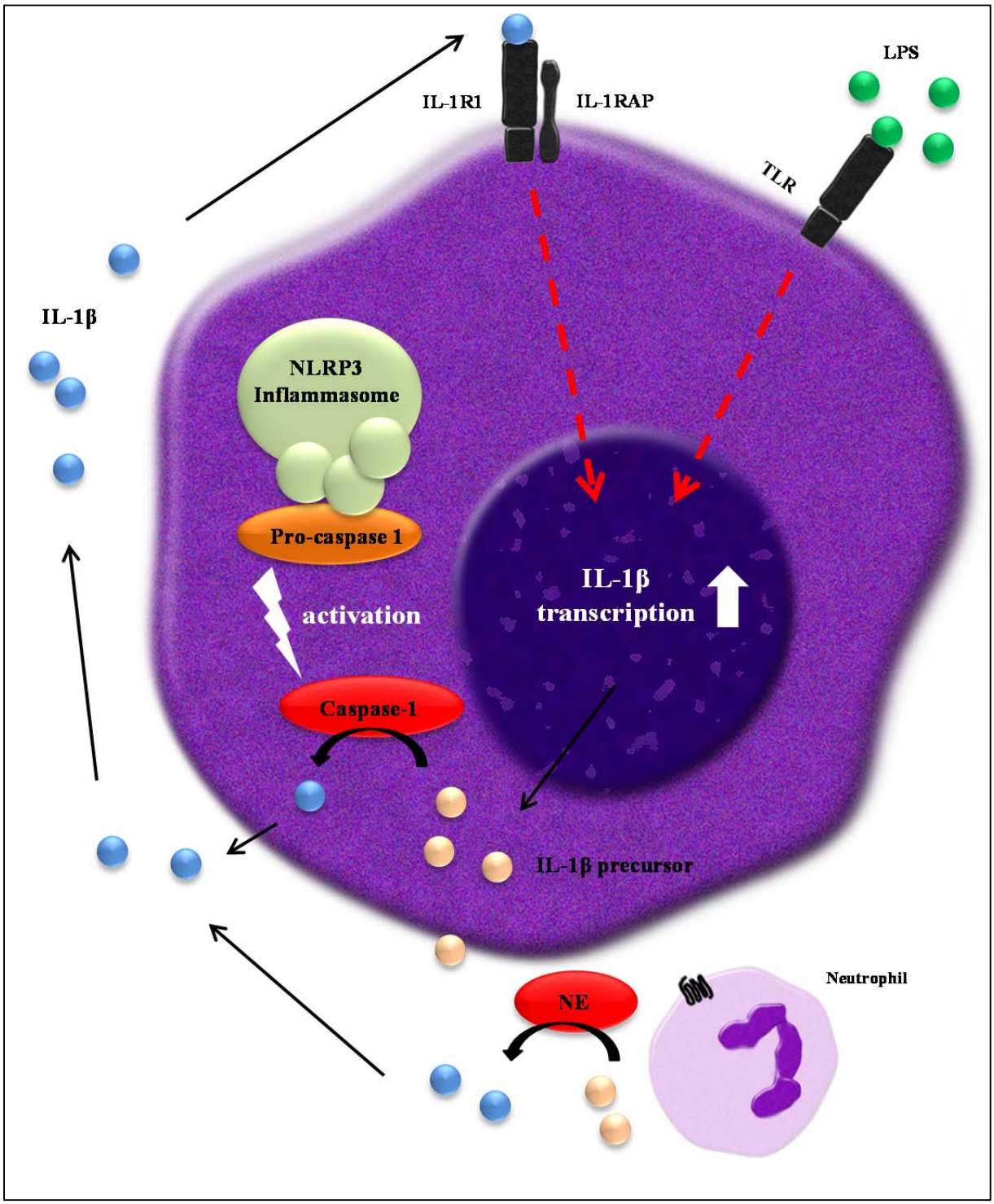

Figure 3: Model of how IL-1β production is induced (adapted from [77, 78])
Bacterial components such as LPS and other "danger signals" released by injured cells induce the formation of the NLRP3-inflammasome and expression of the β1β precursor. Pro-caspase-1 is cleaved and activated by the inflammasome to its bioactive form. In turn, caspase-1 activates IL-1β by cleavage of the IL-1β precursor. Extracellular IL-1β precursor can additionally be activated by NE. IL-1β can now promote its own expression via binding to the IL-1R1 in a positive feedback-loop.

Major producers of IL-1β are monocytes and dendritic cells [71]. As illustrated in **Figure 3**, detection of bacterial components or other "danger signals" induce IL-1β transcription and formation of a multi-protein complex called protein-nucleotide-binding domain and leucine-rich repeat pyrin-containing protein-3 (NLRP3)-inflammasome [75, 77].

Subsequently, the inflammasome cleaves pro-caspase-1, a cysteine protease, resulting in activated caspase-1. In turn, this enzyme cleaves the IL-1β precursor which is then secreted. Notably, the IL-1β precursor may also be cleaved by NE to its bioactive form. Via binding to IL-1R1, IL-1β can enhance its own transcription in a positive feedback-loop [77].

Upon binding to IL-1R1 and IL-1RAP, IL-1α and IL-1β have the ability to induce multiple pathways involved in inflammatory processes (**Figure 4**) [66]. The activation of IL-R1/ IL-1RAP leads to the recruitment of myeloid differentiation primary response gene 88 (MYD88), IL-1 receptor-associated kinases 1/2/4 (IRAK1/2/4) and tumor necrosis factor associated factor 6 (TRAF6) (**Figure 4b**) [79]. Binding of MYD88 to the complex leads to phosphorylation of IRAK1/2/4 [80, 81]. Subsequently, TRAF6 and IRAK1/2 dissociate from the complex and migrate to the cell membrane to form a new complex together with TGF-β activated kinase 1 (TAK1) and TAK1-binding proteins TAB1 and TAB2 (**Figure 4c**) [82]. This complex, excluding IRAK1/2, leaves the membrane and moves to the cytoplasm. TRAF6 gets ubiquitinated and TAK1 phosphorylated (**Figure 4d**) [83]. As illustrated, further signal transduction can proceed via activating nuclear factor kappa B (NF-κB), mitogen-activated kinases (MAPK) p38, c-Jun N-terminal kinases (JNK) and extracellular signal-regulated kinases (ERK) [66]. Regarding the NF-κB path, TAK1 activates the inhibitor of nuclear factor kappa B kinase subunit beta (IKKβ), which in turn phosphorylates the inhibitor of nuclear factor kappa B (IκB) [67]. This leads to the activation of NF-κB, which can now migrate to the nucleus [67]. p38, JNK and ERK are also activated by TAK1 via interaction with MAP kinase kinase (MKK) proteins. Relevant transcription factors induced by these paths are C-Jun and C-Myc [66, 67].

IL-1α and IL-1β are key players in the regulation of local and systemic inflammatory processes [69, 84]. They are found to be increased in COPD patients and might contribute to the detrimental chronic inflammation [85, 86]. By inducing the described pathways, they promote the recruitment and/or activation of a variety of immune cells and immunocompetent cells, such as macrophages, endothelial cells, neutrophils and epithelial cells. Upon activation, these cells can secrete a range of potent pro-inflammatory cytokines such as IL-6 and TNF-α, chemokines such as MCP-1, macrophage inflammatory protein-1α (MIP-1α, CCL3) and

macrophage inflammatory protein-1β (MIP-1β, CCL4), metalloproteases and reactive oxygen species (ROS).

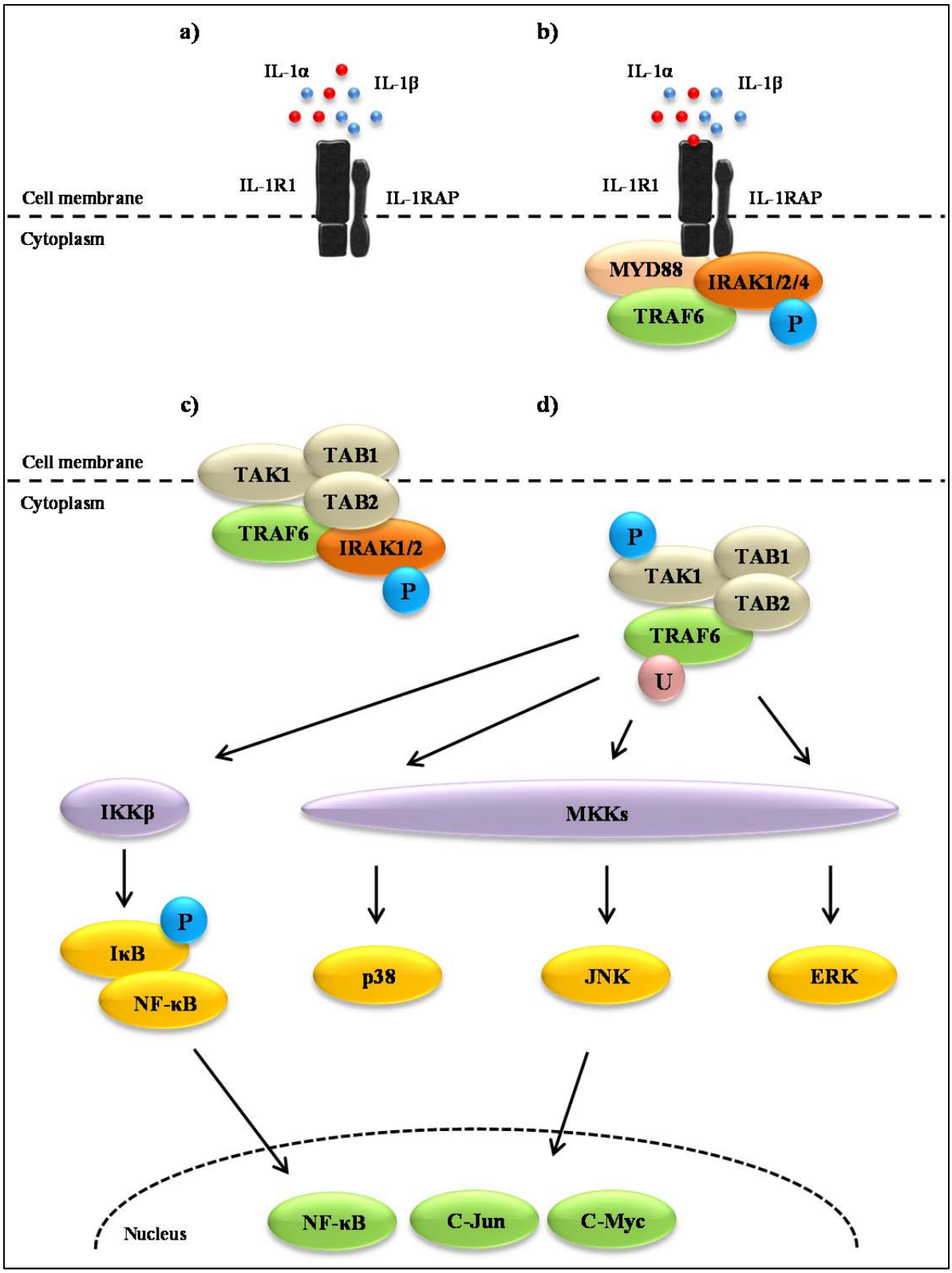

Figure 4: Model of IL-1α and IL-1β signaling pathways
a), b) Upon binding of IL-1α or IL-1β, IRAK1/2/4, TRAF6 and MYD88 are recruited. Recruitment of MYD88 leads to the phosphorylation of IRAK1/2/4. c) IRAK1/2/TRAF6 leave the complex to associate with TAK1/TAB1/TAB2. d) This new complex, excluding IRAK1/2, leaves the membrane and moves to the cytoplasm. TAK1 activates IKKβ thereby activating NF-κB. Moreover, TAK1 activates p38, JNK and ERK via activation of MKKs which leads to activation of transcription factors such as C-Jun and C-Myc.

The release of these inflammatory mediators might lead to further endothelial cell activation, amplified inflammation, and to impaired epithelial barrier function potentially increasing the susceptibility to viral/bacterial infections and subsequent exacerbations in COPD patients [87-90].

Obviously, the IL-1 pathway might provide attractive targets to intervene the inflammatory process of COPD. However, recent clinical Phase II studies using the anti-IL-1β Ab Canakinumab as well as the anti-IL-1R1 MEDI-8968 Ab did not meet their primary endpoints (FEV_1, exacerbation rate) in patients with COPD [91, 92]. Consequently, it remains an open question whether targeting the IL-1 pathway could be a beneficial therapeutic option for the treatment of COPD.

1.1.5 Exacerbations of COPD

Exacerbations of COPD are defined as "events in the natural course of the disease characterized by a change in the patient's baseline dyspnea, cough, and/or sputum and beyond normal day-to-day variations, which is acute in onset and may warrant a change in regular medication" [93, 94]. Periodically, COPD exacerbations induce considerable physiological deterioration in patients [95]. There is evidence that exacerbations result in an accelerated decrease of lung function (**Figure 5**) [96-98]. Therefore, these events have a significant impact on quality of life, morbidity and mortality [3]. In addition to the tremendous impact on disease progression, exacerbations constitute a considerable burden for national healthcare systems, for example due to hospitalizations. In a recent study, Pasquale et al. showed that COPD-related mean annual costs climb from $ 4,069 per individual to $ 6,381 for patients with two or more exacerbations [99, 100]. Furthermore, it was shown that not only the frequency but also the severity of an exacerbation is an important driver of treatment associated costs [101]. Thus, reducing the number and severity of exacerbations in COPD patients could help to disburden not only patients, but also healthcare systems.

Generally, exacerbations are accompanied by an increased inflammation in the airways. Notably, a relationship between the intensity of inflammation and the speed of decrease in FEV_1 has been observed [102]. In particular increased neutrophil numbers are suggested to play a central role in the enhanced inflammation during episodes of exacerbations. Moreover, eosinophils have been associated with higher frequency and severity of these devastating events. Increased levels of eosinophils might be explained by the release of Th2 cytokines such as IL-4 and IL-5 released by Th2 lymphocytes or innate lymphoid cells type 2 (ILC2),

for example upon activation due to viral infections (section 1.1.3) [103, 104]. Levels of TNF-α, IL-1β, IL-6, CXCL1 and CXCL8 are also increased in patients during exacerbations [105-108].

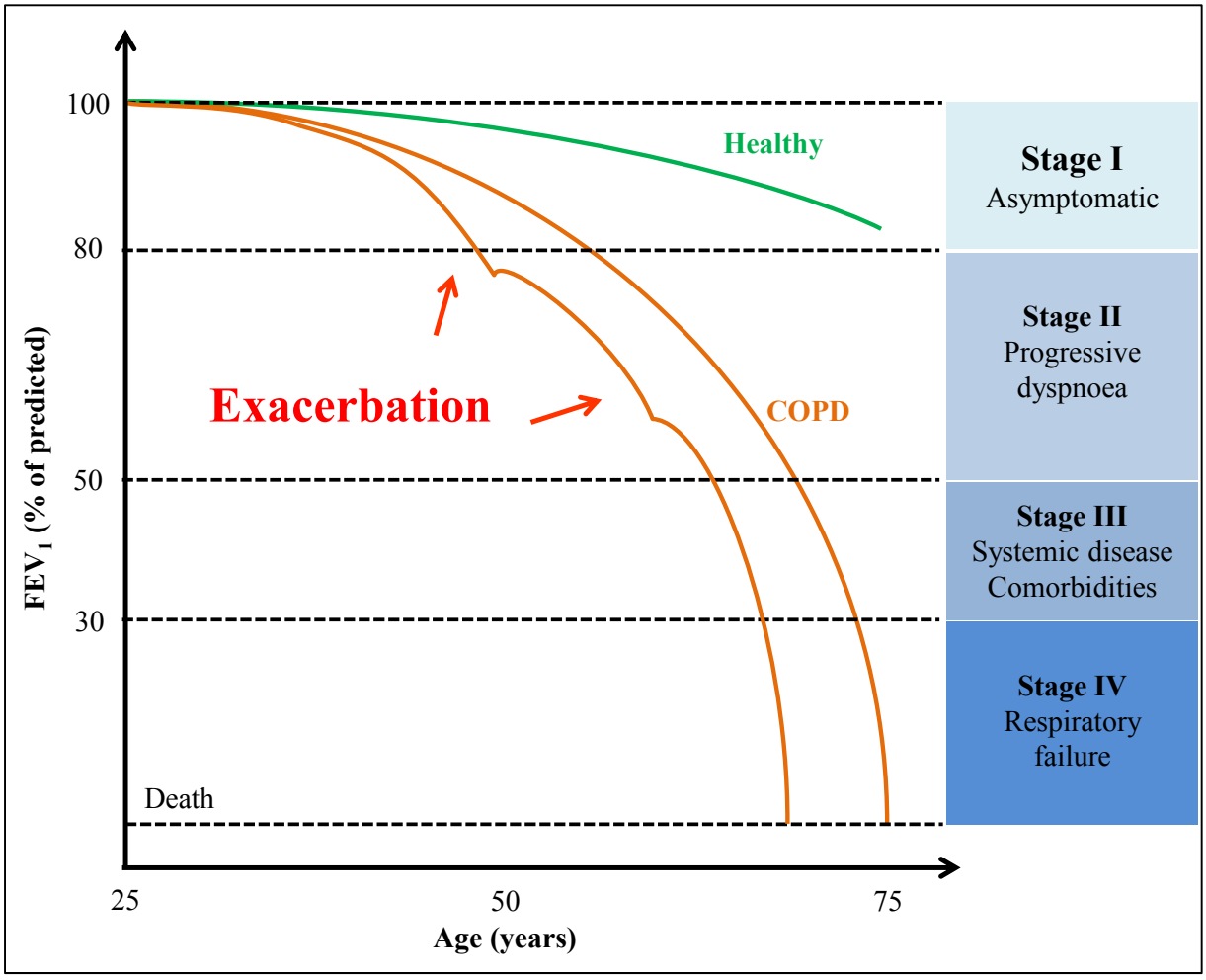

Figure 5: Model of how exacerbations impact the progression of COPD (adapted from [109, 110])
In healthy people, lung function decreases over years as illustrated by a drop in FEV_1 (green line). However, the symptomatic phase will usually not be reached. In contrast, the decline in lung function is much faster in COPD patients (orange lines). The decline magnitude of lung function loss determines the stage of the disease (Stage I -Stage IV). As illustrated, episodes of exacerbations accelerate lung function loss and lead to increased mortality.

Various triggers such as air pollutants and infections of the airways with viruses and bacteria are expected to increase the inflammatory burden in patients thereby leading to a worsening of respiratory symptoms [105].

As described in chapter 1.1.2, air pollution is a major risk factor for the development of COPD. In addition, high amounts of pollutants such as SO_2, O_3 and NO_2 have been linked to aggravated symptoms in COPD patients [111-113]. As mentioned, tissue damage is a major characteristic of COPD. Thus, also ciliary function is impaired and the clearance of particles from the airways is affected negatively. The increase in susceptibility to noxious particles and gases together with the finding that the mentioned pollutants have pro-inflammatory effects in

animal models may explain the observed impact of air pollutants on the frequency of exacerbations [113].

A further cause of increased inflammation in the lungs of COPD patients are infections of the airways with respiratory viruses (**Figure 6**). In the last years, the usage of modern molecular diagnostic techniques revealed that infections, for example with influenza virus or respiratory syncytial virus (RSV), are likely to be predominant triggers of exacerbations [105, 114-116]. Moreover, clinical studies indicate that virus-induced exacerbations are more severe and could be responsible for chronic infections in patients. This condition could promote chronic systemic inflammation in patients, which in turn has been associated with higher exacerbation frequency. Thus, prevention of viral infections, e.g. due to vaccination, could provide an effective tool to reduce exacerbation rates [87, 117, 118].

Air pollutants	Viruses	Bacteria
Nitrogen dioxide	Rhinovirus	*Haemophilus influenzae*
Sulfur dioxide	Influenza	*Streptococcus pneumoniae*
Ozone	Parainfluenza	*Moraxella catarrhalis*
	Coronavirus	*Staphylococcus aureus*
	Adenovirus	*Pseudomonas aeruginosa*
	Respiratory syncytial virus	
	Picornavirus	

Figure 6: Major triggers of COPD exacerbations (adapted from [105])
Distinct air pollutants, viruses and bacteria are expected to increase inflammation in the lungs of COPD patients and thus to be important triggers of exacerbations.

Bacteria are also considered to be major triggers of exacerbations (**Figure 6**) [119-121]. However, they are also detectable in sputum of 20 - 40% of stable COPD patients [121]. Chronic colonization of the airways correlates with the severity of the disease and impaired host defense mechanisms, for example damage of ciliary function. This leads to the inability to clear the bacteria. Chronic colonization is thus an indication for more frequent exacerbations [105]. As bacteria were isolated from patients with stable COPD as well as those with exacerbations, the true impact of these microorganisms on the frequency of exacerbations is difficult to assess. Still, it could be shown that the extent of bacteria in the airways is higher during exacerbations. The importance of the prokaryotes for exacerbations is further supported by the fact that patients benefit from treatment with antibiotics [122, 123].

Conclusively, there is evidence that environmental pollutants, bacteria and viruses have the potential to amplify the inflammatory process underlying COPD and therefore contribute to

the development of exacerbations. However, it must be stressed that the mechanisms which trigger exacerbations of the disease are widely unknown. In addition, inflammatory processes in patients during phases of exacerbations are very variable and patterns of the immunological responses differ. Thus, it is a necessity to identify valid biomarkers for exacerbations in order to develop novel treatments [114].

1.1.6 Influenza virus, respiratory syncytial virus and nontypeable *Haemophilus influenzae*-induced exacerbations of COPD

As listed in **Figure 6**, influenza virus, RSV and nontypeable *Haemophilus influenzae* (NTHi) are expected to be important triggers of COPD exacerbations.

Influenza viruses are enveloped, negative stranded, segmented RNA viruses. They belong to the *Orthomyxoviridae* family and can be further sub-divided in several genera. Of these, in particular influenza virus type A, B and C play a role in human disease. While influenza virus type B and C almost exclusively infect the respiratory tract of humans, animals such as pigs, birds, cats and horses are well-known hosts of the type A [124]. Central for the determination of influenza A virus subtypes are the two surface glycoproteins hemagglutinin (H) and neuraminidase (N). 16 different hemagglutinins and 9 neuraminidases are known and specific reassortments of these two antigens define the virus subtype, for example H1N1 [124]. H binds to sialic acid residues on host cells thereby initiating the infection of those and defining the host specifity [125]. Both H and N are crucial for the assembly and budding process of the virus [126]. Influenza infections have a tremendous impact on human health, not only as important triggers of COPD exacerbations. A prominent example is the spanish influenza, which killed about 50 million humans in 1918 [125].

Like influenza viruses, RSV are enveloped, negative-stranded RNA viruses [127]. They belong to the *Paramyxoviridae* family and are a major cause of airway infection in infants. About 70% of all infants are infected during their first years of life and almost all have come in contact with the virus by the age of 2 years [128]. Usually, RSV infection causes mild infections of the upper airways. However, children or elderly people characterized by risk factors such as immunosuppression or chronic lung diseases frequently develop more severe lower respiratory tract illness [129-132]. While vaccination constitutes an effective protection against influenza virus infection, no potent RSV vaccine is available to date and periodical re-infection with RSV among the human population is common [133].

Airway epithelia are the first line of defense against respiratory viruses. Infection of these cells results in direct effects such as necrosis, increased permeability, release of inflammatory mediators and influx of leukocytes [134]. Several mechanisms are responsible for the induction of inflammatory processes upon viral infection of the airways. For example, ROS are released upon damage of epithelia and lead to activation of NF-κB. Viral activation of NF-κB has been associated with the expression of IL-6, CXCL8, CCL5 and GM-CSF in the airways [135-138].

Important innate mediators which limit the expansion and drive clearance of influenza virus and RSV from the airways are IFNs [139, 140]. Three types (IFNs type I-III) of these mediators are known to date [141]. In particular type I IFNs (IFN-α, IFN-β) and type II IFNs (IFN-γ) are crucial to combat influenza virus and RSV infections [141-146]. IFN production is induced by host cells upon detection of pathogen-associated molecular patterns (PAMPs), for example viral RNA, by pattern recognitions receptors (PRRs) such as toll-like receptors (TLRs) and retinoic acid-inducible gene-I (RIG-I) [139, 147, 148]. Usually, released IFNs trigger specific IFN receptors (IFNR), which further signal through distinct Janus protein tyrosine kinase (JAK)-signal transducers and activators of transcription (STAT) pathways as illustrated in **Figure 7**. Thereby, the expression of several hundred anti-viral downstream IFN response elements such as the STATs are stimulated. Moreover, NOD-like receptor activation and subsequent NLRP3-inflammasome dependent activation of caspase-1 might play a role in virus-induced inflammatory processes [149, 150].

As described in section 1.1.3, IFN-γ promotes the recruitment of T lymphocytes via the release of CXCL9, CXCL10 and CXCL11 by epithelial cells, up-regulates expression of type I MHC and transporter associated with antigen processing I (TAP-1). Thus, it contributes to the recruitment of leukocytes and an effective presentation of viral components which is crucial for the clearance of respiratory viruses from the airways. However, as stated in section 1.1.5, the increased inflammation might trigger exacerbations in patients already suffering from chronic inflammatory processes in the lung.

Besides inducing a significant inflammatory response in the airways, influenza virus and RSV have the potential to alter lung function. On the one hand, airway mechanics such as resistance and compliance might be changed upon virus-induced inflammation due to changed tissue permeability and influx of blood components, which narrow the airways and alter tissue stiffness [151].

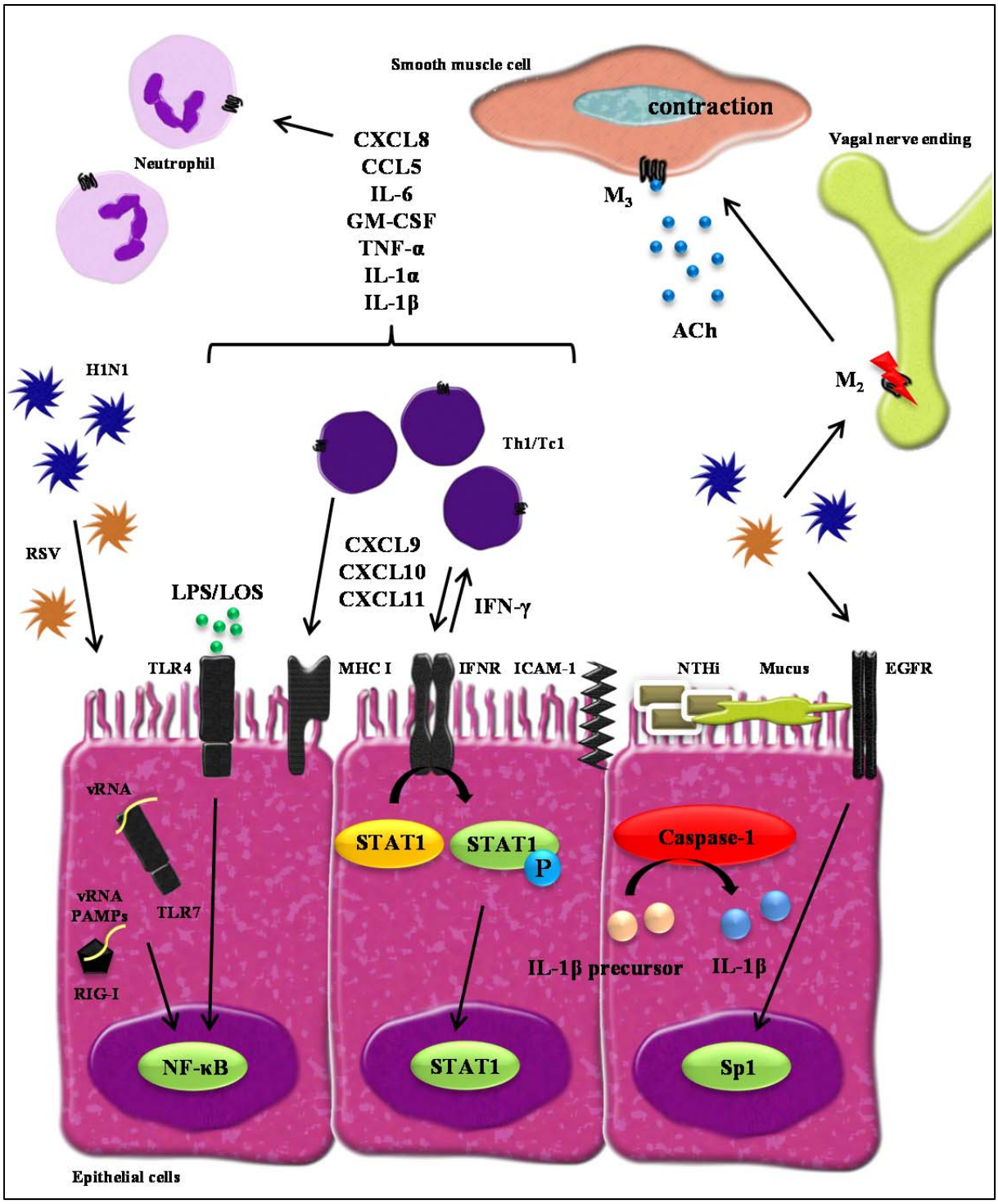

Figure 7: Model of how viral and bacterial infections exacerbate pulmonary inflammation
Influenza virus, RSV and NTHi have the ability to exacerbate pulmonary inflammation and worsen lung function in patients by affecting several inflammatory pathways or influencing the cholinergic system in the lungs.

On the other hand, it has been shown that respiratory viruses influence the muscarinic system (**Figure 7**). For example, TNF-α released upon viral infection was shown to directly reduce M_2 muscarinic receptor expression and function on vagal airway nerves [152]. Usually, activation of this receptor counteracts the release of the neurotransmitter acetylcholine (ACh) thereby limiting activation of M_3 muscarinic receptor activation on smooth muscle cells. This

regulating negative feedback loop is disrupted upon viral infection and might lead to enhanced bronchoconstriction [153-155].

In addition to triggering inflammatory processes in the airways directly, influenza virus and RSV were reported to modulate the structural integrity of epithelia and responsiveness regarding bacteria. For example, RSV was shown to up-regulate TLR4 on airway epithelial cells which sense PAMPs such as Lipopolysaccharides (LPS) or Lipooligosaccharides (LOS), respectively. Notably, airway epithelia are unresponsive to these PAMPs under normal circumstances [156]. Furthermore, virus-induced necrosis of cells has the ability to destroy the epithelial barrier promoting subsequent secondary bacterial infection, for example with NTHi, thereby leading to enhanced inflammation and exacerbations [157].

NTHi, a gram-negative coccobacillus, colonizes the nasopharynx of healthy adults and can be considered as part of the normal microbiome of healthy humans [157]. Notably, NTHi has to be distinguished from the typeable strains which are characterized by the presence of a polysaccharide capsule. While NTHi is a mucosal pathogen, the encapsulated strains are typically responsible for systemic diseases, for example meningitis. Based on variations in the outer membrane proteins, a huge variety of NTHi can be identified [158, 159].

Despite being a commensal in the upper airways, NTHi can also infect the lower respiratory tract thereby inducing a strong inflammatory response. Specific factors such as impaired ciliary function, structural damage or viral infections might facilitate lower respiratory tract infections [157]. The finding that influenza virus up-regulates ICAM-1 expression of airway epithelial cells, which in turn acts as a receptor for NTHi, is just one example of how viruses might promote a secondary infection with NTHi [160-162]. To date, the mechanisms which determine the pathogeny of NTHi are not completely understood and further investigations are needed to clarify why NTHi induces a strong inflammatory response in the lower airways while it does not in the upper airways [157].

As published, NTHi-induced lower airway inflammation is predominately mediated by TLR4 signaling induced by LOS and subsequent activation of the NF-κB signaling pathway [157, 163]. The infection with the bacteria has been associated with strong induction of IL-1β, TNF-α, CXCL8 and IL-6 release [164, 165]. Furthermore, there is evidence that NTHi infection, similar to an infection with influenza virus or RSV, triggers activation of the EGFR [166-168] (**Figure 7**). As outlined in section 1.1.3, EGFR is up-regulated in COPD patients and its activation induces mucus production which can thus be promoted by influenza virus, RSV or NTHi.

A reason why NTHi is a less prominent inducer of systemic inflammation might be that it is susceptible to killing by the complement system. Notably, immune responses in the lower airways often fail to clear the bacteria from the lungs resulting in persistent inflammation [157]. This might be one reason why NTHi appears to be a pivotal bacterial trigger of COPD exacerbations.

Conclusively, both infections with influenza virus and RSV have the ability to exacerbate inflammation in the airways directly by inducing specific immune responses. Moreover, infections with the viruses have to be considered as crucial promoters of lower respiratory tract infection with NTHi, which itself has the ability to aggravate inflammation in the lungs of COPD patients thereby inducing exacerbations. The assumption that both individual viral or NTHi infection or combined infection with virus and NTHi could be important when considering triggers of COPD exacerbations is supported by clinical studies, for example conducted by Bandi et al. [169].

1.1.7 Treatment options

To date, no treatment is able to stop the progression of COPD [170]. As outlined in sections 1.1.3 and 1.1.5, a chronic inflammatory process is expected to be causative for COPD pathologies. In particular, exacerbations accompanied by an increased inflammation have been associated with an accelerated disease progression and thus increased morbidity and mortality (section 1.1.5). Currently, most available treatments aim at reducing symptoms and slowing down the decline in lung function by dampening the devastating inflammatory processes thereby reducing exacerbation rates. Further important approaches aim at improving lung function [170].

Prominent anti-inflammatory treatments are corticosteroids, for example Dexamethasone or Fluticasone [170, 171]. Regarding the treatment of COPD, inhaled corticosteroids (ICS) such as Fluticasone are frequently used to reduce inflammation in patients [170, 172]. However, the role of ICS in COPD treatment is controversial. Studies have shown that ICS treatment does not attenuate neutrophil-driven inflammation and disease progression [170, 172, 173]. Furthermore, adverse effects have been reported to be associated with ICS treatment, including an increased risk for candidiasis, cataracts and fractures [172]. In addition, a large randomized, double-blind clinical trial with 6,112 patients revealed an increased risk of pneumonia (TORCH study), and withdrawal of ICS did not adversely affect the rate of exacerbations in COPD patients (WISDOM study) [172, 174, 175].

Further important anti-inflammatory drugs are phosphodiesterase-4 (PDE-4) inhibitors such as Roflumilast [176]. They act through blocking PDE-4, an enzyme which metabolizes intracellular cAMP in T lymphocytes, neutrophils and macrophages thereby contributing to the induction of inflammatory pathways [176, 177]. Roflumilast is approved for the treatment of severe COPD with frequent exacerbations [176].

Besides trying to dampen inflammation in the airways generally with broadly acting anti-inflammatory compounds such as ICS or PDE-4 inhibitors, more specific biologicals/antibodies (Abs) targeting specific inflammatory mediators recently entered the focus of interest. Important examples are chemokine inhibitors or anti-TNF-α Abs [170]. Moreover, as already described explicitly in section 1.1.4, Abs targeting members of the IL-1 pathway are currently under investigation for their potential to control an important driver of lung inflammation in patients.

The set of potential anti-inflammatory approaches currently under investigation for the treatment of COPD treatment is completed by adhesion molecule inhibitors, NF-κB inhibitors, p38 MAP kinase inhibitors. Moreover, anti-proteases and protease inhibitors aim at counteracting the devastating uncontrolled protease activity in the lungs of COPD patients. Prominent examples include α1-antitrypsin and MMP inhibitors. They might help to slow down the development of emphysema [170].

As mentioned, bronchoconstriction is a hallmark of COPD and especially during exacerbations patients suffer from a reduction in lung function [178, 179]. Therefore, the utilization of bronchodilators is currently a standard approach to help patients [179]. On the one hand, short- and long-acting β2 agonists such as Salbutamol or Formoterol are widely used options. On the other hand short- or long-acting muscarinic receptor antagonists provide a promising approach. A well-known long-acting muscarinic receptor antagonist is Tiotropium bromide [170, 179]. The drug blocks M_3 receptors of airway smooth muscle cells and thereby prevents binding of acetylcholine and subsequent bronchoconstriction [180]. Treatment with Tiotropium was shown to have a positive effect on lung function, quality of life and the frequency and severity of exacerbations (UPLIFT and POET study) [181, 182]. Interestingly, recent studies suggest that Tiotropium also has additional anti-inflammatory effects, possibly contributing to the efficacy seen in patients suffering from exacerbations [183, 184]. For example, Wollin et al. found that Tiotropium significantly reduced IL-6, TNF-α, MCP-1, MIP-1α and KC levels and neutrophil cell counts in bronchoalveolar lavage (BAL) fluid of CS-exposed mice [185]. Furthermore, Tiotropium also reduced inflammation

and remodeling in several models of asthma [186-190]. In addition, several *in vitro* studies also attest anti-inflammatory properties to Tiotropium [191-194].

In addition to the above mentioned treatment options which reduce inflammation and/or improve lung function, further treatments which remove viral or bacterial exacerbation stimuli should not be neglected in the context of COPD treatment options. As already mentioned in section 1.1.6, vaccination against viruses such as influenza can help to avoid exacerbations. Moreover, the utilization of antibiotics such as Azithromycin might help to reduce the bacterial burden and thus inflammation [195]. Azithromycin is a macrolide antibiotic which blocks the 50S subunit of bacterial ribosomes, thereby inhibiting mRNA translation and protein synthesis [196]. Long-term treatment with Azithromycin has been associated with decreased exacerbation frequency. However, prophylactic usage of Azithromycin must be considered carefully against the backdrop of the emergence of adverse effects and macrolide resistance development [197].

1.2 Relevance of pre-clinical mouse models in COPD research

To date, pre-clinical mouse models are crucial for the development of novel therapies to treat COPD [198]. In particular, they bridge the gap between *in vitro* and human studies and can help to gain new insights in the underlying disease mechanism and support the identification of attractive targets for therapeutic intervention [199, 200]. The fact that effective treatments which are able to stop the progression of COPD are not available and that the global dimension of the disease continues to rise implicates a huge unmet medical need (section 1.1.1). Thus, intensive research including the usage of pre-clinical mouse models is of central importance.

In the past years, several model organisms such as rodents, guinea-pigs, dogs, sheep and monkeys have been used to investigate aspects of COPD. In particular, mice are well-suited for the investigation of relevant disease pathways, primarily because of their physiological proximity to humans, the fact that they depict a (genetically) well characterized model system, the ability to produce many genetically engineered strains, the availability of Ab probes and low costs [198, 199]. So far, characteristic features of COPD have been modeled in mice by exposing them to exogenous stimuli such as proteases, chemicals, particles and most importantly CS [185, 198-202]. For example, Wollin et al. exposed C57BL/6 mice to CS thereby inducing a COPD-like inflammation characterized by increased total cells and neutrophils in BAL fluid, increased cytokines in lung homogenate and perivascular infiltrates

in the lungs. Furthermore, the authors used LPS in order to induce pulmonary inflammation [185]. As published, long-term CS-exposure provides the opportunity to model emphysema in mice. For example, Rinaldi et al. exposed C57BL/6 mice to CS for a total of six months. Thereby they were able to model emphysema and moreover systemic symptoms of COPD such as skeletal muscle dysfunction [203]. Besides inducing specific pathologies by external exposure to stimuli, genetically engineered mice have been utilized. For example, D'Armiento et al. used transgenic mice with up-regulated expression of metalloprotease-1 (MMP-1) in the lungs and thus were able to induce destruction of the alveolar walls [204]. Previously, exacerbations of COPD have been modeled in mice by administration of poly(I:C) or infection with viruses on top of CS-exposure [198]. Using influenza infection of CS-exposed C57BL/6 mice, Staempfli et al. were able to depict an exacerbated COPD phenotype [205].

Despite having the ability to model specific aspects of COPD in mice, a number of difficulties and limitations have to be considered. First and foremost, anatomical and physiological differences have to be taken into account. Moreover, one has to consider the fact that mice do not develop major pathological characteristics such as mucus overproduction, emphysema and airway remodeling to the same extent as human COPD patients. Notably, the set of inflammatory mediators of mice differs from the human one. For example, the role of important pro-inflammatory cytokines humans such as CXCL8 is not ascertained in mice and MMP-1 is not present in the animals [200].

Presently, no animal model is able to depict all characteristics of COPD [198]. However, as demonstrated by the mentioned examples, it is possible to model and investigate specific aspects of the disease which supports the development of novel therapies. The aim of this study was to develop and characterize pre-clinical mouse models which depict relevant aspects of viral and bacterial-induced COPD exacerbations to test novel therapies.

2 Material and Methods

2.1 *In vivo* experiments

2.1.1 Animals

Female BALB/cAnNCrl, C57BL/6J or C.C3-Tlr4LPS-d/J (TLR4-deficient) mice, 8-12 weeks of age, were purchased from Charles River (Germany). The Animals were kept in a specific pathogen-free facility at 20 – 25°C and a humidity of 46 – 65%. They received water and food *ad libitum*. All experimental procedures were performed under biosafety level 2 conditions and were in accordance with European and German national guidelines and legal regulations (Regierungspräsidium Tübingen, Germany, approved animal experimental licenses TVV 12-009, 12-016, 12-017, 14-016, 15-013).

2.1.2 Cigarette smoke-exposure

Mice were exposed to CS of 4 cigarettes daily (Roth-Händle without filters, tar 10 mg, nicotine 1.0 mg, carbonmonoxide 6 mg, Badische Tabakmanufaktur Roth-Händle, Germany) inside a perspex box for 8, 9 or 10 days as described previously [185]. Detailed experimental schemes can be found in section 2.1.16. On each day, the animals were exposed to CS of 4 cigarettes. Whole body CS exposure per cigarette was 16 minutes followed by an 8 minute period of fresh air. After the second cigarette, fresh air was transmitted into the box for 24 minutes, followed by two more cycles of CS exposure. CS exposure was controlled by a semi-automatic cigarette lighter and smoke generator (Boehringer Ingelheim Pharma GmbH & Co. KG, Germany). CS boxes were heated by a heating plate under the apparatus set to 40°C to maintain physiological body temperature of the animals.

2.1.3 Influenza virus and RSV infection of mice

Infection with influenza virus A/PR/8/34 (H1N1) or RSV strain A2 was performed as previously published [206]. In brief, mice were anaesthetized with 3% isoflurane and infected 2 hours after CS exposure by administering 50 µl virus in PBS intranasally. H1N1 was kindly provided by Boehringer Ingelheim (Canada). RSV strain A2 was obtained from Tebu-bio (USA). Details about the infection and re-infection schemes can be found in section 2.1.16.

2.1.4 NTHi growth and infection of mice

NTHi strain 3198-R with a spontaneous streptomycin resistance was kindly provided by the Institute of Molecular Biosciences, University of Graz, Austria. NTHi was plated on Mueller-Hinton agar plates supplemented with 0.005 mg/ml yeast extract, 0.015 mg/ml hemine, 0.015 mg/ml NAD and 0.1 mg/ml streptomycin. After a 16 hours period of incubation at 37°C, 4-6 colonies were scraped off the plate and fresh Mueller-Hinton broth medium supplemented with 0.005 mg/ml yeast extract, 0.015 mg/ml hemine, 0.015 mg/ml NAD and 0.1 mg/ml streptomycin was inoculated with the bacteria. Blank broth medium was used as sterile control. After overnight incubation at 37°C, 225 rpm in a MaxQ 4450 Benchtop Orbital Shaker (Thermo Scientific, USA), optical density at 490 nm (OD_{490}) was determined using a Nanodrop8000 UV-Vis Spectrophotometer (Thermo Scientific, USA). Fresh broth medium was inoculated with the overnight culture to an OD_{490} of 0.01. NTHi was grown to an OD_{490} of 0.11 (exponential phase), which was reached after approximately 5 hours as illustrated in **Figure 8**.

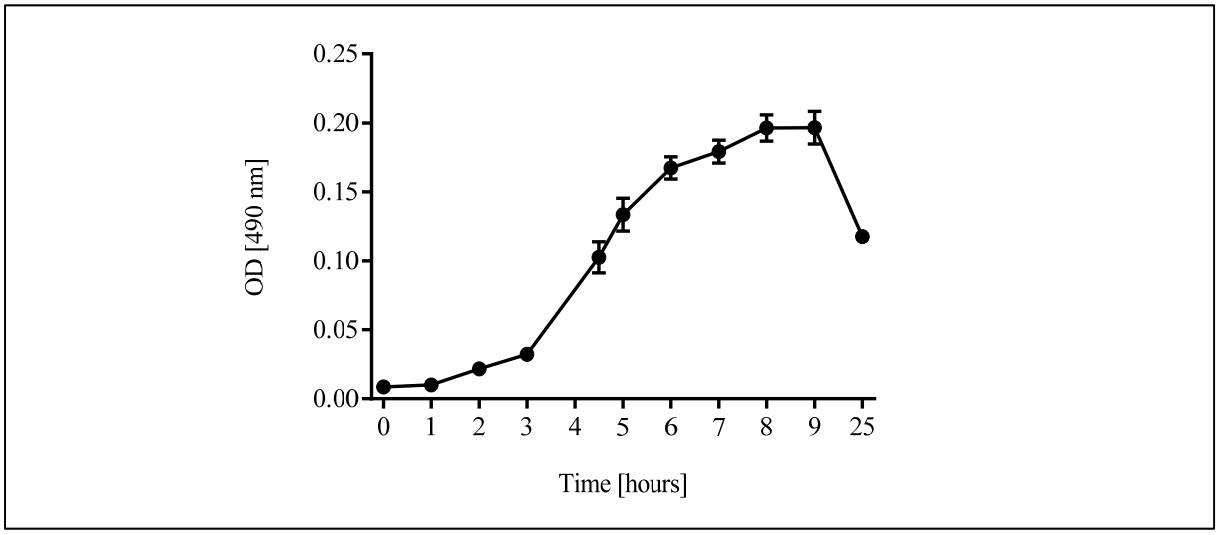

Figure 8: NTHi growth curve
Illustrated is a representative growth curve of NTHi in Mueller-Hinton broth medium supplemented with 0.005 mg/ml yeast extract, 0.015 mg/ml hemine, 0.015 mg/ml NAD and 0.1 mg/ml streptomycin at 37°C.

Subsequently, bacteria were washed twice with 10 ml PBS and adjusted to an OD_{490} of 0.11 in PBS which was equivalent to approximately 10^9 colony forming units (CFU)/ml. This stock was further diluted in PBS and used for infection (infection stock). 100 µl PBS, sterile control or infection stock were plated on Mueller-Hinton agar plates as controls. Heat-killing (HK) of NTHi was performed by heating the infection stock 45 min at 80°C. **Figure 9** illustrates plated NTHi, HK-NTHi, PBS and sterile control samples. Infection of mice was performed 4 hours after CS exposure by intranasal administration of 50 µl infection stock

under 3% isoflurane anesthesia. Details about the NTHi infection schemes can be found in section 2.1.16.

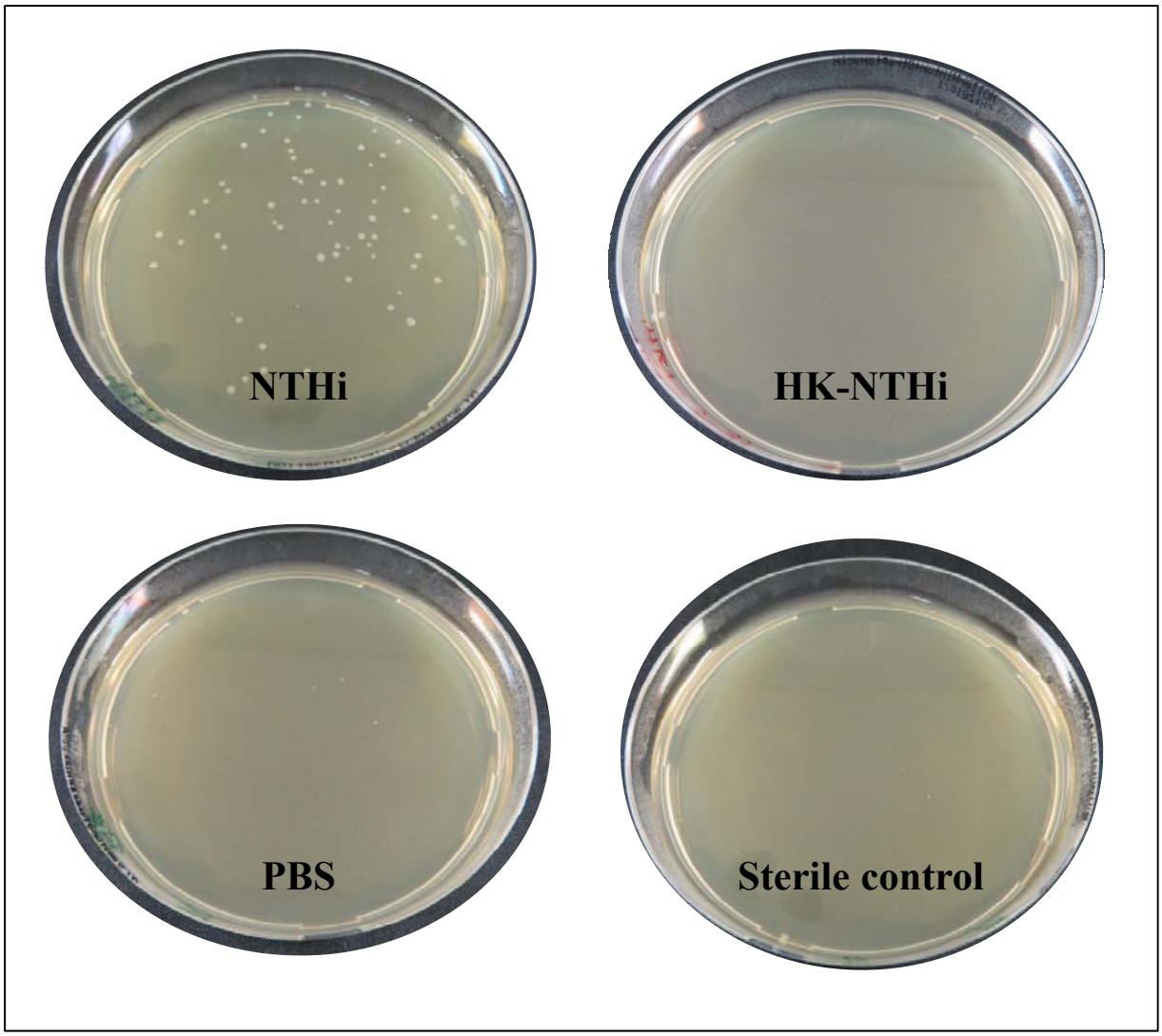

Figure 9: Plated NTHi, HK-NTHi, PBS, sterile control samples on Mueller-Hinton agar plates
Shown are representative Mueller-Hinton agar plates supplemented with 0.005 mg/ml yeast extract, 0.015 mg/ml hemine, 0.015 mg/ml NAD and 0.1 mg/ml streptomycin. 100µl plated NTHi, HK-NTHi, PBS and sterile control samples are depicted.

2.1.5 Measurement of lung function and airway hyperresponsiveness

Lung function was investigated by means of non-invasive whole body plethysmography measuring enhanced pause (Penh) values. Mice were placed in a whole body plethysmograph (Buxco Research Systems, USA) and breathing-induced changes in pressure were measured as illustrated in **Figure 10**. During the experiments airflow in the plethysmograph chamber was kept at 1 l/min. Penh values were calculated from the obtained breathing-induced changes in pressure according to the formula given in **Figure 10** [207].

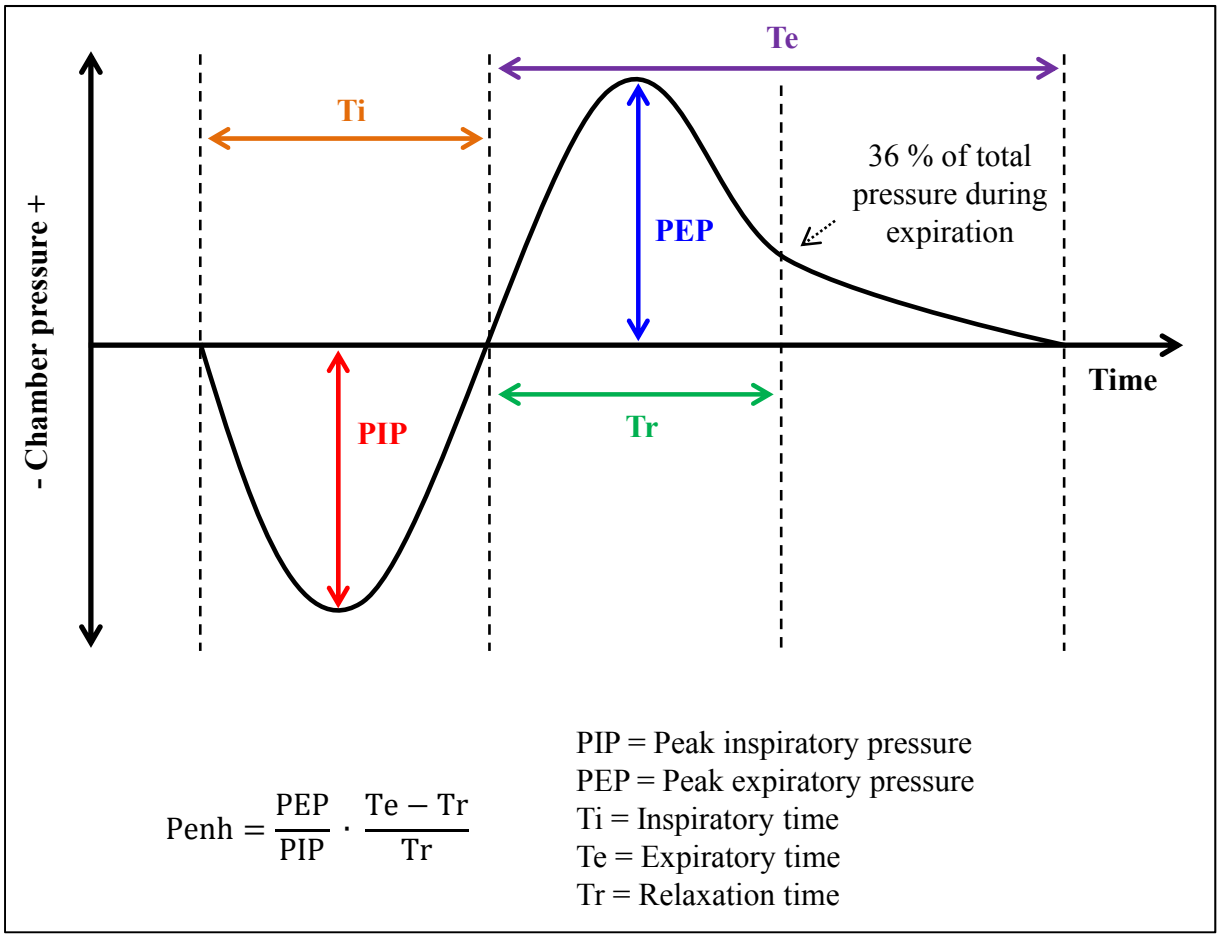

Figure 10: Parameters obtained from a whole body plethysmograph during one breathing cycle (adapted from [207]) Illustrated are the recorded breathing-induced changes in pressure during one breathing cycle of a mouse in a whole body plethysmograph. Enhanced pause (Penh) is calculated using the depicted parameters and formula.

The Penh value depicts the changes in the waveform of the measured pressure signal in combination with differences in the late/early expiration time (pause) and allows to measure altered lung function and responsiveness which might be triggered for example by inflammatory processes [207]. Notably, this method also has weaknesses. For example, the Penh value can easily be influenced by temperature, water vapor pressure or compressibility of the air. Therefore, the determination of the true impact of airway mechanics on the assessed changes in pressure and time is difficult [208, 209].

Given the mentioned weaknesses of the Penh assessment, minimal invasive lung function test to assess airway resistance and dynamic compliance was conducted as an alternative to detect changes in lung mechanics and AHR. For this purpose, mice were anestizised using a combination of 0.5 mg/kg metedomidin, 5 mg/kg midazolam and 0.05 mg/kg fentanyl. Subsequently, the animals were intubated and connected to the DSI's Buxco® FinePointe Series Resistance and Compliance sites. Using the corresponding FinePointe software, changes in the trans-pulmonary pressure (ΔP [cm H_2O]), the respiratory flow (ΔF [ml/s]) and the tidal volume (ΔV [ml]) were assessed. Baseline values were recorded. Moreover, MCh

(Sigma-Aldrich, Germany) at concentrations of 0.625, 2.5, 5 and 12.5 mg/ml in PBS were nebulized while continuing recording to investigate AHR. Increased airway resistance (Rl) indicates narrowing of the airways and was calculated according to the following equation [151]:

$$\mathrm{Rl} = \frac{\Delta \mathrm{P}}{\Delta \mathrm{F}} \ [\mathrm{cm\ H2O/ml/s}]$$

The dynamic lung compliance (Cdyn) describes the elasticity of the lung and was calculated as illustrated [151]:

$$\mathrm{Cdyn} = \frac{\Delta \mathrm{V}}{\Delta \mathrm{P}} \ [\mathrm{ml/cm\ H2O}]$$

2.1.6 Bronchoalveolar lavage

Four hours after the last CS exposure, mice were sacrificed by intraperitoneal (i.p.) injection of pentobarbital (Narcoren 160 mg/ml, Merial GmbH, Germany) diluted in 0.9% saline (400 mg/kg). Following, a cannula was inserted into the trachea of the animals and fixed with cord. The lungs were flushed with 0.8 ml of lavage buffer (PBS containing 1% BSA) twice. BAL fluid was extracted, collected in VACUETTE® tubes (Greiner Bio-One, Austria) and stored on ice until measurement by a Sysmex XT-1800i automated haematology analyzer (Sysmex Europe GmbH, Germany). The lavage volume was recorded in order to calculate total cells in BAL fluid.

2.1.7 Measurement of cell numbers and NTHi load in BAL fluid

Cell counts in BAL fluid were measured and differentiated using a Sysmex XT-1800i automated haematology analyzer. For determination of NTHi load, BAL fluid was diluted in PBS and plated on Mueller-Hinton agar plates supplemented with 0.005 mg/ml yeast extract, 0.015 mg/ml hemine, 0.015 mg/ml NAD and 0.1 mg/ml streptomycin. Colonies were counted after overnight incubation at 37°C.

2.1.8 Lung preparation

After sacrificing the animals, the lungs were removed, cleaned briefly in PBS and transferred into FastPrep Lysing Matrix tubes D (MP Biomedicals, USA). They were frozen in liquid nitrogen immediately after extraction and stored at -80˚C. For preparation of lung homogenates, the organs were thawed and weighed. The same amount of Hank's Solution

containing 0.1% 0.5 M EDTA pH 8.0, 1% BSA and one protease inhibitor cocktail tablet (Roche Diagnostics, Germany) corresponding to the weight of the lungs was added to the tubes and they were then put into the FastPrep-24 Sample Preparation System (MP Biomedicals, USA). If samples were meant to be used for quantitative polymerase-chain-reaction (qPCR) analysis, RNase inhibitor (Qiagen, Germany) was added (100 units/ml). Subsequently, lung homogenates were spun for 15 minutes at 14,800 g and 4°C to remove debris. Lung homogenates were stored at -80°C. If needed for histological analysis, left lungs were fixed in 4% paraformaldehyde (PFA) and further prepared as described in section 2.1.10.

2.1.9 Cytokine measurement in lung homogenate

Cytokine levels were measured in lung homogenate. Levels of IFN-γ, IL-1β, IL-2, IL-4, IL-5, IL-6, KC, IL-10, IL-12p70, TNF-α, GM-CSF, RANTES, IL-17, IL-13, IL-23, MCP-1, MIP-1α and MIP-1β were assessed using MSD multiplex technology (Meso Scale Discovery, USA) according to the manufacturer's instructions. In brief, 25 µl of MSD assay diluent were added to each well of a MSD 96-well multi-spot plate and incubated for 30 minutes. Next, 25 µl BAL fluid or lung homogenate were dispensed into each well and incubated for 2 hours. The plate was washed three times with PBS containing 0.05% Tween 20 (Fluka tablet, Sigma, Germany) and 1 µg/ml detection Ab was added to each well. After incubation for 2 hours at room temperature the plate was washed three times with PBS containing 0.05% Tween 20 and analyzed on a MESO QuickPlex SQ 120.

2.1.10 Histology

For the analysis of pathological changes in the lung tissue, left lungs were fixed in 4% paraformaldehyde (PFA) for at least 24 hours and subsequently embedded in paraffin wax. 3 µm transversal slices of the entry point of the main bronchus were sliced and stained using standard tissue staining protocols. Directly before staining, slices were heated for 45 min at 65°C. Hematoxylin and eosin (H&E) reagent (Merck, Germany) were used for staining of inflammatory infiltrates in a Varistain™ Gemini ES Automated Slide Stainer (Thermo Scientific, Germany). Stained sections were visualized using a Mirax Scan microscope scanner (Zeiss, Germany).

Staining protocol:

Step	H&E staining
1	Hematoxylin 8:00 min
2	Deionized water 0:10 s
3	HCL EtOH solution 0:30 s
5	Tap water 9:00 min
5	EtOH 80% 0:10 s
6	EtOH 96% 0:10 s
7	Eosin-Phloxin 0:20 s
8	EtOH 96% 0:20 s
9	EtOH 96% 0:20 s
10	EtOH 100% 0:30 s
11	EtOH 100% 0:30 s
12	Xylol 0:30 s
13	Xylol 0:30 s

2.1.11 RNA purification, cDNA generation and qPCR

300 µl of guanidinium chloride containing buffer RLT (Qiagen, Germany) containing 1% ß-mercaptoethanol were added to 50 µl lung homogenate. The samples were transferred onto Qiagen Shredder tubes and spun for 2 minutes at 10,000 g. Subsequently, 350 µl 70% ice-cold ethanol was added to the flow-throughs. The samples were transferred onto RNeasy spin columns (Qiagen, Germany) and connected to a QIAvac 24 Plus vacuum manifold (Qiagen, Germany). The columns where washed with 350 µl buffer RW1 (Qiagen, Germany). After that, 80 µl of RNase-Free DNase (Qiagen, Germany) solution was added to each tube and incubated for 15 min at room temperature according to the manufacturer's instruction to remove potential DNA contamination. Subsequently, samples were washed twice with buffer RPE (Qiagen, Germany) and eluted with 50 µl RNase-free water. Total RNA amount in samples was determined using a Nanodrop8000 UV-Vis Spectrophotometer (Thermo Scientific, USA).

High Capacity cDNA Reverse Transcription Kit (Applied Biosystems, USA) was used to generate cDNA according to the manufacturer's instructions in 96-well format. The following reverse transcription mix and cycler setup was used:

1 x RT master mix		Cycler setup	
10 x Reverse Transcription buffer	6 µl	1.	25 °C, 10 min
25 x dNTPs	2.4 µl	2.	37 °C, 120 min
10 x Random primers	6 µl	3.	85 °C, 5 min
Multiscribe Reverse Transcriptase (50 U/µl)	3 µl	4.	4 °C, ∞

1-3 µg RNA of each samples were added to 1x RT master mix. RNase free water was added to achieve a total volume of 60 µl in each well. The reaction mixes were then loaded into a Mastercyler Pro S (Eppendorf, Germany).

qPCR was performed to detect RSV or H1N1 in samples using Taqman technology. For this purpose, the following custom manufactured primers and probe were obtained from Sigma, Germany:

H1N1	
Forward 1	5'-GGACTGCAGCGTAGACGCTT-3'
Forward 2	5'-CATCCTGTTGTATATGAGGCCCAT-3'
Reverse	5'-CATTCTGTTGTATATGAGGCCCAT-3'
Probe	5'-CTCAGTTATTCTGCTGGTGCACTTGCCA-3'
RSV	
Forward	5'-AGATCAACTTCTGTCATCCAGCAA-3'
Reverse	5'-TTCTGCACATCATAATTAGGAGTATCAAT-3'
Probe	5'-CACCATCCAACGGAGCACAGGAGAT-3'

The probes were labeled with the 5' reporter dye 6-carboxyfluorescein (FAM) and the 3' quencher dye 6-carboxytetramethylrhodamine (TAMRA).

For the detection of MUC5 A/C and ICAM-1, ready-to-use gene expression assays were sourced from Life Technologies, USA.

In Taqman experiments, the quencher suppresses the fluorescence of the reporter dye linked to the probe when it is in close proximity. The probe binds specifically to its target gene (if present in the sample) and is cleaved during qPCR amplification process by the DNA polymerase. Consequently, the reporter dye is released and fluorescence is detectable. The fluorescence intensity is thus proportional to the amount of target DNA.

The following qPCR mixture and cycler setup was used:

1 x qPCR master mix (H1N1)		**Cycler setup**
Nuclease-free water	9.2 µl	Stage 1
QuantiFast PCR MasterMix 2 x (Qiagen, Germany)	20 µl	95 °C, 10 min
Primer forward 1 10 µM	0.8 µl	Stage 2
Primer forward 2 10 µM	0.8 µl	a) 95 °C, 15 sec
Primer reverse 10 µM	0.8 µl	b) 60 °C, 1 min
Probe 5 µM	0.4 µl	
1 x qPCR master mix (RSV)		
Nuclease-free water	10 µl	
QuantiFast PCR MasterMix 2 x (Qiagen, Germany)	20 µl	
Primer forward 10 µM	0.8 µl	
Primer reverse 10 µM	0.8 µl	
Probe 5 µM	0.4 µl	
1 x qPCR master mix (Gene expression assays)		
Nuclease-free water	10 µl	
QuantiFast PCR MasterMix 2 x (Qiagen, Germany)	20 µl	
Life technologies gene expression assay	2 µl	

8 µl of cDNA, generated by reverse transcription, were added to 1 x qPCR master mix to achieve a total volume of 40 µl in each well of a 96 well plate. 3 x 10 µl of these reaction mixes in each well were subsequently transferred to wells of a 384 well plate to generate 3 technical replicates. Additional reaction mixes containing 8 µl water instead of cDNA were used as no template controls.

qPCR data is presented either as ΔC_T or as fold change. These values were determined as described in the following. The cycle threshold (C_T) is defined as the number of PCR cycles needed until the fluorescence signal crosses the set threshold indicating significant and specific amplification of the target gene. The C_T value is inversely proportional to the amount of the target gene. 18S rRNA was used as endogenous control in the qPCR experiments. This reference gene was used for normalization and exclusion of variations during sample preparation, RNA isolation, reverse transcription, etc.

The normalized ΔC_T value was calculated by subtracting the C_T value of the endogenous control from the C_T value of the target gene. To illustrate the relative change in gene

expression of one sample (group) to another sample (group), the fold change was calculated according to standard qPCR instructions:

$$\Delta\Delta C_T = \Delta C_T \text{ (sample/group 1)} - \Delta C_T \text{ (sample/group 2)}$$

$$2^{-\Delta\Delta CT} = \text{fold change}$$

2.1.12 Detection of influenza virus and RSV in lung homogenate

Amount of H1N1 in lung homogenate was either determined using qPCR as described in section 2.1.11 or using an immunofocus assay. In brief, MDCK cells were seeded in 96-well dishes at a density of $2x10^4$ cells/well. 50 µl lung homogenate were incubated with the cells for 2 hours at 37°C. Next, the wells were washed with PBS and 200 µl DMEM containing 1% FBS and glutamine were added. After overnight incubation at 37°C, cells were fixated using acetone/methanol and blocked for 1 hour with 2% normal goat serum in PBS. Biotinylated anti-H1N1 Ab NP MAB8258 (Millipore, USA) was used for detection of infected cells. After addition of streptavidin-peroxidase conjugate diluted 1:4000 in 2% normal goat serum and true blue substrate, stained cells were counted via light microscopy.
RSV in 50 µl lung homogenate was determined by means of qPCR as described in section 2.1.11. Quantification was performed from standard curves of a pMA plasmid carrying a fragment of the RSV N-gene (provided by life technologies/GenArt®). Results are expressed in fold change compared to the control group.

2.1.13 Tiotropium, Fluticasone, Dexamethasone and Roflumilast treatment

Tiotropium bromide, Dexamethasone and Roflumilast were administered 1 hour prior to CS exposure. Tiotropium (Boehringer Ingelheim Pharma GmbH & Co. KG, Germany) was solved in 0.9% saline. For drug administration the animals were placed in wire-mesh cages inside a custom made perspex box (Boehringer Ingelheim Pharma GmbH & Co. KG, Germany). Mice were exposed to nebulized Tiotropium for 5 min. Fluticasone propionate (Boehringer Ingelheim Pharma GmbH & Co. KG, Biberach, Germany) was micronized and solved in 1 ml PBS/0.04% Tween 80, further diluted in PBS, and administered intranasally under isoflurane anesthesia. Dexamethasone (Sigma, Germany) was solved in PBS, further diluted in 0.5% hydroxyethylcellulose (Merck, Germany) and administered by oral gavage. Roflumilast (Boehringer Ingelheim Pharma GmbH & Co. KG, Germany) was micronized and solved in PBS/0.02% Tween 80. The drug was administered by oral gavage. Experimental schemes and used doses are described in detail in section 2.1.16.

2.1.14 Antibodies

For the *in vivo* studies, Abs against mouse IL-1α (clone ALF-161, haIgG, eBioscience, USA) and mouse IL-1R1 (clone JAMA-147, haIgG, BioXCell, USA) were sourced commercially, as well as the isotype control Ab eBio299Arm (haIgG, eBioscience, USA). Anti-mouse IL-1β Ab #315B4G5 (mIgG1) was developed and characterized in-house and kindly provided by NBE discovery colleagues; MOPC-21 (mIgG1, BioXCell, USA) was used as isotype control. In brief, all Abs were tested for endotoxin content (Endosafe-PTS, Charles River, USA), aggregation (Äkta chromatography, GE Healthcare, United Kingdom) and cellular potency (data not shown). All contained < 5 EU/mg endotoxin and were > 95% monomeric.

Target engagement models were developed using i.t. application of recombinant mouse IL-1α (#14-8011, eBioscience, USA) or IL-1β (#200-01B, Peprotech, Germany), respectively, to determine the efficacious dose for each Ab for subsequent experiments. In brief, dose-range finding and kinetic studies suggested 10 ng recombinant IL-1α or 10 ng recombinant IL-1β administered i.t. to induce submaximal phosphorylation of ERK in the lungs, peaking 20 min after administration (data not shown). Subsequently, the anti-IL-1α Ab, the anti-IL-1β Ab or the anti-IL-1R1 Ab, respectively, was administered i.p. 18 h before the i.t. stimulus. 20 min after stimulation with the recombinant ligand, the animals were sacrificed; the lungs were removed and subjected to homogenization. The ratio pERK/total ERK was determined according to the instructions of the manufacturer (Meso Scale Discovery, USA). Treatment with the respective Abs 18 h prior to the i.t. stimulation with mouse IL-1α or IL-1β revealed strong suppressive effects on the phosphorylation of ERK when using ≥ 100 µg anti-IL-1α Ab, ≥ 300 µg anti-IL-1β Ab, or ≥ 300 µg anti-IL-1R1 Ab (data not shown).

2.1.15 Antibody treatment

Based on data generated in the target engagement models, mice were treated i.p. with Abs directed against IL-1α (200 µg/mouse) or IL-1β (300 µg/mouse) or with Abs antagonizing the IL-1R1 (300 µg/mouse). Treatment was performed on day 1, 3, 5, 8, 10 of the experiment as illustrated in the experimental scheme in section 2.1.16. Isotype controls were used to adjust the amount of protein per mouse. Notably, all mice received the same amount of Abs, either as anti-target Ab or as isotype control Ab or as combinations thereof.

2.1.16 Experimental schemes

The effects of Tiotropium bromide, Fluticasone, Dexamethasone and Roflumilast were tested in the CS/H1N1 model as illustrated in the experimental scheme below.

CS/H1N1 model and treatments

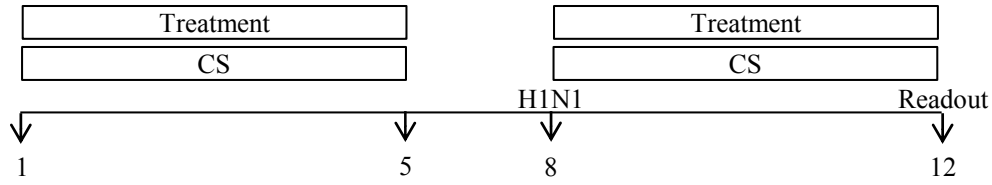

Drug	Type	Concentration/Dose	Route of administration
Tiotropium	Muscarinic receptor antagonist	0.1, 0.3 mg/ml	Inhalation
Fluticasone	Steroid	0.3, 0.5 mg/kg	Oral gavage
Dexamethasone	Steroid	1.0, 3.0 mg/kg	Oral gavage
Roflumilast	PDE4-inhibitor	0.2, 1.0 mg/kg	Oral gavage

Doses were chosen based on previous in-house experience. Drugs were administered in a preventive manner for a total of ten days (day 1-5 and day 8-12) 1 hour prior to CS exposure and infection.

For the CS/RSV model, a re-infection protocol was used, because similar to mice humans do not generate a protective memory response against RSV and are often re-infected with the virus [210, 211]. Moreover, re-infection of CS-exposed mice resulted in a more robust exacerbation phenotype compared to a single infection (data not shown).

CS/RSV model and treatments

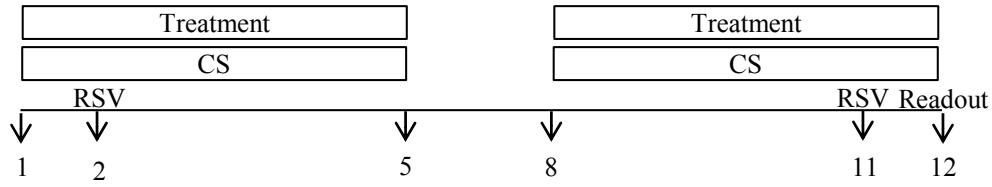

Drug	Type	Concentration/Dose	Route of administration
Tiotropium	Muscarinic receptor antagonist	0.1, 0.3 mg/ml	Inhalation
Fluticasone	Steroid	0.1, 0.3 mg/kg	Oral gavage
Roflumilast	PDE4-inhibitor	0.2, 1.0 mg/kg	Oral gavage

Neutralizing Abs were tested in the established CS/H1N1 model, targeting IL-1α, IL-1β and the IL-1R1. Abs were administered as shown in the experimental scheme below. Further

details about the sourcing/generation/characterization of the Abs can be found in section 1.1.14 and 1.1.15.

CS/H1N1 antibody studies

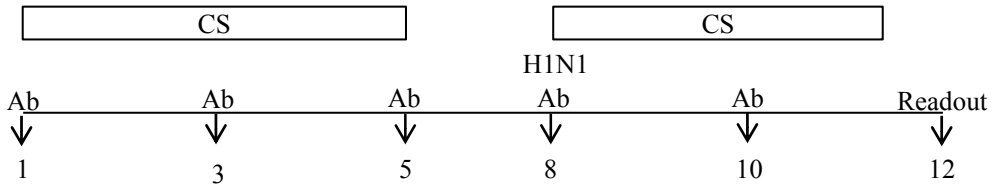

Antibody	Type	Concentration/Dose	Route of administration
Anti-IL-1α	ALF-161	200 µg/mouse	Intraperitoneal
Anti-IL-1β	#315B4G5	300 µg/mouse	Intraperitoneal
Anti-IL-1R1	JAMA-147	300 µg/mouse	Intraperitoneal

For the establishment of the CS/NTHi model, mice were exposed to CS and infected with the bacteria as illustrated below. The infection setup was based on previous dose-response and time-course experiments.

CS/NTHi model and treatments

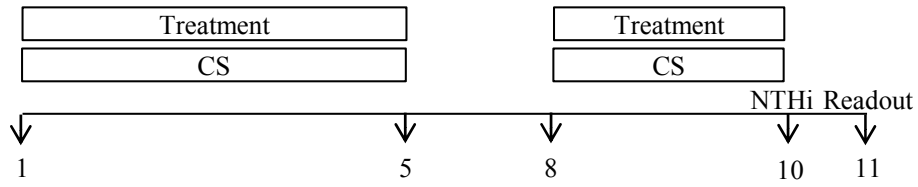

Drug	Type	Concentration/Dose	Route of administration
Dexamethasone	Steroid	0.1, 0.3, 1.0 mg/kg	Oral gavage
Roflumilast	PDE4-inhibitor	1, 3, 10, 30 mg/kg	Oral gavage
Azithromycin	Macrolide	5, 25, 50, 100 mg/kg	Oral gavage

H1N1 infections have been associated with secondary bacterial pneumonia [124]. Therefore, a CS/H1N1/NTHi combination model was established. For this purpose, mice were exposed to CS, infected with H1N1 and subsequently with NTHi as depicted in the following experimental scheme.

CS/H1N1/NTHi model and treatments

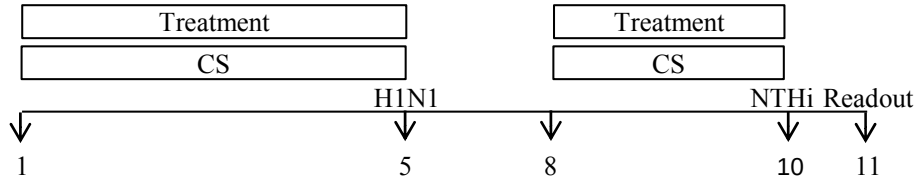

Drug	Type	Concentration/Dose	Route of administration
Dexamethasone	Steroid	0.1, 0.3, 1.0 mg/kg	Oral gavage
Roflumilast	PDE4-inhibitor	1, 3, 10, 30 mg/kg	Oral gavage
Azithromycin	Macrolide	5, 25, 50, 100 mg/kg	Oral gavage

2.2 *In vitro* experiments

2.2.1 Submerged NCI-H292 cell culture and Tiotropium, Fluticasone, Dexamethasone and Roflumilast treatment

30,000 NCI-H292 cells/well were seeded on day 1 in 24 well format. On day 2, Tiotropium bromide, Fluticasone propionate, Dexamethasone or Roflumilast were added. Drugs were solved in DMSO and further diluted in culture medium (RPMI1640 containing 5% FCS). Final drug concentrations were 10, 100, 1000 nM. On day 5, culture medium was removed and H1N1 or RSV diluted in 100 µl PBS was added. Infection dose was $1x10^5$ IU for H1N1 and $1x10^6$ PFU for RSV. After incubation for 3 hours at 37°C the wells were washed with 200 µl PBS and 600 µl medium containing the above mentioned treatments was added.

NCI-H292 cell culture and treatments

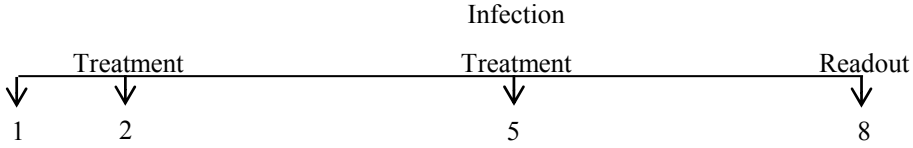

Drug	Type	Concentration	Treatment mode
Tiotropium	Muscarinic receptor antagonist	10, 100, 1000 nM	Solved in Medium
Fluticasone	Steroid	10, 100, 1000 nM	Solved in Medium
Dexamethasone	Steroid	10, 100, 1000 nM	Solved in Medium
Roflumilast	PDE4-inhibitor	10, 100, 1000 nM	Solved in Medium

On day 8, the medium was removed and 200 µl buffer RLT containing 1% ß-mercaptoethanole was added to each well. Notably, the experimental setup was based on infection time-course and dose-response studies (data not shown). RNA was isolated from cell lysate (Qiagen, Germany) and High Capacity cDNA Reverse Transcription Kit (Applied Biosystems, USA) was used for generation of cDNA according to the manufacturer's instructions and as described in sections 2.1.11. 2.5 µg of total RNA were used for reverse transcription. Detection of H1N1 and RSV was performed by means of qPCR as described in section 2.1.11.

2.2.2 Primary human bronchial epithelial air-liquid interface cell culture and antibody treatment

Normal human bronchial epithelial cells (Product code CC-2540S, Lot no. 0000313831) were obtained from Lonza, Germany. As stated by Lonza, the cells were isolated from donated human tissue after obtaining permission for their use in research applications by informed consent or legal authorization. Cells were thawed and cultured in a T75 culture flask overnight in expansion medium (PneumaCult-Ex basal medium containing 10% PneumaCult-Ex supplements, 1 µl/ml hydrocortisone, 10 µl/ml penicillin/streptomycin). Cells were grown to a confluency of 80%. Subsequently, reagent pack subculture reagents (Lonza, Germany) where used for trypsination. Cells were counted and transferred into a falcon tube. 35,000 cells were added onto Transwell® Permeable Support filters (6.5 mm Insert, 0.4 µm polyester membrane, Costar, USA). Four days after addition of the cells onto the transwell filters, apical medium was removed and basal medium was switched to differentiation medium (Pneumacult-ALI basal medium containing 10% Pneumacult-ALI supplements, 1% Pneumacult-ALI maintenance supplements, 2 µl/ml 0.2% heparin sodium salt in PBS, 4 µl/ml hydrocortisone, 10 µl/ml penicillin/streptomycin). Air-liquid-interface (ALI) cells were grown for at least three weeks. Medium was changed every second or third day. Apical mucus was removed as required by washing with PBS. Hydrocortisone and penicillin/streptomycin was removed from the medium five days prior to treatment and H1N1 infection.

IL-1α was neutralized using 100 nM of clone #4414 (mIgG2A, R&D Systems, USA; isotype control clone #20102, R&D Systems, USA), IL-1β by 100 nM Canakinumab (hIgG1, Komptur Apotheke, Germany; isotype control #BIBH1, Boehringer Ingelheim Pharma GmbH & Co KG). These concentrations were chosen as they reached maximal efficacy in cellular assays using whole blood (data not shown). Abs were added to the basal medium 6 hours prior to infection with $1.5x10^5$ IU H1N1 in 30 µl PBS, which was added on the apical side of

the cells. Appropriate isotypes (anti-IgG2a and anti-IgG1) were used as controls. Readout was performed 48 hours p.i.

Transepithelial electrical resistance (TEER) was measured using an EVOM device (World Precision Instruments, USA). Cytokines were measured in supernatant using MSD multiplex technology as described in section 2.1.9.

Detailed information about the study design are given in the experimental scheme below. Appropriate time points and doses for the study were determined based on previous infection time-course and dose-response studies (data not shown).

Primary air-liquid-interface cell culture and treatments

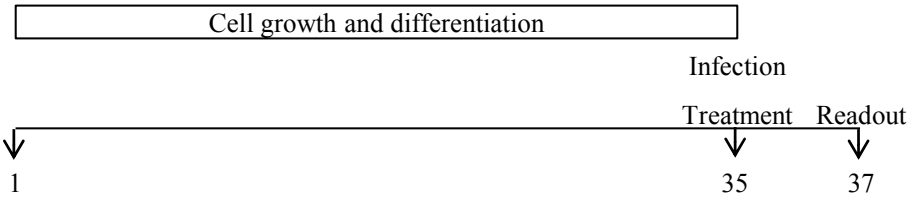

Drug	Type	Concentration	Treatment mode
Anti-IL-1α	MAB200	100 nM	Solved in Medium
Anti-IL-1β	Canakinumab	100 nM	Solved in Medium

2.3 Software and statistical analysis

Microsoft Office 2010 and GraphPad Prism 6.01 were used for data analysis and presentation. Multiple comparisons were performed by one-way ANOVA with Dunnett post-test. Non-parametric Kruskal-Wallis test was used upon unequal variances. For comparison of two groups, unpaired t-test was used. Data is expressed as mean ± standard error of mean (SEM). ****$p < 0.0001$, ***$p < 0.001$, **$p < 0.01$, *$p < 0.05$ represents significant differences compared to the control.

3 Results

3.1 Cigarette smoke/H1N1 exacerbation model

H1N1 infections are associated with exacerbations in COPD patients (section 1.1.6). Thus, this virus was used to develop murine models which reflect aspects of virus-induced COPD exacerbations.

3.1.1 CS/H1N1 exacerbation model establishment

Mice were exposed to CS and infected with different doses of H1N1 as published previously [206]. **Figure 11A** illustrates a protocol using 30 IU H1N1 for infection, which depicts relevant aspects of an exacerbation.

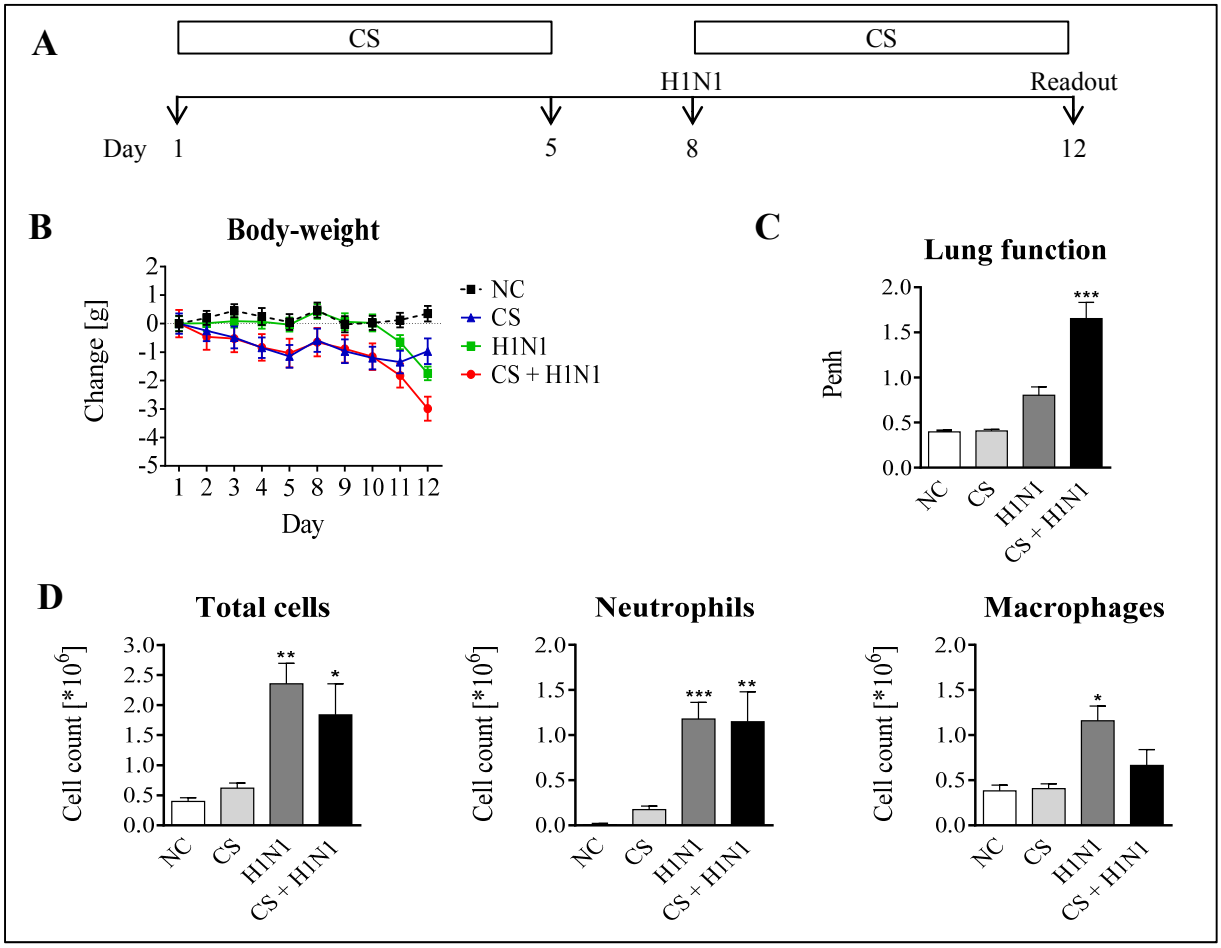

Figure 11: H1N1 infection of CS-exposed mice [206]
(A) Mice were exposed to CS for a total of 10 days (light gray bars). Additional mice were infected with only H1N1 on day 8 (dark gray bars) or CS-exposed and infected with H1N1 on day 8 (black bars). White bars show the results from untreated negative control (NC) animals. (B) Body-weight change in NC animals (black dotted line), CS-exposed (blue line), H1N1-infected (green line), or CS-exposed and H1N1-infected (red line) mice. (C) Lung function, (D) total cell, neutrophil and macrophage numbers in BAL fluid. Mean values ± SEM of n = 7-8 animals in the H1N1- and CS-exposed mice groups and n = 4 in the NC group are shown. ****p < 0.0001, ***p < 0.001, **p < 0.01, and *p < 0.05 represent significant differences compared with the NC group.

While CS-exposure or H1N1 infection resulted in a low or moderate loss of body-weight, combination of the stimuli led to a significant loss of body-weight (**Figure 11B**). As shown in **Figure 11C**, neither CS-exposure nor H1N1 infection alone resulted in significantly increased Penh values. In contrast, lung function was significantly impaired upon CS-exposure and additional H1N1 infection. Measured Penh value was 1.65 ± 0.18 compared to 0.40 ± 0.014 of the control animals. Infection of mice with H1N1 significantly increased accumulation of total cells, neutrophils and macrophages in BAL fluid (**Figure 11D**). Surprisingly, additional CS-exposure of H1N1-infected mice did not further increase cellular influx into the lungs in this experiment.

While CS-exposure alone did not increase cytokine levels in lung homogenate significantly, H1N1 infection of the animals resulted in significantly increased levels of IL-6, KC, TNF-α, IL-1ß and IFN-γ (**Figure 12A**). However, H1N1-induced cytokine influx was lower in comparison to animals receiving CS and H1N1. In CS-exposed and H1N1-infected animals IL-6, KC, TNF-α, IL-1β and IFN-γ were significantly elevated. Furthermore, quantification of H1N1 load in lung homogenate revealed that the amount of virus was highest in mice which were exposed to CS prior to infection with the virus (**Figure 12B**).

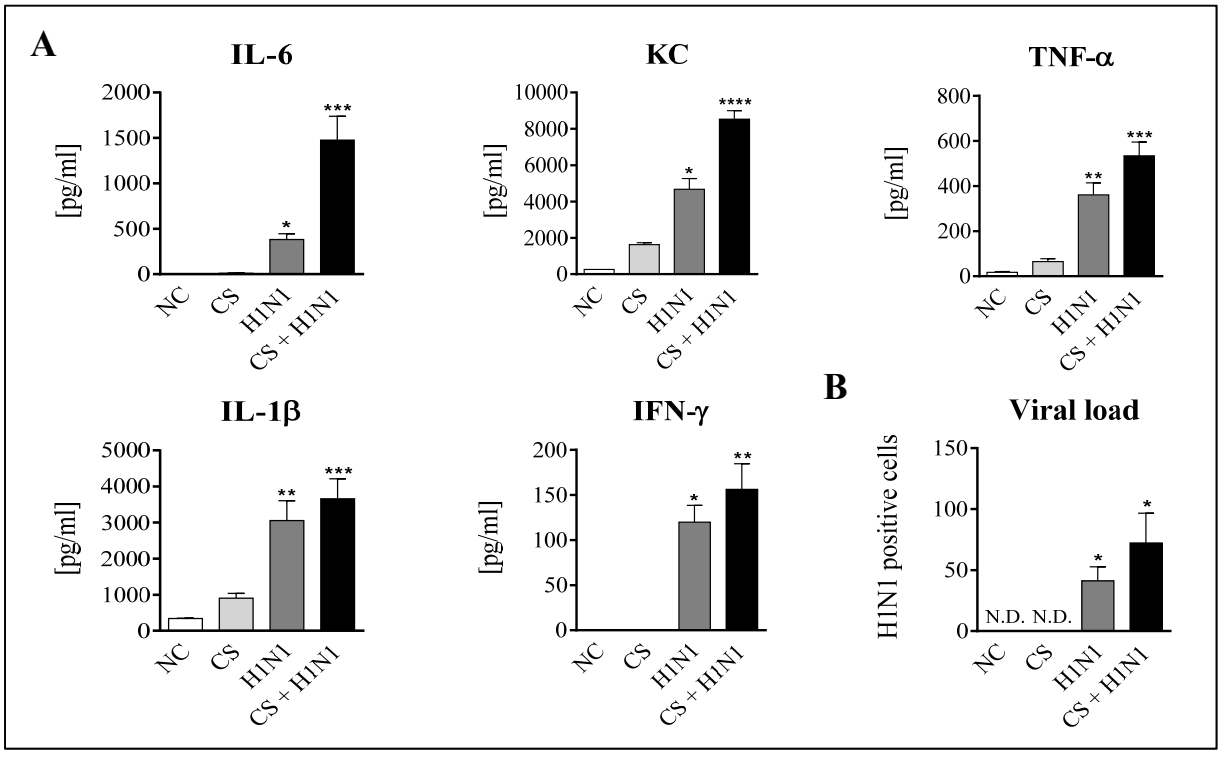

Figure 12: Cytokine levels of CS-exposed and H1N1-infected mice [206]
Mice were exposed to CS for a total of 10 days (light gray bars). Additional mice were infected with only H1N1 on day 8 (dark gray bars) or CS-exposed and infected with H1N1 on day 8 (black bars). White bars show the results from untreated negative control (NC) animals. (A) Cytokine levels in lung homogenate and (B) viral load in lung homogenate. Mean values ± SEM of n = 7-8 animals in the H1N1- and CS-exposed mice groups and n = 4 in the NC group are shown. ****$p < 0.0001$, ***$p < 0.001$, **$p < 0.01$, and *$p < 0.05$ represent significant differences compared with the NC group.

3.1.2 Tiotropium attenuates H1N1-induced pulmonary inflammation in CS-exposed mice

In order to investigate whether Tiotropium shows anti-inflammatory effects in the CS/H1N1-exposed mice, the animals were treated with the drug for a total of ten days (**Figure 13A**).

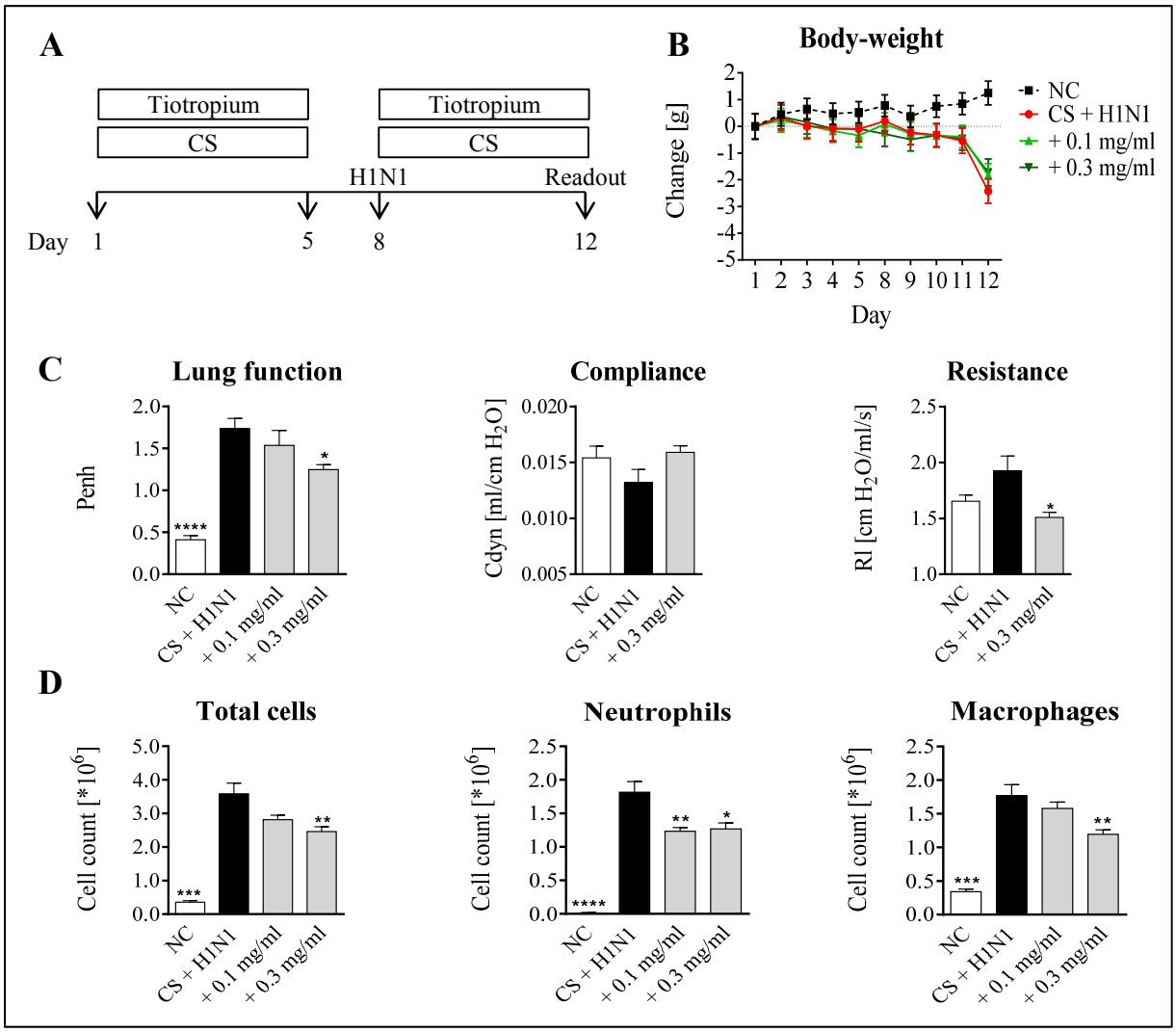

Figure 13: Tiotropium treatment of CS-exposed and H1N1-infected mice [206]
(A) CS-exposed and H1N1-infected mice (black bars) were treated for a total of 10 days with 0.1 mg/ml or 0.3 mg/ml nebulized Tiotropium (gray bars). White bars show the results from untreated negative control (NC) animals. (B) Body-weight change in NC mice (black dotted line), untreated CS-exposed and H1N1-infected mice (red line), CS-exposed and H1N1-infected mice treated with 0.1 mg/ml (light green line) or 0.3 mg/ml (dark green line) nebulized Tiotropium. (C) Lung function, resistance, compliance and (D) total cell, neutrophil and macrophage numbers in BAL fluid. Mean values ± SEM of n = 7-8 animals in the H1N1- and CS-exposed mice groups and n = 4 in the NC group are shown. ****p < 0.0001, ***p < 0.001, **p < 0.01, and *p < 0.05 represent significant differences compared with CS-exposed and H1N1-infected group.

Treatment with Tiotropium did not influence body-weight (**Figure 13B**). At a concentration of 0.3 mg/ml Tiotropium decreased Penh values and airway resistance significantly indicating improved lung function (**Figure 13C**). In addition, Tiotropium significantly reduced total cells, neutrophils and macrophages in BAL fluid (**Figure 13D**).

Cytokine levels of IL-6 and IFN-γ were reduced in lung homogenate of animals treated with Tiotropium (**Figure 14**).

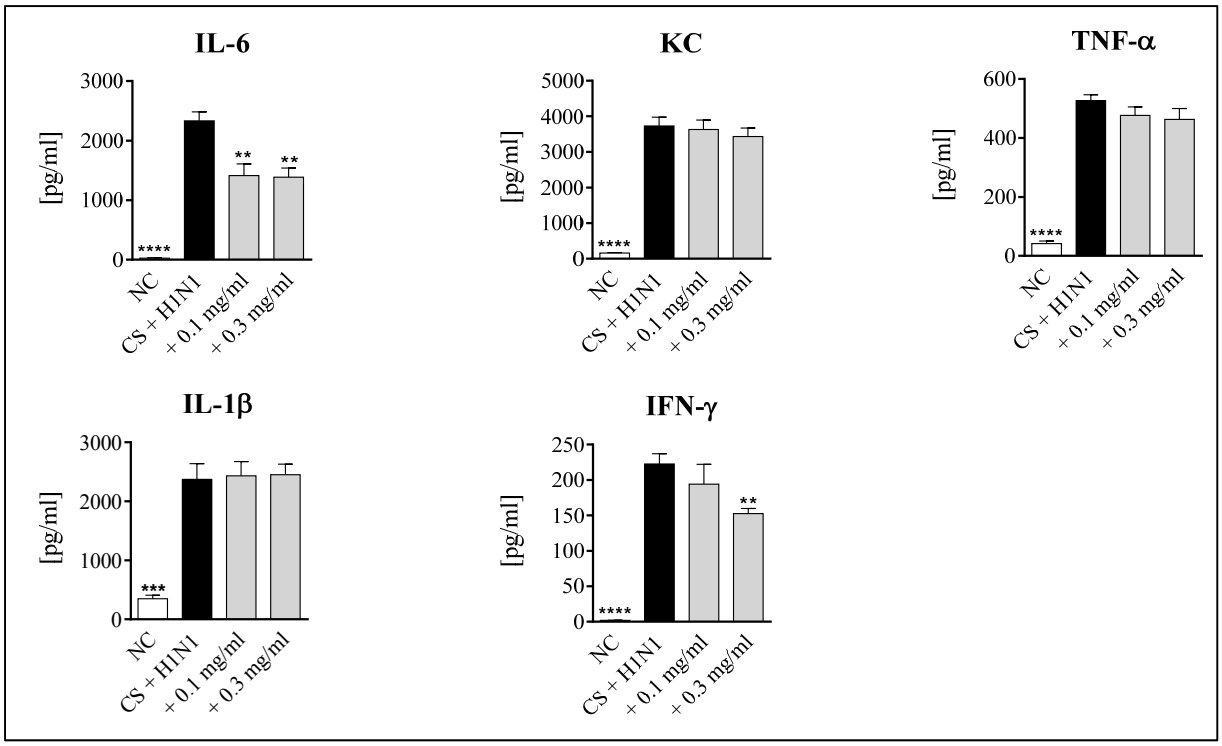

Figure 14: Cytokine levels of Tiotropium-treated CS-exposed and H1N1-infected mice [206]
CS-exposed and H1N1-infected mice (black bars) were treated for a total of 10 days with 0.1 mg/ml or 0.3 mg/ml nebulized Tiotropium (gray bars). White bars show the results from untreated negative control (NC) animals. Cytokine levels in lung homogenate. Mean values ± SEM of n = 7-8 animals in the H1N1- and CS-exposed mice groups and n = 4 in the NC group are shown. ****p < 0.0001, ***p < 0.001, **p < 0.01, and *p < 0.05 represent significant differences compared with CS-exposed and H1N1-infected group.

3.1.3 Steroid treatment fails to reduce pulmonary inflammation, increases the loss of body-weight and the viral load

Next, the effect of the corticosteroid Fluticasone was investigated in the CS/H1N1 model. The protocol shown in **Figure 15A** illustrates the experimental scheme. Upon treatment with 0.3 mg/kg or 0.5 mg/kg, an aggravated loss of body-weight was observed in comparison to CS-exposed and H1N1-infected mice without treatment (**Figure 15B**). Furthermore, Penh values increased significantly in a dose dependent manner upon Fluticasone treatment and compliance values were lowered significantly (**Figure 15C**). While Penh value was 1.86 ± 0.21 for the CS-exposed and additionally H1N1-infected mice, it peaked at a value of 6.30 ± 0.94 in mice treated with 0.5 mg/kg of the corticosteroid. In contrast to its described anti-inflammatory effect [212], treatment with Fluticasone failed to reduce cytokine levels in lung homogenate or cell counts in BAL fluid in the CS-exposed and H1N1-infected mice (**Figure 15D**). As illustrated in **Figure 15E**, drug administration moreover increased levels of IL-6, KC and TNF-α significantly.

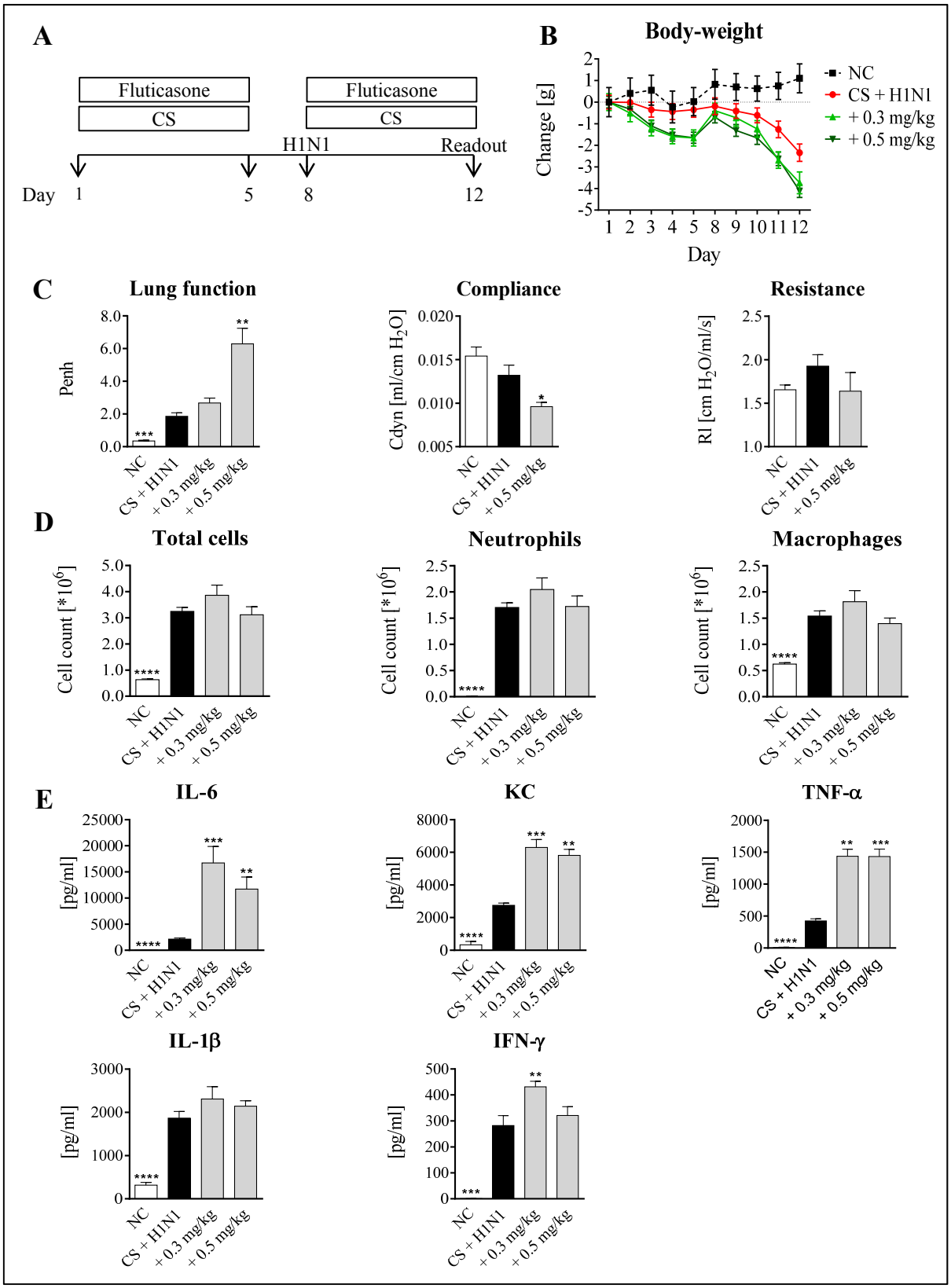

Figure 15: Fluticasone treatment of CS-exposed and H1N1-infected mice [206]
(A) CS-exposed and H1N1-infected mice (black bars) were treated with 0.3 mg/kg or 0.5 mg/kg Fluticasone (gray bars). White bars show the results from untreated negative control (NC) animals. (B) Body-weight loss in NC mice (black dotted line), untreated CS-exposed and H1N1-infected mice (red line), CS-exposed and H1N1-infected mice treated with 0.3 mg/kg (light green line) or 0.5 mg/kg (dark green line) Fluticasone. (C) Lung function, resistance, compliance, (D) total cell, neutrophil and macrophage numbers in BAL fluid, (E) cytokine levels in lung homogenate. Mean values ± SEM of n = 4–8 animals in the H1N1- and CS-exposed mice groups and n = 4 in the NC group are shown. ****p < 0.0001, ***p < 0.001, **p < 0.01, and *p < 0.05 represent significant differences compared with CS-exposed and H1N1-infected group.

These results were surprising. Therefore, it was investigated whether they are Fluticasone-specific or a general corticosteroid effect. For this purpose the effects of Dexamethasone were tested in the CS/H1N1 model. As illustrated in **Figure 16,** Dexamethasone also increased weight loss and had no positive effect on airway resistance and compliance or neutrophil numbers in the CS/H1N1-exposed mice.

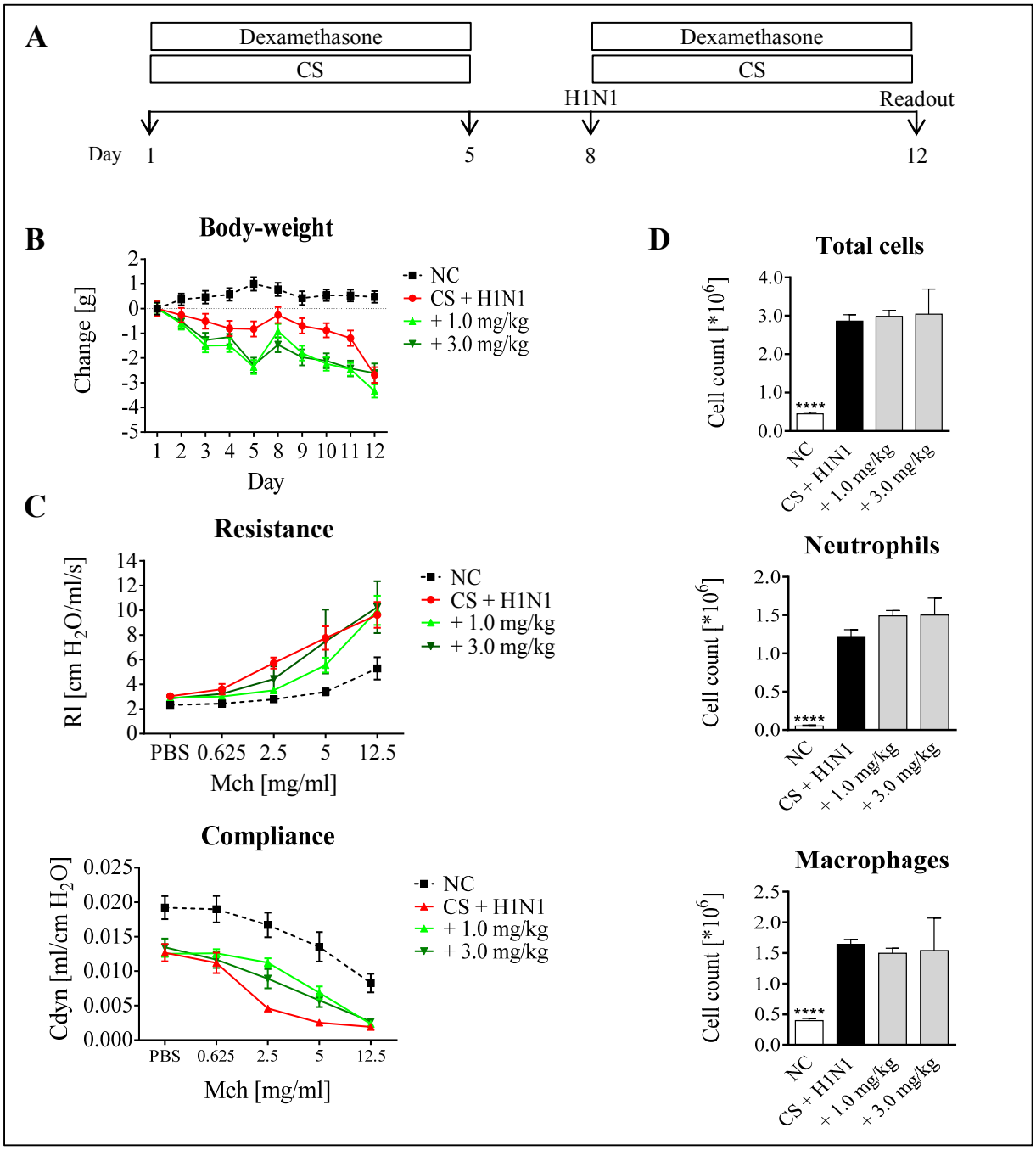

Figure 16: Dexamethasone treatment of CS-exposed and H1N1-infected mice [206]
(A) CS-exposed and H1N1-infected mice (black bars) were treated for a total of ten days with 1.0 mg/kg or 3.0 mg/kg Dexamethasone (gray bars). (B) Body-weight loss in negative control (NC) mice (black dotted line), untreated CS-exposed and H1N1-infected mice (red line), CS-exposed and H1N1-infected mice treated with 1.0 mg/kg (light green line) or 3.0 mg/kg (dark green line) Dexamethasone. (C) Resistance and compliance, (D) total cell, neutrophil and macrophage numbers in BAL fluid. Mean ± SEM of n = 7-8 animals per group are shown. ****$p < 0.0001$, ***$p < 0.001$, **$p < 0.01$, *$p < 0.05$ represent significant differences compared to the CS-exposed and H1N1-infected group.

However, in contrast to Fluticasone, Dexamethasone treatment reduced levels of KC, IL-6, IL-1ß and IFN-γ in these animals (**Figure 17**).

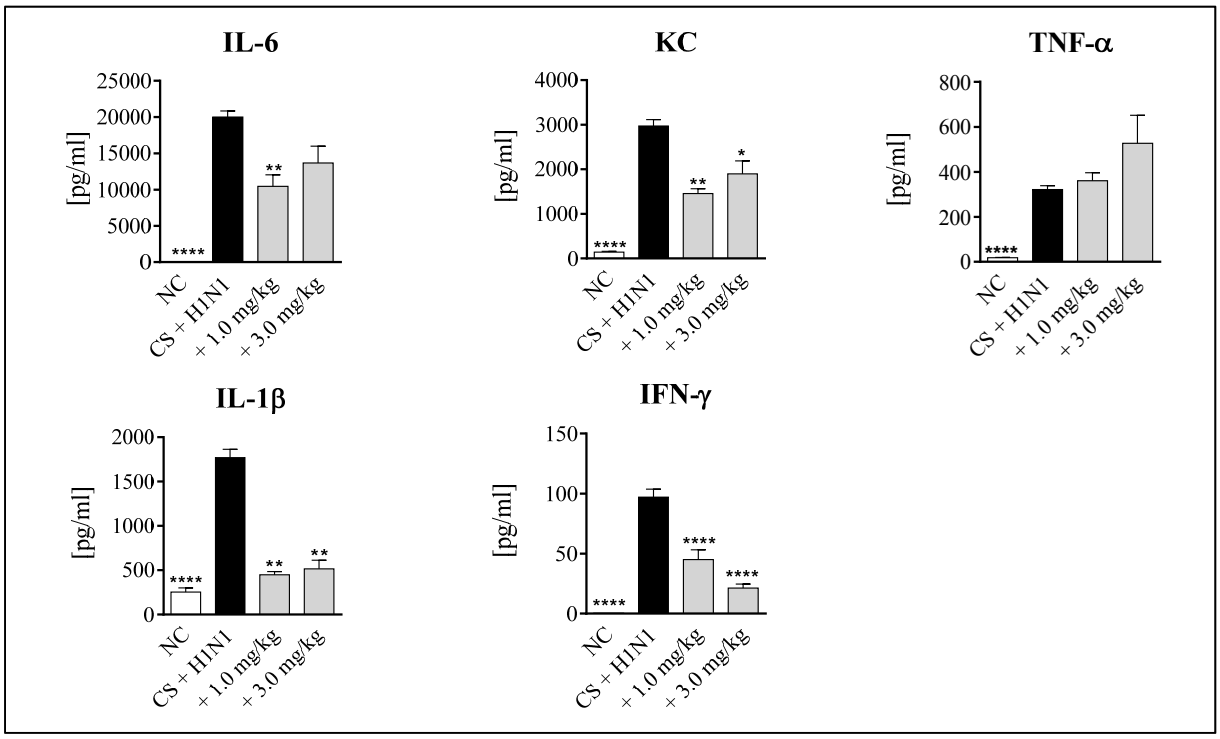

Figure 17: Dexamethasone treatment of CS-exposed and H1N1-infected mice [206]
CS-exposed and H1N1-infected mice (black bars) were treated for a total of ten days with 1.0 mg/kg or 3.0 mg/kg Dexamethasone (gray bars). Cytokine levels in lung homogenate are shown. Mean ± SEM of n = 7-8 animals per group are shown. ****p < 0.0001, ***p < 0.001, **p < 0.01, *p < 0.05 represent significant differences compared to the CS-exposed and H1N1-infected group.

3.1.4 Roflumilast decreases levels of cytokines and cell counts but does not improve lung function

The effect of the PDE-4 inhibitor Roflumilast treatment was investigated in the CS/H1N1 combination model. The experimental scheme is illustrated in **Figure 18A**. Drug administration had no effect on the loss of body-weight (**Figure 18B**). Moreover, it had no effect on Penh values or lung resistance and compliance (**Figure 18C**). As shown in **Figures 18D** and **18E**, both cytokine levels and cell counts decreased upon treatment. Levels of IL-6, KC and IFN-γ were significantly lower in lung homogenate and total cells and macrophages decreased significantly in BAL fluid at a dose of 1.0 mg/kg.

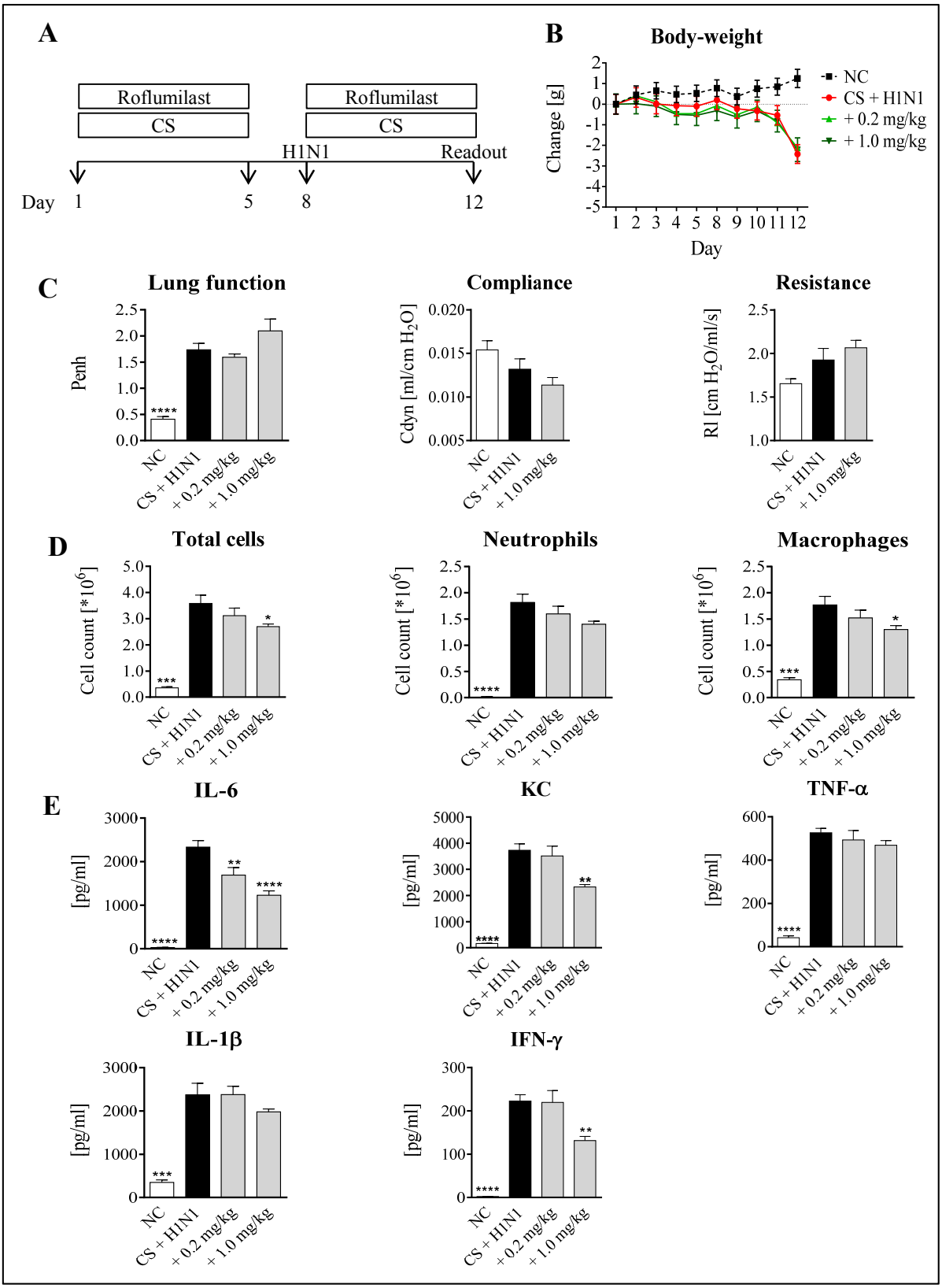

Figure 18: Roflumilast treatment of CS-exposed and H1N1-infected mice [206]
(A) CS-exposed and H1N1-infected mice (black bars) were treated with 0.2 mg/kg or 1.0 mg/kg Roflumilast (gray bars). White bars show the results from untreated negative control (NC) animals. (B) Body-weight loss in NC mice (black dotted line), untreated CS-exposed and H1N1-infected mice (red line), CS-exposed and H1N1-infected mice treated with 0.2 mg/kg (light green line), or 1.0 mg/kg (dark green line) Roflumilast. (C) Lung function, resistance, compliance and (D) total cell, neutrophil and macrophage numbers in BAL fluid. (E) Cytokine levels in lung homogenate. Mean values ± SEM of n = 7-8 animals in the H1N1- and CS-exposed mice groups and n = 4 in the NC group are shown. ****$p < 0.0001$, ***$p < 0.001$, **$p < 0.01$, and *$p < 0.05$ represent significant differences compared with the CS-exposed and H1N1-infected group.

3.1.5 Fluticasone and Dexamethasone treatment increases the amount of H1N1 *in vivo* and *in vitro*

The amount of H1N1 in the lungs of CS-exposed mice and the effects of treatment with Tiotropium, Roflumilast, Fluticasone and Dexamethasone were investigated. In addition, the effect of the mentioned treatments was tested in human bronchial epithelial cell culture. **Figure 19A** shows that treatment with Tiotropium or Roflumilast did not increase the amount of virus present in the lungs of mice compared to the control group. In contrast, the amount of H1N1 increased significantly in the lungs of the Fluticasone- or Dexamethasone-treated mice compared to the controls. Consistent with these findings, the viral load also increased significantly *in vitro* upon treatment of H1N1-infected cells with Fluticasone or Dexamethasone but not Tiotropium or Roflumilast (**Figure 19B**).

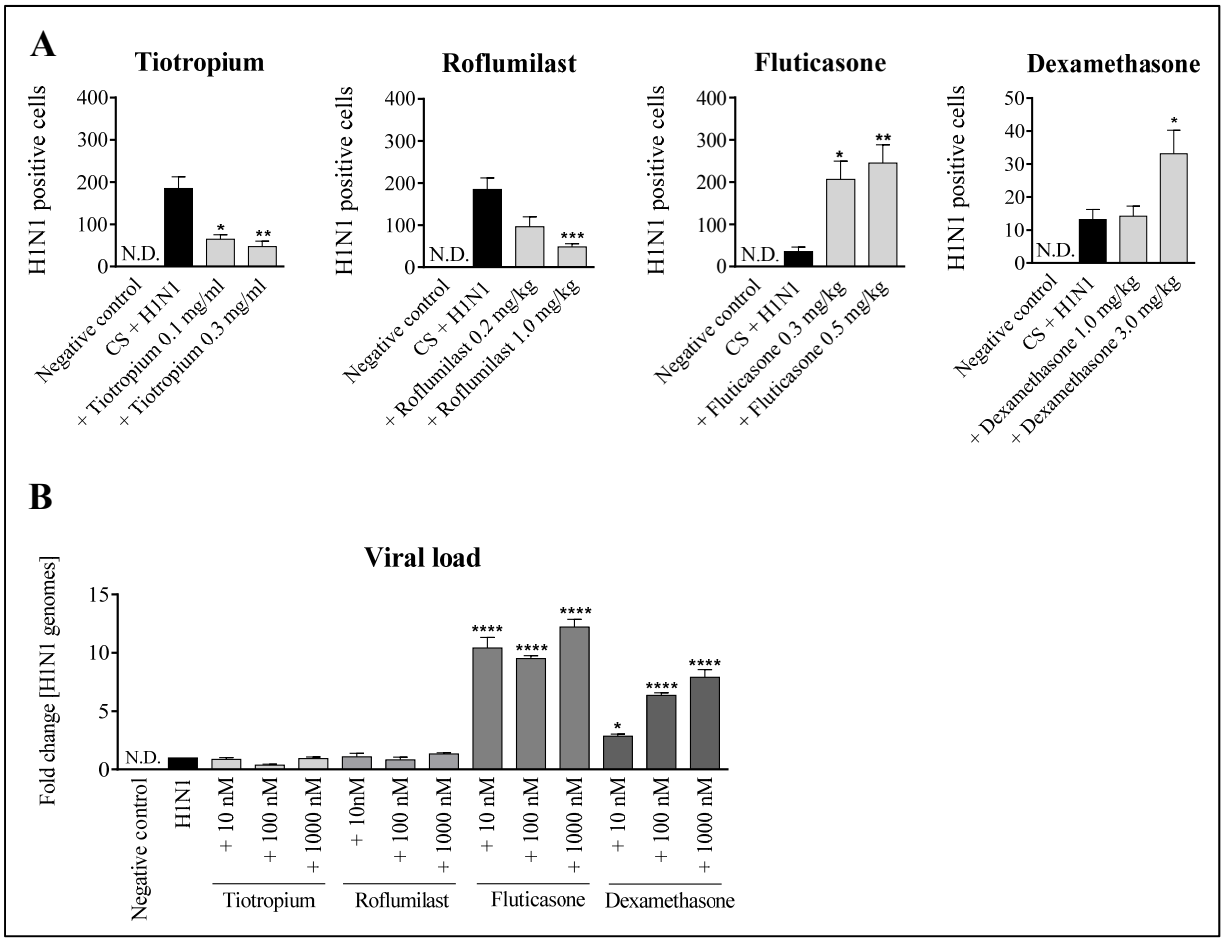

Figure 19: H1N1 virus load in CS-exposed and H1N1-infected mice after treatment with Tiotropium, Fluticasone, Dexamethasone or Roflumilast [206]
(A) Mice were exposed to CS and infected with H1N1 and additionally treated with Tiotropium (0.1 mg/ml or 0.3 mg/ml), Roflumilast (0.2 mg/kg or 1.0 mg/kg), Fluticasone (0.3 mg/kg or 0.5 mg/kg), or Dexamethasone (1.0 mg/kg or 3.0 mg/kg). Shown is the mean ± SEM viral load in lung homogenate of n = 7-8 mice per group measured by immunofocus assay. (B) NCI-H292 cells were infected with H1N1 and treated with Tiotropium, Fluticasone, Dexamethasone or Roflumilast. Changes in virus load were measured in cell lysates using qPCR (Mean values ± SEM of n = 4 wells per group are shown. ****$p < 0.0001$, ***$p < 0.001$, **$p < 0.01$, and *$p < 0.05$ represent significant differences compared with the CS-exposed and H1N1-infected group or the H1N1-infected cells.

3.1.6 H&E stainings of lung sections of the CS/H1N1-exposed mice treated with the different drugs

Figure 20 shows H&E-stained lung sections of the negative control and CS/H1N1-exposed animals which were additionally treated with Tiotropium, Fluticasone or Roflumilast.

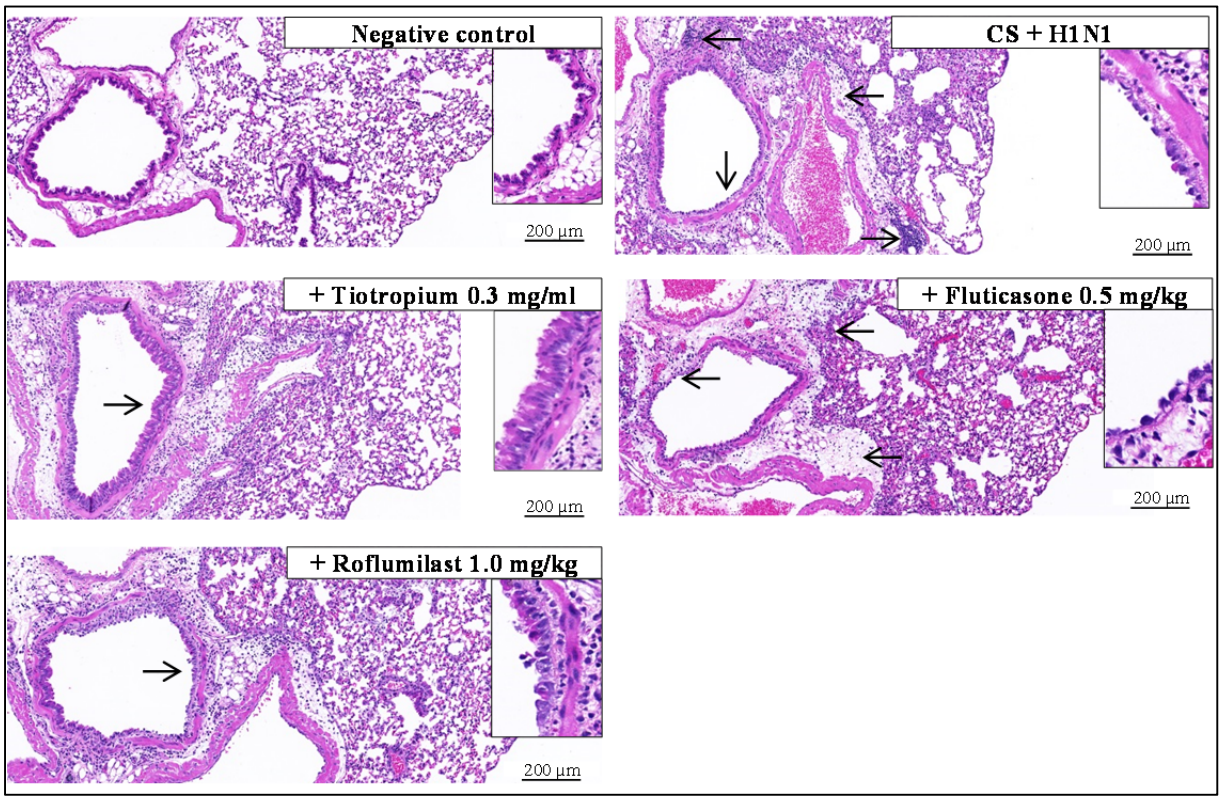

Figure 20: H&E stainings of lung sections of H1N1-infected and CS-exposed mice after treatment with Tiotropium, Fluticasone, or Roflumilast [206]
Mice were exposed to CS and infected with H1N1 and additionally treated with Tiotropium (0.3 mg/ml), Fluticasone (0.5 mg/kg), or Roflumilast (1.0 mg/kg). H&E stainings of lung sections from untreated negative control mice, mice exposed to CS and H1N1, or CS/H1N1-exposed mice which were additionally treated with Tiotropium, Fluticasone, or Roflumilast. Arrows indicate areas of inflammation or structural changes. Lungs of n = 6–8 mice per group were analyzed and representative sections shown.

Negative control mice show normal lung morphology. Lungs of mice which were exposed to CS and infected with H1N1 exhibited peribronchial disseminated inflammation. Upon treatment with 0.5 mg/kg Fluticasone, loss of epithelial cells in the main bronchus was increased. In contrast, integrity of epithelia of the main bronchi in lungs of mice treated with 0.3 mg/ml Tiotropium was less affected. No changes were detectable in lungs of mice treated with 1.0 mg/kg Roflumilast when compared with the lungs of mice of the CS/H1N1 group.

3.1.7 Tiotropium down-regulates choline acetyltransferase and sialic acid synthase expression in CS/H1N1-exposed mice

The impact of Dexamethasone, Fluticasone, Roflumilast and Tiotropium on gene expression of choline acetyltransferase (ChAT) and sialic acid synthase (NANS) were investigated as described in section 2.1.11.

ChAT catalyzes the synthesis of acetylcholine and both are ubiquitously expressed throughout the airways and furthermore are involved in inflammatory processes [213-215]. NANS is an important enzyme for the biosynthesis of sialic acid, a receptor for influenza virus [216, 217]. The expression of both genes was significantly up-regulated in mice challenged with CS and H1N1 (**Figure 21**). Dexamethasone, Fluticasone or Roflumilast treatment had no effect on ChAT or NANS expression. In contrast, a strong and significant down-regulation of ChAT and NANS expression was observed in lung homogenate of mice treated with Tiotropium.

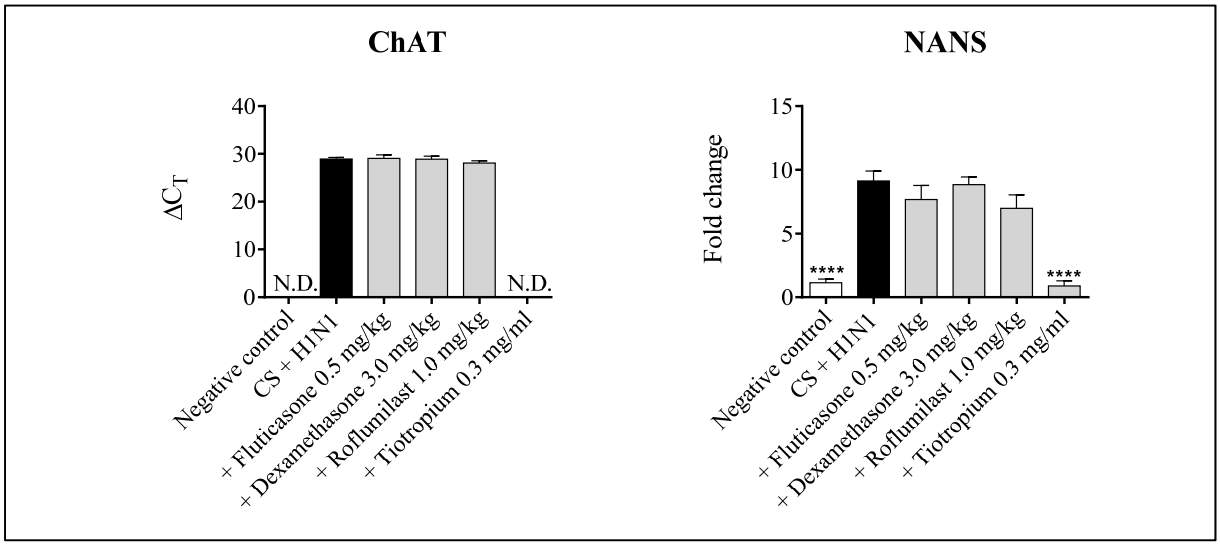

Figure 21: ChAT and NANS expression in CS-exposed and H1N1-infected mice after treatment with Dexamethasone, Fluticasone, Roflumilast, or Tiotropium [206]
Mice were exposed to CS and infected with H1N1 and additionally treated with Dexamethasone (3.0 mg/kg), Fluticasone (0.5 mg/kg), Roflumilast (1.0 mg/kg), or Tiotropium (0.3 mg/ml). Changes in mRNA levels of ChAT and NANS are illustrated by ΔC_T values or as fold change normalized to 18S rRNA. Mean values ± SEM of n = 4–8 animals per group are shown. ****p < 0.0001, ***p < 0.001, **p < 0.01, and *p < 0.05 represent significant differences compared with the CS-exposed and H1N1-infected group.

3.2 Cigarette smoke/RSV exacerbation model

As outlined in section 1.1.6, RSV is expected to be an important trigger of COPD exacerbations. A re-infection protocol was used for the establishment of the CS/RSV model as it yielded a more pronounced exacerbation phenotype compared to a single infection (data not shown). Furthermore, no protective memory response against RSV is generated in humans as well as in mice and re-infections are common (section 2.1.16).

3.2.1 Tiotropium but not Fluticasone or Roflumilast has anti-inflammatory effects in a CS/RSV re-infection model

The anti-inflammatory effects of Tiotropium were investigated in the CS/RSV combination model. For this purpose, mice were exposed to CS and re-infected with the virus as illustrated in **Figure 22A**.

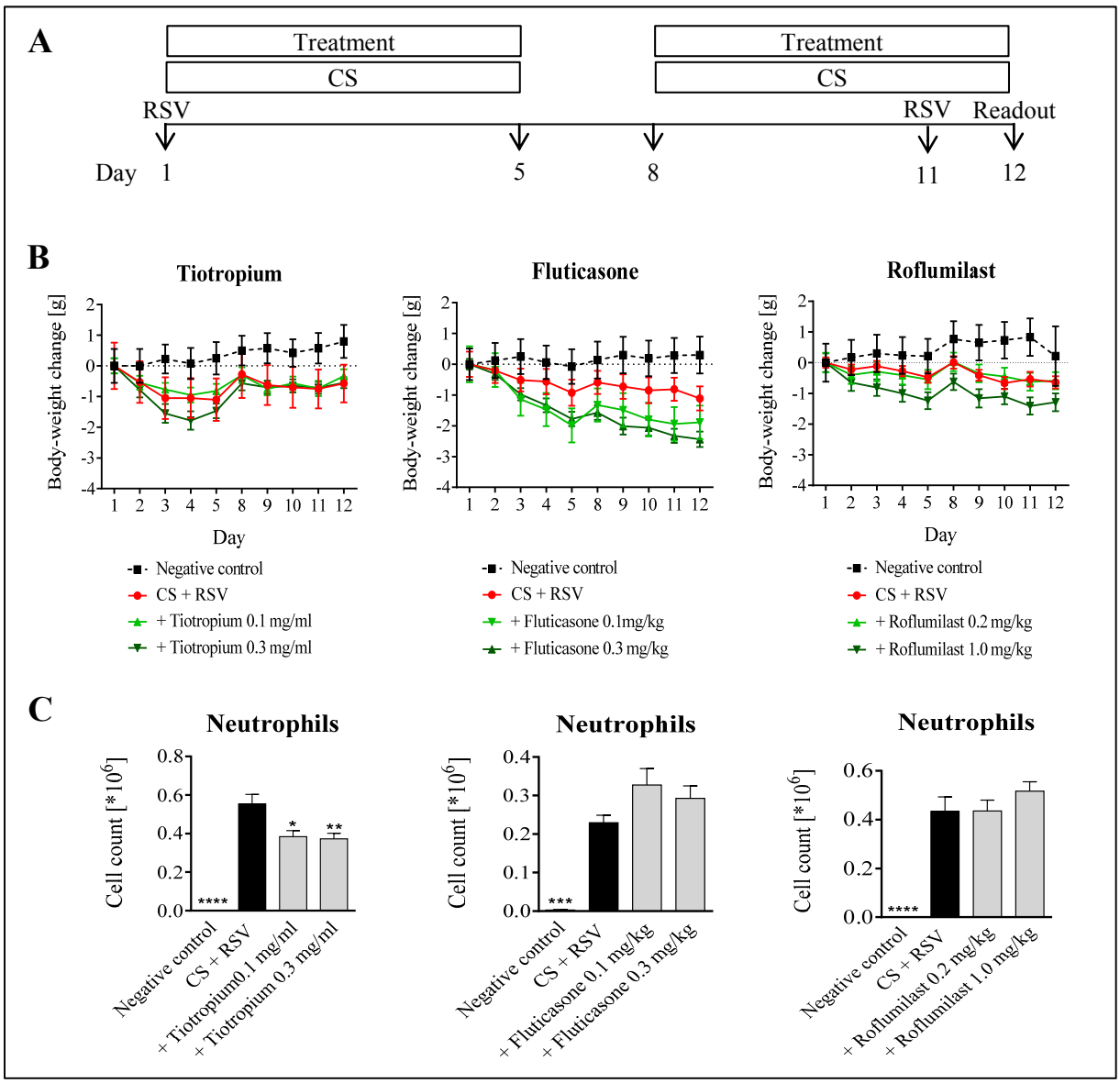

Figure 22: Tiotropium, Fluticasone, and Roflumilast treatment in a CS/RSV re-infection model [206]
(A) Mice were exposed to CS and infected with RSV on day 1 and re-infected with the virus on day 11. CS- and RSV-exposed mice were treated with Tiotropium (0.1 mg/ml or 0.3 mg/ml), Fluticasone (0.1 mg/kg or 0.3 mg/kg), or Roflumilast (0.2 mg/kg or 1.0 mg/kg). (B) Development of body-weight over time and (C) neutrophil numbers in the BAL fluid. Mean values ± SEM of n = 4–8 animals per group are shown. ****$p < 0.0001$, ***$p < 0.001$, **$p < 0.01$, and *$p < 0.05$ represent significant differences compared with the CS-exposed and RSV-infected group.

Administration of Roflumilast and in particular of Fluticasone increased the loss of body-weight in the CS/RSV combination model while Tiotropium did not (**Figure 22B**). Treatment with Tiotropium but not Fluticasone or Roflumilast reduced the neutrophil cell count in BAL

fluid significantly (**Figure 22C**). None of the drugs reduced macrophage numbers (data not shown).

Table 1 shows cytokine levels in lung homogenate of CS/RSV-exposed and drug-treated mice. Tiotropium reduced levels of IL-6, IFN-γ, TNF-α and KC, being significant for IL-6, IFN-γ and TNF-α. Treatment with Fluticasone decreased IFN-γ levels but increased the amount of KC. Roflumilast increased the level of KC without having any effects on the other measured cytokine levels.

Cytokine [pg/ml]	**Negative control**	**Smoke + RSV**	**+ Tiotropium 0.1 mg/ml**	**+ Tiotropium 0.3 mg/ml**
IL-6	20.4 ± 3.1 **	173.9 ± 35.9	128.2 ± 20.9	87.5 ± 10.7 *
KC	99.9 ± 28.0 ***	673.6 ± 61.5	523.0 ± 72.4	499.0 ± 37.9
TNF-α	0.9 ± 0.4 ***	37.1 ± 5.1	21.5 ± 1.8 **	25.0 ± 2.4 *
IL-1β	60.5 ± 13.0 **	500.4 ± 92.9	578.0 ± 52.0	575.5 ± 44.5
IFN-γ	< 3.1	336.1 ± 46.4	169.2 ± 28.8 *	182.6 ± 34.3 *
	Negative control	**Smoke + RSV**	**+ Fluticasone 0.1 mg/kg**	**+ Fluticasone 0.3 mg/kg**
IL-6	< 25.5	47.7 ± 9.8	88.8 ± 21.1	122.4 ± 55.0
KC	154.0 ± 19.2 ****	720.6 ± 39.9	1932.1 ± 134.3 ***	1462.0 ± 169.2 *
TNF-α	4.0 ± 1.1 ****	24.7 ± 1.4	27.0 ± 2.1	22.9 ± 2.1
IL-1β	51.4 ± 10.8 ****	532.4 ± 40.7	1184.6 ± 169.3 ***	811.9 ± 94.7
IFN-γ	0.3 ± 0.1 ***	81.8 ± 10.0	53.4 ± 6.9 *	39.2 ± 5.7 **
	Negative control	**Smoke + RSV**	**+ Roflumilast 0.2 mg/kg**	**+ Roflumilast 1.0 mg/kg**
IL-6	10.5 ± 3.6 ***	72.0 ± 10.7	63.1 ± 25.3	44.0 ± 6.2
KC	116.9 ± 35.2 **	344.7 ± 46.4	459.9 ± 30.7	592.9 ± 36.7 ***
TNF-α	< 3.1	37.4 ± 7.7	33.9 ± 5.9	31.1 ± 4.3
IL-1β	66.4 ± 4.9 ***	581.2 ± 86.6	1015.3 ± 141.4 *	569.5 ± 55.5
IFN-γ	0.6 ± 0.0 **	118.6 ± 24.9	54.9 ± 16.6	75.0 ± 16.1

Table 1: Cytokine levels in the lungs of CS/RSV-exposed mice after treatment with Tiotropium, Fluticasone, and Roflumilast [206]
Mice were exposed to CS, infected and re-infected with RSV, and treated with Tiotropium, Fluticasone, or Roflumilast. Cytokine levels in lung homogenate. Mean values ± SEM of n = 4–8 animals per treatment group and n = 4 for negative control group are shown.

3.2.2 Fluticasone treatment increases the amount of RSV *in vivo* and *in vitro*

Consistent with previous findings for H1N1, treatment with Fluticasone increased the amount of virus in the airways of CS-exposed and RSV-infected mice compared to controls (**Figure 23A**). RSV load in human bronchial epithelial cell culture was also significantly elevated upon treatment with Fluticasone. In contrast, Tiotropium and Roflumilast treatment had no effect on the amount of RSV load in the CS/RSV-exposed mice and NCI-H292 cell culture (**Figure 23B**).

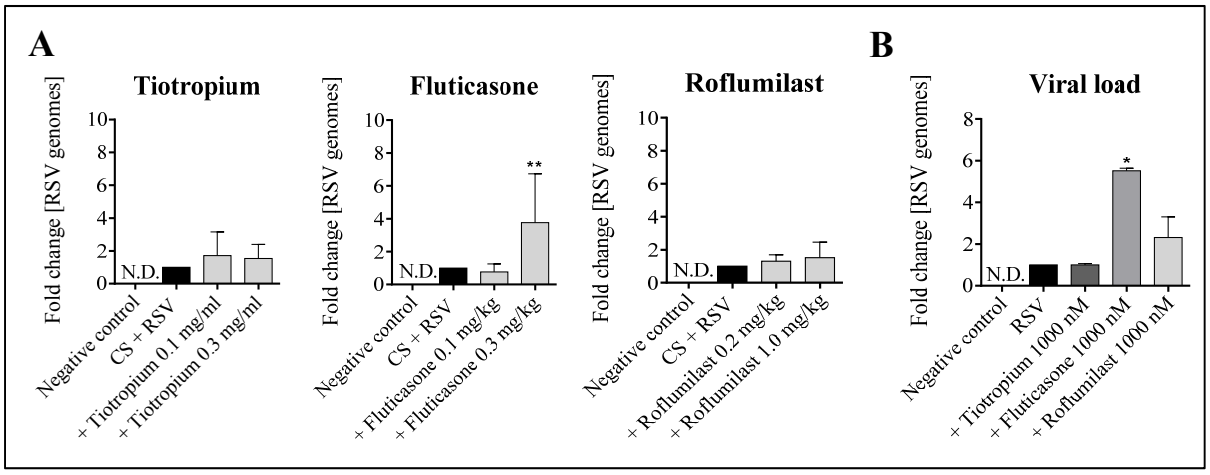

Figure 23: Amount of RSV *in vivo* and *in vitro* [206]
Mice were exposed to CS and infected with RSV on day 1 and re-infected with the virus on day 11. They were treated with Tiotropium (0.1 mg/ml or 0.3 mg/ml), Fluticasone (0.1 mg/kg or 0.3 mg/kg), or Roflumilast (0.2 mg/kg or 1.0 mg/kg). (A) The viral load in lung homogenate. Mean values ± SEM from n = 4–8 animals per group are shown. (B) NCI-H292 cells were infected with RSV and treated with 10, 100, or 1000 nM Tiotropium, Fluticasone, or Roflumilast. The amount of virus was measured in cell lysates. Mean values ± SEM of n = 4 wells are shown. ****p < 0.0001, ***p < 0.001, **p < 0.01, and *p < 0.05 represent significant differences compared with the CS-exposed and RSV-infected group or the RSV-infected cells.

3.3 The role of IL-1α and IL-1β in combined cigarette smoke/H1N1-induced airway inflammation

The pro-inflammatory IL-1 family members IL-1α and IL-1β are increased in COPD patients and might contribute to disease pathology (section 1.1.4). The individual or combined inhibition of IL-1α, IL-1β or blockade of the IL-1R1 by respective Abs was investigated in CS-exposed and H1N1-infected BALB/c mice. In order to determine doses for each Ab that result in high target occupancy in the lung *in vivo*, mechanistic target engagement models were established as described in material and methods. Doses were considered suitable when using ≥ 100 µg anti-IL-1α Ab ≥ 300 µg anti-IL-1β Ab, or ≥ 300 µg anti-IL-1R1 Ab (data not shown).

3.3.1 Anti-IL-1α but not anti-IL-1β treatment reduces inflammatory cell numbers in BAL fluid

Based on the target engagement results, CS/H1N1-exposed mice were treated with Abs against IL-1α (200 µg/mouse) or IL-1β (300 µg/mouse). **Figure 24A** shows the experimental scheme. Ab treatment had no effect on the development of body-weight (**Figure 24B**).

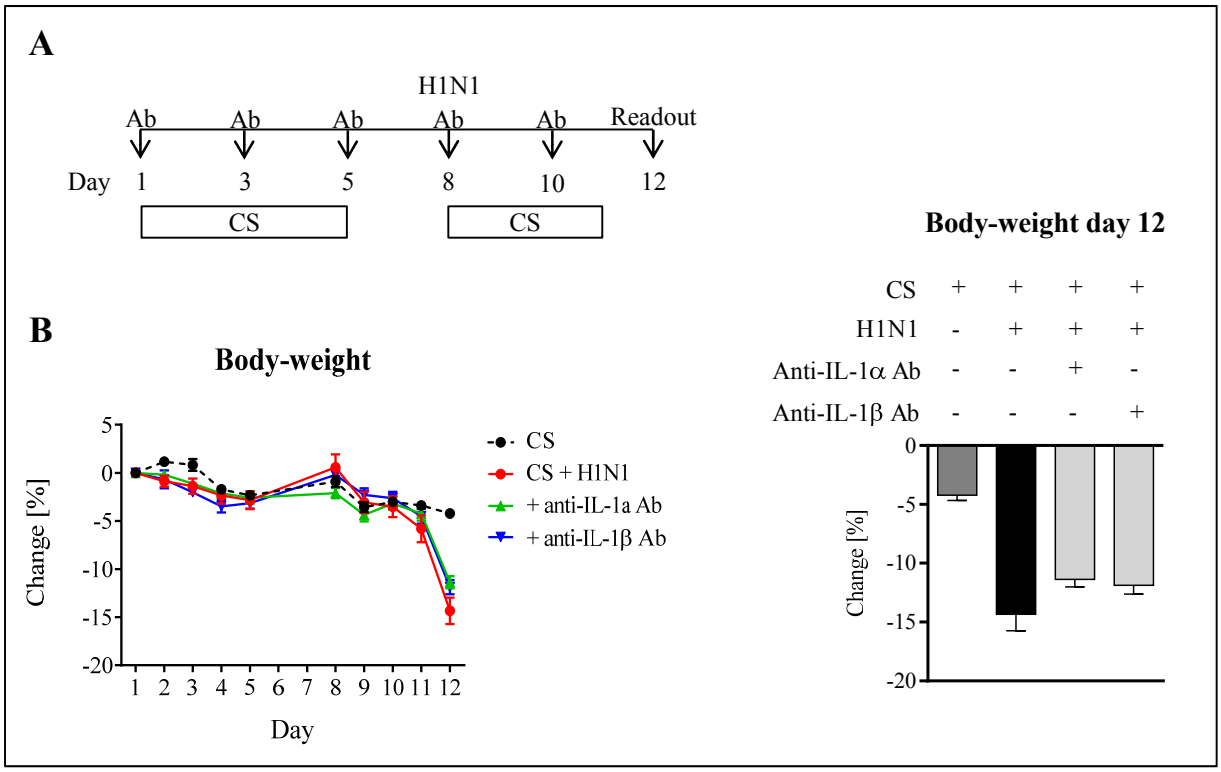

Figure 24: Treatment of CS-exposed and H1N1-infected mice with anti-IL-1α or anti-IL-1β Abs
(A) Mice were exposed to CS for a total of nine days and infected with H1N1 on day 8. Every second or third day, respective mice were treated with Abs targeting IL-1α or IL-1β and adjusted with isotype control Abs. (B) Body-weight loss as time course and as % change at day 12. Mean values ± SEM of n = 7-8 mice are shown. ****p < 0.0001, ***p < 0.001, **p < 0.01, *p < 0.05 represent significant differences compared to the CS/H1N1 group.

Neutralization of IL-1β failed to reduce the loss of body-weight and the total cell, neutrophil, or macrophage numbers in BAL fluid significantly (**Figure 25**). In contrast, neutralization of IL-1α resulted in significantly reduced levels of total cells (-37.4%), neutrophils (-34.4%) and macrophages (-40.8%).

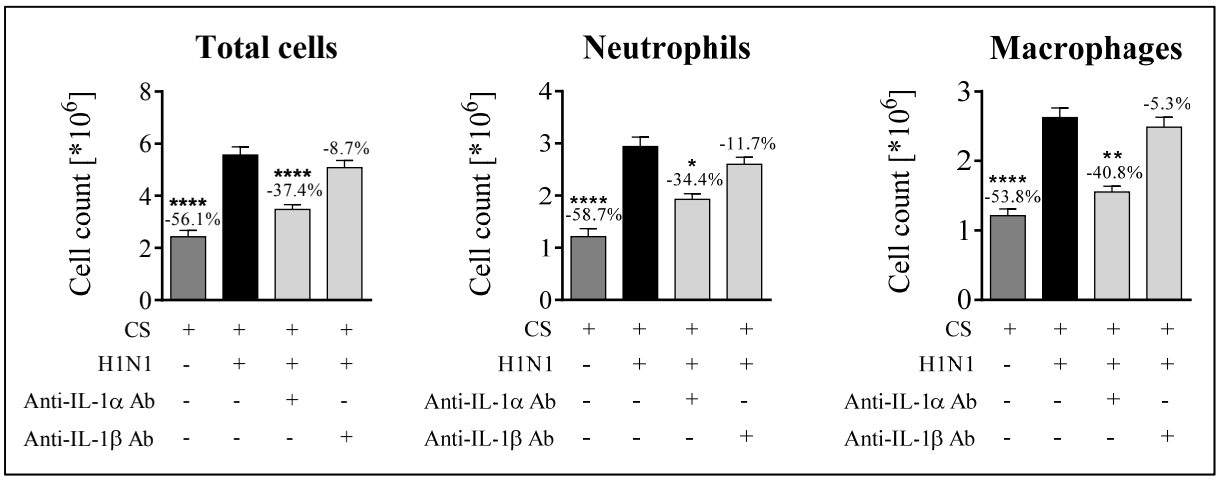

Figure 25: Treatment of CS-exposed and H1N1-infected mice with anti-IL-1α or anti-IL-1β Abs
Mice were exposed to CS for a total of nine days and infected with H1N1. Every second or third day, respective mice were treated with Abs targeting IL-1α or IL-1β and adjusted with isotype control Abs. Total cell, neutrophil and macrophage counts in BAL fluid. Mean values ± SEM of n = 7-8 mice are shown. ****p < 0.0001, ***p < 0.001, **p < 0.01, *p < 0.05 represent significant differences compared to the CS/H1N1 group.

Previously, commercially available Abs against IL-1α and IL-1β have been explored in CS models [85, 86]. Therefore, the effects of IL-1α and IL-1β neutralization were also investigated head-to-head in a one-week CS-model. As in the CS/H1N1 model, neutralization of IL-1α was able to reduce inflammatory cell influx significantly, whereas neutralization of IL-1β had no effect (data not shown).

3.3.2 IL-1α antagonization reduces KC in lung homogenate of CS/H1N1-challenged mice

Pro-inflammatory cytokine and chemokine levels were measured in lung homogenate of CS/H1N1-challenged mice treated with Abs against IL-1α (200 µg/mouse) or IL-1β (300 µg/mouse). The results are displayed in **Table 2**. The murine CXCL8 homologue KC was reduced significantly upon inhibition of IL-1α (49.7%) while administration of the anti-IL-1β had no effect. Levels of IL-6, TNF-α, MCP-1, MIP-1α or MIP-1β were not reduced by individual neutralization of IL-1α or IL-1β.

Group	Amount ± SEM [pg/ml]	% Change	Amount ± SEM [pg/ml]	% Change
	KC		IL-6	
CS	444.0 ± 24.7	- 82.3 ****	46.3 ± 9.4	- 99.5 ****
CS + H1N1	2502.6 ± 120.2		9174.4 ± 571.2	
Anti-IL-1α	1259.5 ± 107.9	- 49.7 ****	11423.6 ± 1093.0	+ 24.5
Anti-IL-1β	2624.9 ± 131.4	+ 4.9	7386.4 ± 720.3	- 19.5
	TNF-α		MCP-1	
CS	35.4 ± 3.5	- 89.8 ****	258.1 ± 18.4	- 93.9 ****
CS + H1N1	347.3 ± 16.1		4246.9 ± 193.9	
Anti-IL-1α	320.5 ± 24.7	- 7.7	4570.2 ± 399.1	+ 7.6
Anti-IL-1β	392.5 ± 22.6	+ 13.0	3732.9 ± 227.6	- 12.1
	MIP-1α		MIP-1β	
CS	1215.2 ± 115.4	- 85.3 ****	1273.3 ± 104.4	- 93.9 ****
CS + H1N1	8258.0 ± 517.1		20960.6 ± 1602.0	
Anti-IL-1α	15275.6 ± 2586.0	+ 85.0 ***	19926.7 ± 1907.0	- 4.9
Anti-IL-1β	9059.6 ± 595.0	+ 9.7	22310.5 ± 1135.0	+ 6.4

Table 2: Cytokine levels in the lung homogenate of CS/H1N1-exposed mice after treatment with individual anti-IL-1α or anti-IL-1β Abs
Mice were treated according to the experimental scheme in Figure 24. Cytokine levels in lung homogenate. Mean values ± SEM of n = 7-8 mice are shown. ****p < 0.0001, ***p < 0.001, **p < 0.01, *p < 0.05 represent significant differences compared to the CS/H1N1 group.

3.3.3 Anti-IL-1α but not anti-IL-1β treatment has anti-inflammatory activity in H1N1-infected air-liquid-interface cell culture

To investigate the effects of anti-IL-1α or anti-IL-1β Ab treatment in primary human bronchial epithelial cells, an ALI cell culture was used according to section 2.2.2. This system is considered suited to mimick aspects of human airway epithelia, including ciliated, basal and

secretory cells [218]. **Figure 26A** illustrates the experimental scheme. ALI cells were infected with H1N1 and treated with the Abs. Upon infection, the TEER values dropped significantly in H1N1-infected cells and increased TNF-α and IL-6 levels were detectable in supernatant (**Figure 26B**).

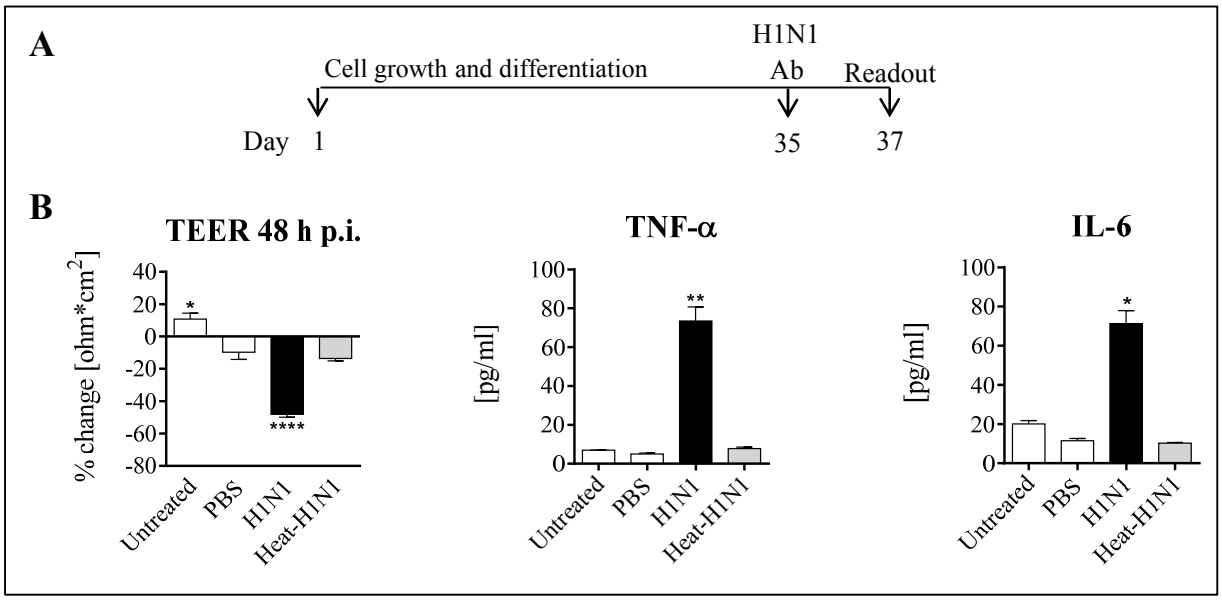

Figure 26: H1N1 infection of primary human bronchial epithelial cells
(A) Experimental scheme of H1N1 infection of primary human bronchial epithelial cells in an air-liquid-interface setup. (B) TEER and levels of TNF-α and IL-6 in supernatant. Mean values ± SEM of n = 4 wells are shown. ****p < 0.0001, ***p < 0.001, **p < 0.01, *p < 0.05 represent significant differences compared to the PBS group.

In line with the *in vivo* studies, treatment with the anti-IL-1α Abs but not with the anti-IL-1β Abs had anti-inflammatory activity and reduced levels of TNF-α and IL-6 significantly (**Figure 27 A, B**). No effects of treatments were observed on TEER values (data not shown).

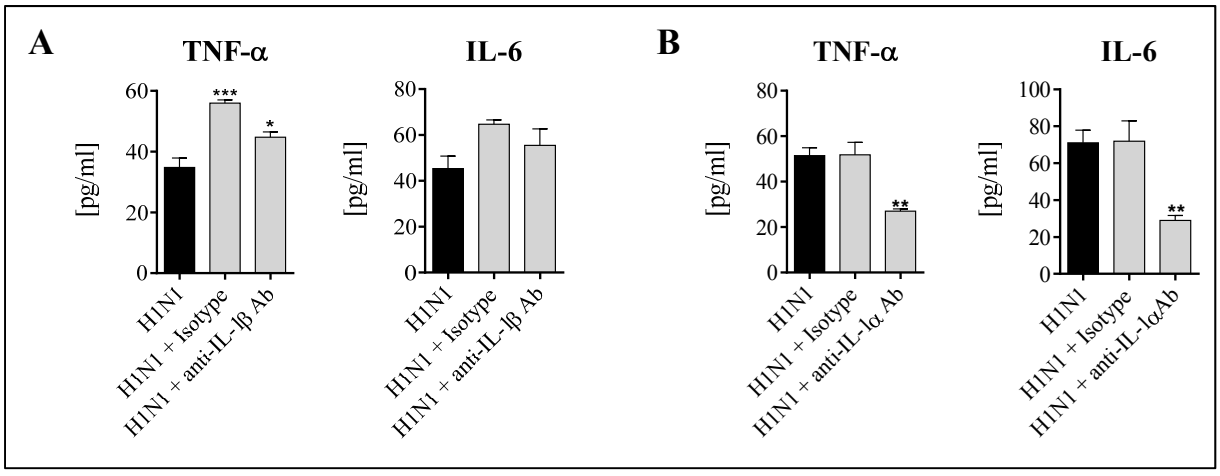

Figure 27: Treatment of primary human bronchial epithelial cells with anti-IL-1α and anti-IL-1β Abs
Human primary bronchial epithelial cells were grown under air-liquid-interface conditions, infected with H1N1 and treated with Abs. Cytokine levels in supernatant after (A) anti-IL-1α or (B) anti-IL-1β Ab treatment. Mean values ± SEM of n = 4 wells are shown. ****p < 0.0001, ***p < 0.001, **p < 0.01, *p < 0.05 represent significant differences compared to the H1N1 group.

3.3.4 IL-1α/IL-1β neutralization is superior in reducing inflammatory cells and the loss of body-weight compared to blockade of IL-1R1 in CS/H1N1-challenged mice

The effect of combined anti-IL-1α/anti-IL-1β treatment on CS/H1N1-driven inflammatory cell influx in BAL fluid was investigated. Furthermore, mediator neutralization was compared to the effects of IL-1R1 blockade. The experimental scheme is shown in **Figure 28A**.

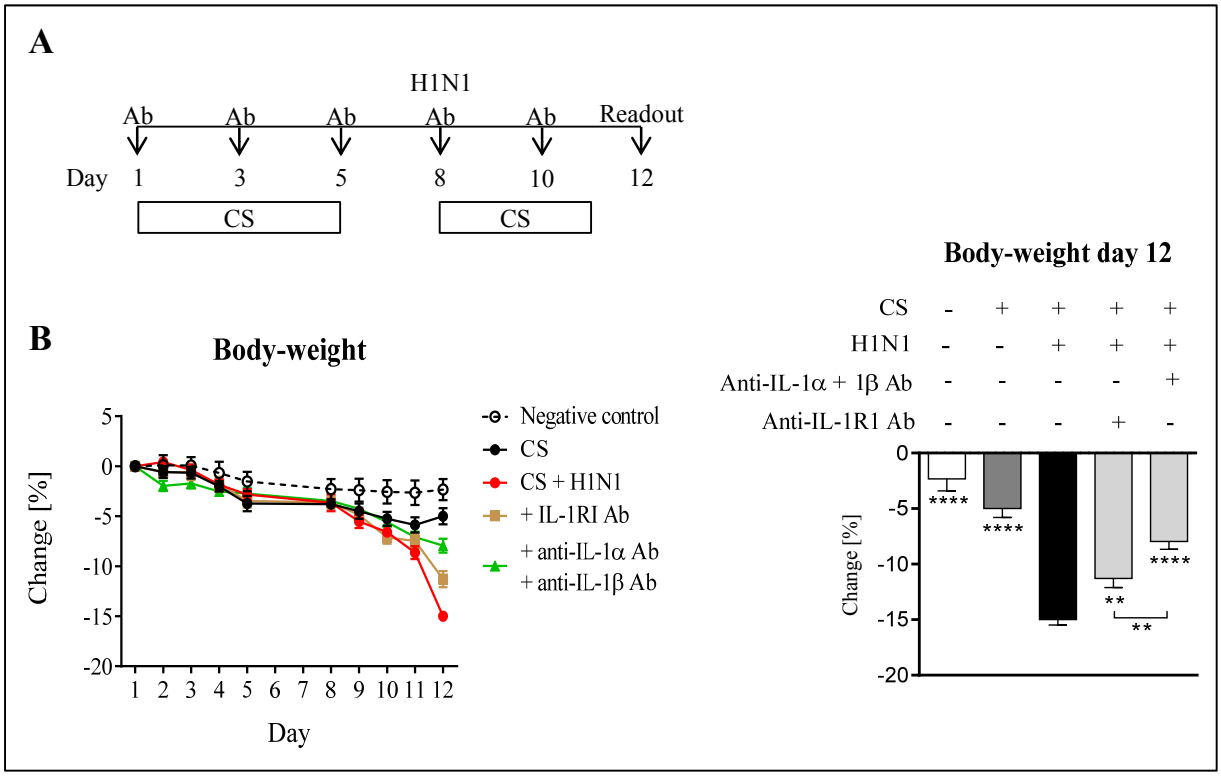

Figure 28: Treatment of CS-exposed and H1N1-infected mice with combined anti-IL-1α/anti-IL-1β Abs or anti-IL-1R1 Abs
(A) Mice were exposed to CS for a total of nine days and infected with H1N1 on day 8. They were treated with Abs targeting IL-1R1 or IL-1α and IL-1β. (B) Body-weight loss is displayed as time course and as % change at day 12. Mean values ± SEM of n = 7-8 mice are shown. ****p < 0.0001, ***p < 0.001, **p < 0.01, *p < 0.05 represent significant differences compared to the CS/H1N1 group.

IL-1α/IL-1β neutralization resulted in a strong and significant reduction of CS/H1N1-induced increase of inflammatory cells. Total cell numbers were reduced by 68.3%, neutrophil counts by 75.6% and macrophage counts by 59.6%. Blockade of the IL-1R1 decreased counts of total cells (-49.6%), neutrophils (-53.4%) and macrophages (-45.2%) (**Figure 29**). The reduction of inflammatory cell counts was less pronounced upon antagonism of IL-1R1 compared to combined neutralization of its soluble ligands IL-1α/IL-1β. The changes in inflammatory cells were also reflected by changes in the loss of body-weight (**Figure 28B**). All treatments reduced the model-induced loss of body-weight significantly. As seen for inflammatory cells, combined neutralization of both IL-1α/IL-1β revealed a stronger effect compared to blockade of the IL-1R1. The effect of additional antagonization of IL-18 on top of IL-1α/IL-1β or

IL-1R1 blockade was tested. No significant further suppressive effect on cell numbers was observed (data not shown).

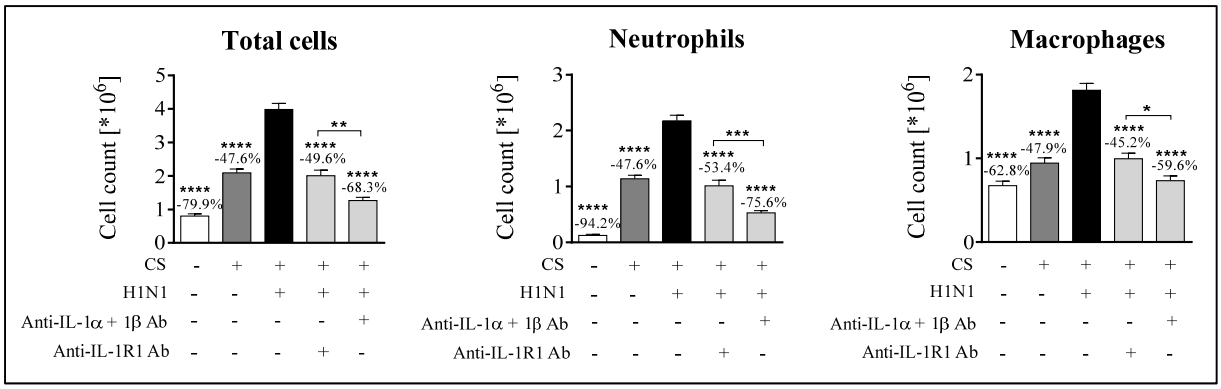

Figure 29: Treatment of CS-exposed and H1N1-infected mice with combined anti-IL-1α/anti-IL-1β Abs or anti-IL-1R1 Abs

Mice were exposed to CS for a total of nine days and infected with H1N1 on day 8. Mice were treated with combinations of Abs targeting IL-1α/IL-1β or IL-1R1 and adjusted with isotype control Abs. Total cells, neutrophils and macrophages in BAL fluid. Mean values ± SEM of n = 7-8 mice are shown. ****p < 0.0001, ***p < 0.001, **p < 0.01, *p < 0.05 represent significant differences compared to the CS/H1N1 group.

3.3.5 Combined IL-1α/IL-1β neutralization reduces levels of KC, IL-6, TNF-α, MCP-1, MIP-1α or MIP-1β in lung homogenate of CS/H1N1-challenged mice

Group	Amount ± SEM [pg/ml]	% Change	Amount ± SEM [pg/ml]	% Change
	KC		IL-6	
Neg. control	72.0 ± 5.2	- 97.8 ****	8.9 ± 0.6	- 99.9 ****
CS	426.8 ± 26.3	- 87.0 ****	29.8 ± 1.8	- 99.8 ****
CS + H1N1	3272.0 ± 215.5		15549.0 ± 1341.0	
Anti-IL- 1R1	839.2 ± 131.2	- 74.35	7299.8 ± 317.6	- 53.1
Anti-IL- 1α+1β	275.4 ± 19.5	- 91.58 ***	4176.3 ± 282.6	- 73.1 ***
	TNF-α		MCP-1	
Neg. control	11.1 ± 0.5	- 97.3 ****	41.2 ± 2.0	- 99.1 ****
CS	29.0 ± 0.8	- 93.0 ****	216.1 ± 17.2	- 95.3 ****
CS + H1N1	416.3 ± 23.2		4597.0 ± 344.0	
Anti-IL- 1R1	398.7 ± 21.4	- 4.2	4140.5 ± 201.0	- 9.9
Anti-IL- 1α+1β	268.9 ± 20.0	- 35.4 ****	2844.4 ± 328.9	- 38.1 ***
	MIP-1α		MIP-1β	
Neg. control	1368.1 ± 161.5	- 81.6 ****	595.1 ± 70.0	- 97.0 ****
CS	1221.8 ± 81.6	- 83.6 ****	854.7 ± 74.1	- 95.7 ****
CS + H1N1	7449.0 ± 533.9		19900.2 ± 1908.0	
Anti-IL- 1R1	7720.6 ± 613.6	+ 3.6	16430.6 ± 1431.0	- 17.4
Anti-IL- 1α+1β	4750.2 ± 427.0	- 36.2 **	12600.5 ± 1564.0	- 36.7 *

Table 3: Cytokine levels in the lung homogenate of CS/H1N1-exposed mice after treatment with combined anti-IL-1α/anti-IL-1β or anti-IL-1R1 Abs

Mice were treated according to the experimental scheme in Figure 28. Cytokine levels were assessed in lung homogenate. Mean values ± SEM of n = 7-8 mice are shown. ****p < 0.0001, ***p < 0.001, **p < 0.01, *p < 0.05 represent significant differences compared to the CS/H1N1 group.

Table 3 shows cytokine/chemokine levels measured in lung homogenate of CS/H1N1-challenged mice after neutralization of IL-1α/IL-1β or blockade of IL-1R1. Treatment with the Ab combination had strong effects and reduced levels of KC, IL-6, TNF-α, MCP-1, MIP-1α or MIP-1β significantly. Blockade of the IL-1R1 resulted in reduced cytokine levels of KC and IL-6. When testing the effect of antagonization of IL-18 on top of IL-1α/IL-1β or IL-1R1 blockade, additional suppressive effects on some parameters such as MCP-1 were observed (data not shown).

3.3.6 Effects of IL-1α, IL-1β neutralization on the viral load, MUC5 A/C and ICAM-1 expression

Beyond the effects on inflammatory mediators, the effect of treatment of CS/H1N1-exposed mice with single or combined anti-IL-1α, anti-IL-1β Abs or Abs blocking the IL-1R1 on the viral load was investigated using qPCR. Furthermore, MUC5 A/C and ICAM-1 mRNA expression in the lungs was investigated. Increased MUC5 A/C gene expression is associated with mucus production in the airways of COPD patients (section 1.1.3). ICAM-1 is an important receptor in the airways and acts as receptor for NTHi (section 1.1.6). **Figures 30A and 30B** illustrate the ΔC_T-values for the experiments according to section 2.1.11. In all cases, viral genomes were detectable in the infected animals. A significant reduced viral load was observed in the combined anti-IL-1α/IL-1β Ab-treated mice, indicated by a higher ΔC_T-value of 24.4 compared to the control animals with a ΔC_T-value of 17.6. MUC5 A/C was up-regulated in CS/H1N1-challenged mice. Ab treatment showed a tendency to reduce MUC5 A/C expression. However, the effects were statistically not significant. A significant up-regulation in ICAM-1 expression was observed after CS exposure that was further enhanced by additional infection with H1N1. The group treated with the anti-IL-1α/IL-1β Abs showed significant lower expression levels of ICAM-1, whereas individual anti-IL-1α, anti-IL-1β or anti-IL-1R1 Ab treatment had no effect.

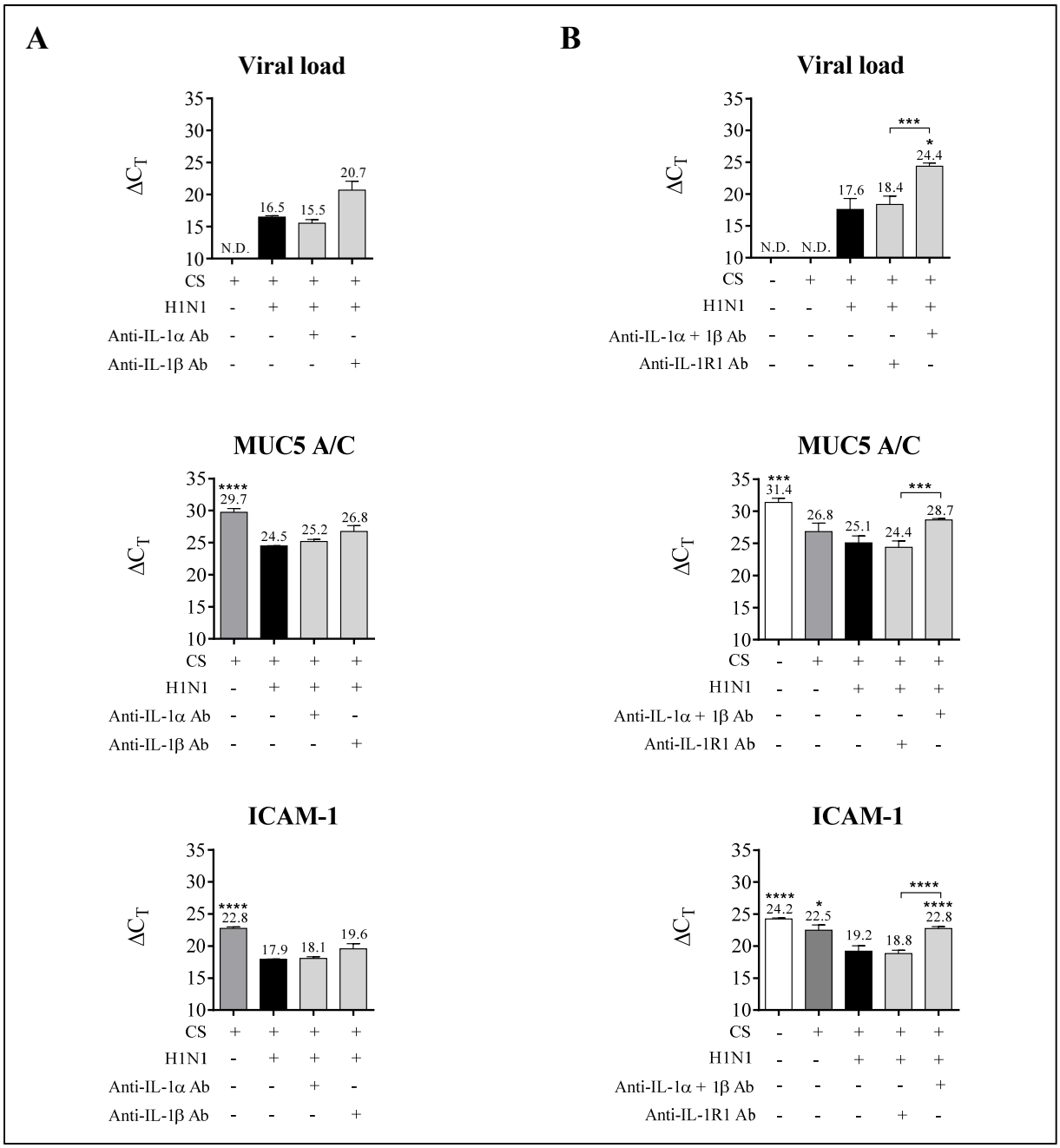

Figure 30: Detection of H1N1 and gene expression analysis of ICAM-1 and MUC5 A/C
Mice were exposed to CS for a total of nine days and infected with H1N1 on day 8. Mice were treated with individual (A) or combined (B) Abs as described before. qPCR was used for detection of viral genomes and for gene expression analysis of ICAM-1 and MUC5 A/C as described in material and methods. ΔC_T-values are illustrated. Mean values ± SEM of n = 7-8 mice are shown. ****$p < 0.0001$, ***$p < 0.001$, **$p < 0.01$, *$p < 0.05$ represent significant differences compared to the CS/H1N1 group.

3.4 Cigarette smoke/NTHi exacerbation model

Besides viral infections, also bacteria are expected to play a pivotal role in triggering exacerbations of COPD in patients. NTHi is considered to be one of the most important triggers of COPD exacerbations in patients (section 1.1.6). Thus, the bacteria were used for the infection of CS-exposed mice to mimic aspects of a bacterial-induced exacerbation in the animals.

3.4.1 CS/NTHi model establishment

In order to determine an appropriate infection dose of NTHi to induce significant pulmonary inflammation in mice, dose-response (data not shown) and time-course experiments were performed. Moreover, the inflammatory response was investigated and compared in BALB/c and C57BL/6 mice. $5x10^6$ CFU were found optimal to induce pulmonary inflammation in mice while still being well tolerated.

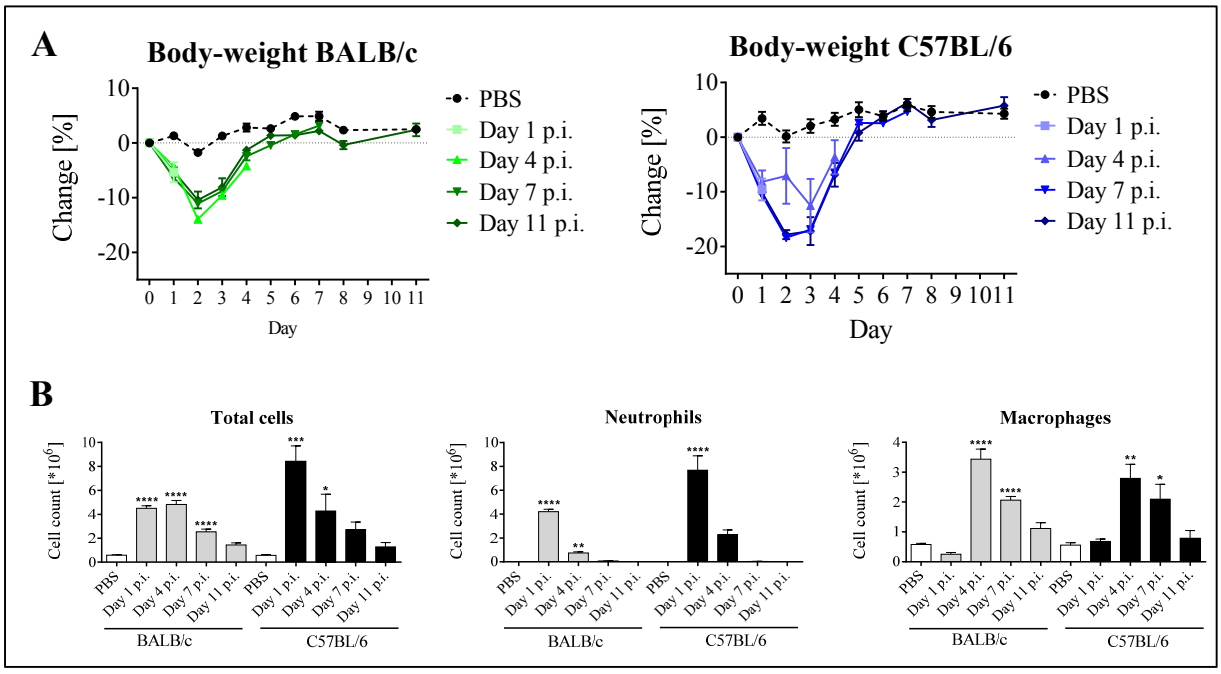

Figure 31: NTHi infection time course in BALB/c and C57BL/6 mice
BALB/c or C57BL/6 mice were infected with NTHi. (A) Development of body-weight. (B) Total, neutrophil and macrophage cell counts in BAL fluid on day 1, 4, 7, 11 p.i. Mean values ± SEM of n = 4 mice are shown. ****p < 0.0001, ***p < 0.001, **p < 0.01, *p < 0.05 represent significant differences compared to the PBS group.

As shown in **Figure 31A**, infection with $5x10^6$ CFU NTHi induced a strong loss of body-weight in both mouse strains peaking on day 2 post infection (p.i). Neutrophil counts and levels of IFN-γ, MCP-1, TNF-α, IL-6, KC and IL-17 peaked on day 1 p.i. (**Figure 31B and Figure 32A**). Plated BAL fluid samples revealed that NTHi was cleared rapidly from the lungs of mice. Replication competent NTHi was detectable only in BAL fluid samples 1 day

p.i. (**Figure 32B**). Notably, most cytokine signal-to-background ratios and the NTHi load were larger/higher in BALB/c mice when compared to C57BL/6 mice.

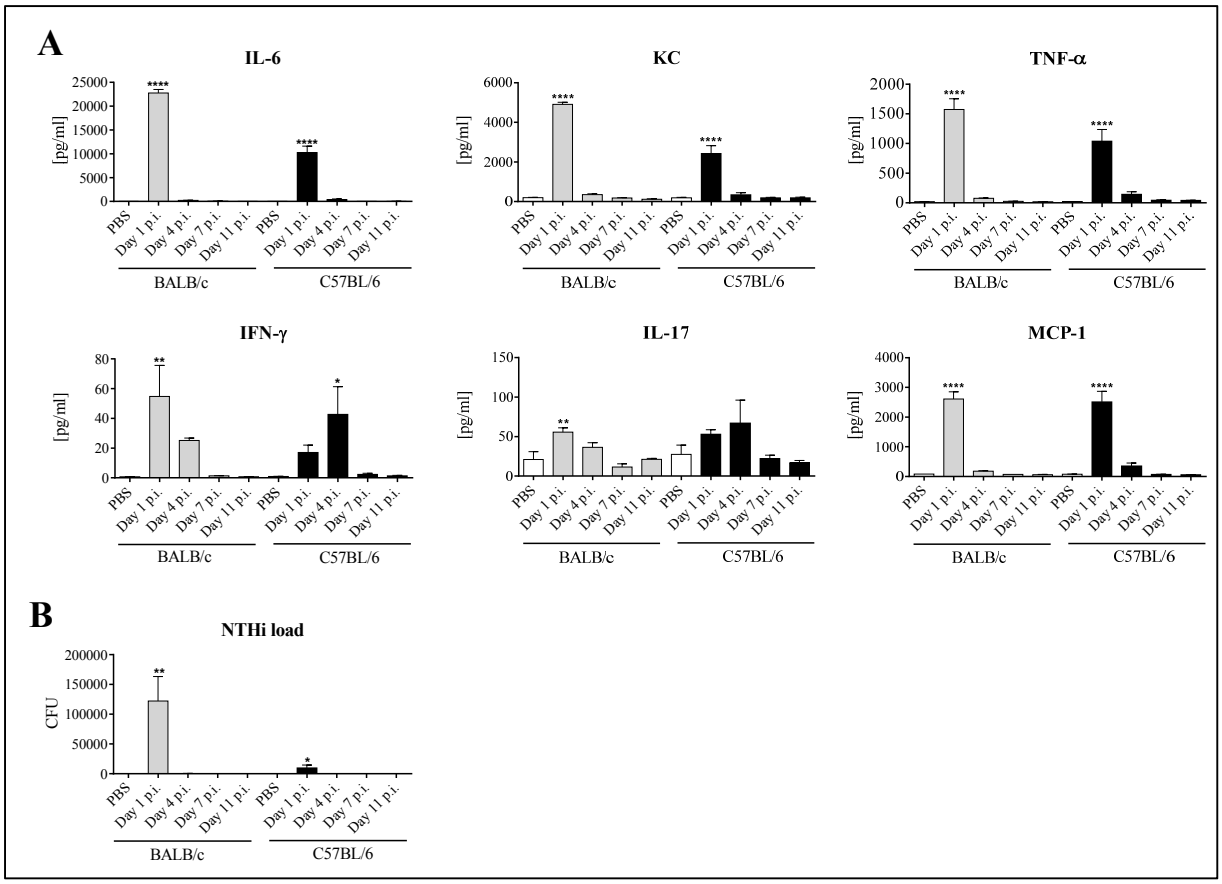

Figure 32: NTHi infection time course of BALB/c and C57BL/6 mice
BALB/c or C57BL/6 mice were infected with NTHi. (A) Cytokine levels in lung homogenate. (B) The NTHi load in BAL fluid. Mean values ± SEM of n = 4 mice are shown. ****p < 0.0001, ***p < 0.001, **p < 0.01, *p < 0.05 represent significant differences compared to the PBS group.

3.4.2 Infection of CS-exposed mice with NTHi exacerbates pulmonary inflammation

Based on the dose-response and time-course experiments, BALB/c mice were exposed to CS and infected with $5x10^6$ CFU NTHi or HK-NTHi 1 day prior to the readout as illustrated in **Figure 33A**. Different infection doses were investigated in CS-exposed BALB/c mice (data not shown). $5x10^6$ CFU were considered to be the optimal infection dose for obtaining an exacerbation phenotype. Individual NTHi infection or CS-exposure significantly increased total cell counts in BAL fluid of the animals (**Figure 33B**). Upon NTHi infection of CS-exposed mice total cell, neutrophil and macrophage numbers were significantly elevated compared to the individual stimuli. Infection with HK-NTHi-induced significant accumulation of total cells in BAL fluid. However, infection of CS-exposed mice failed to exacerbate total cells, macrophages or neutrophils.

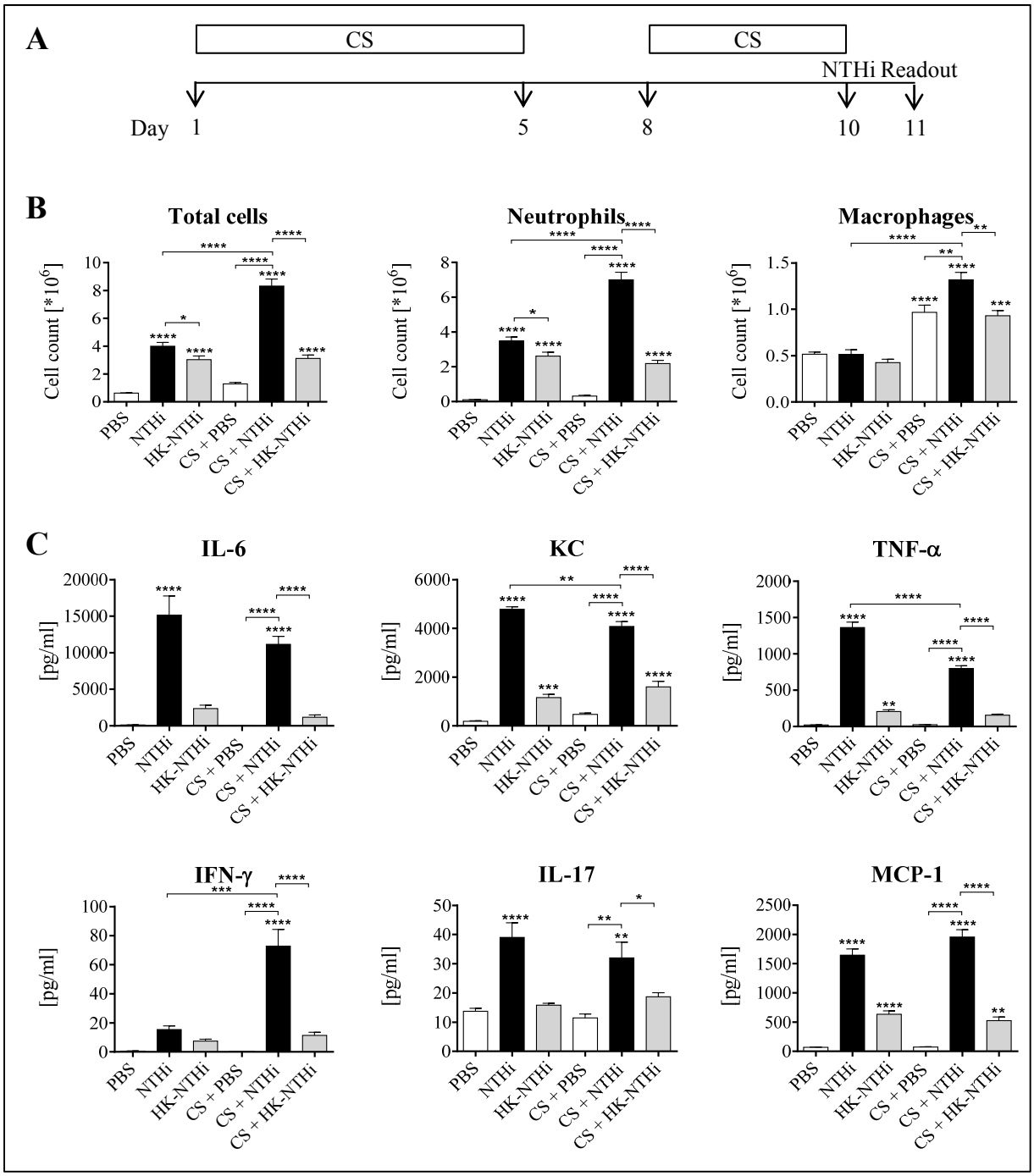

Figure 33: Infection of CS-exposed mice with NTHi or HK-NTHi
(A) Mice were exposed to CS for eight days over a period of two weeks and infected with NTHi or HK-NTHi on day 10, one day prior to readout. (B) Total, neutrophil and macrophage cell counts in BAL fluid and (C) levels of cytokines in lung homogenate. Mean values ± SEM of n = 6-8 mice are shown. ****p < 0.0001, ***p < 0.001, **p < 0.01, *p < 0.05 represent significant differences compared to the PBS group and between the groups.

Figure 33C shows that NTHi infection of CS-exposed mice exacerbated levels of IFN-γ and MCP-1 in lung homogenate. As observed for cell counts, infection of CS-exposed mice with HK-NTHi did not exacerbate any of these mediators. Levels of TNF-α, IL-6, KC and IL-17 were not increased additionally in CS/NTHi-challenged mice in comparison to mice which were only infected with NTHi.

3.4.3 NTHi-induced pulmonary inflammation is partly mediated by TLR4

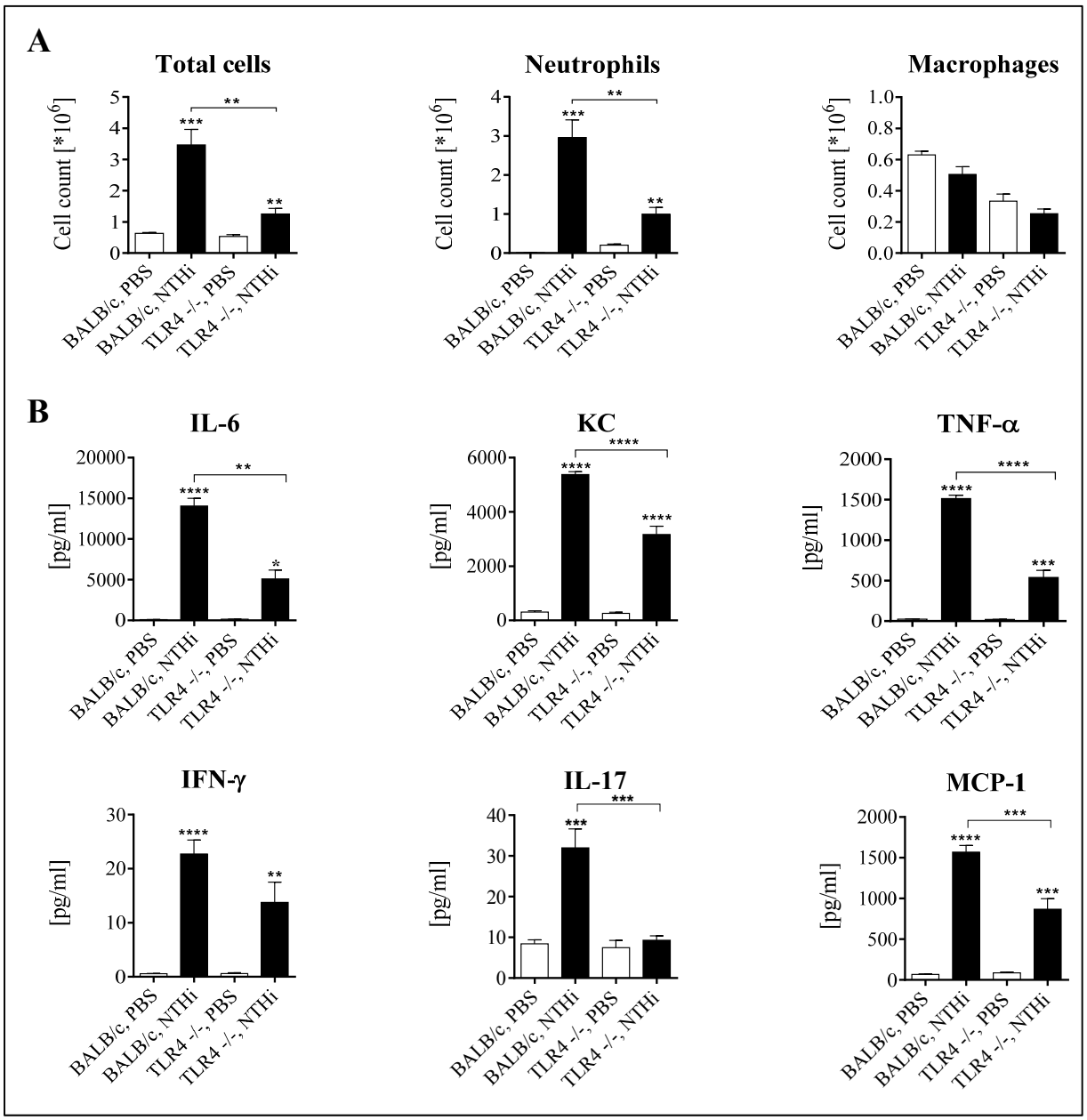

Figure 34: Infection of BALB/c or TLR4-/- mice with NTHi
Mice were infected with $5x10^6$ CFU NTHi. (A) Total cells, neutrophils, macrophages in BAL fluid and (B) cytokine levels in lung homogenate one day 1 p.i. Mean values ± SEM of n = 6 mice are shown. ****$p < 0.0001$, ***$p < 0.001$, **$p < 0.01$, *$p < 0.05$ represent significant differences compared to the corresponding PBS group or between the groups.

The contribution of TLR4 to NTHi-induced inflammation in mice was investigated. For this purpose, TLR4 deficient animals were infected with the bacteria. **Figure 34A** shows that NTHi infection induced a significant influx of total cells and neutrophils in BAL fluid. In contrast, cell counts in BAL fluid of TLR4 deficient mice were significantly lower upon infection. In addition, the NTHi-induced increased levels of MCP-1, TNF-α, IL-6, KC and IL-17 were significantly reduced in mice lacking TLR4 (**Figure 34B**). Moreover, TLR4 deficient mice were protected from infection-induced loss of body-weight (**Figure 35B**).

Notably, the bacterial load was elevated in BAL fluid of the TLR4 deficient mice as illustrated in the representative pictures in **Figure 35A**.

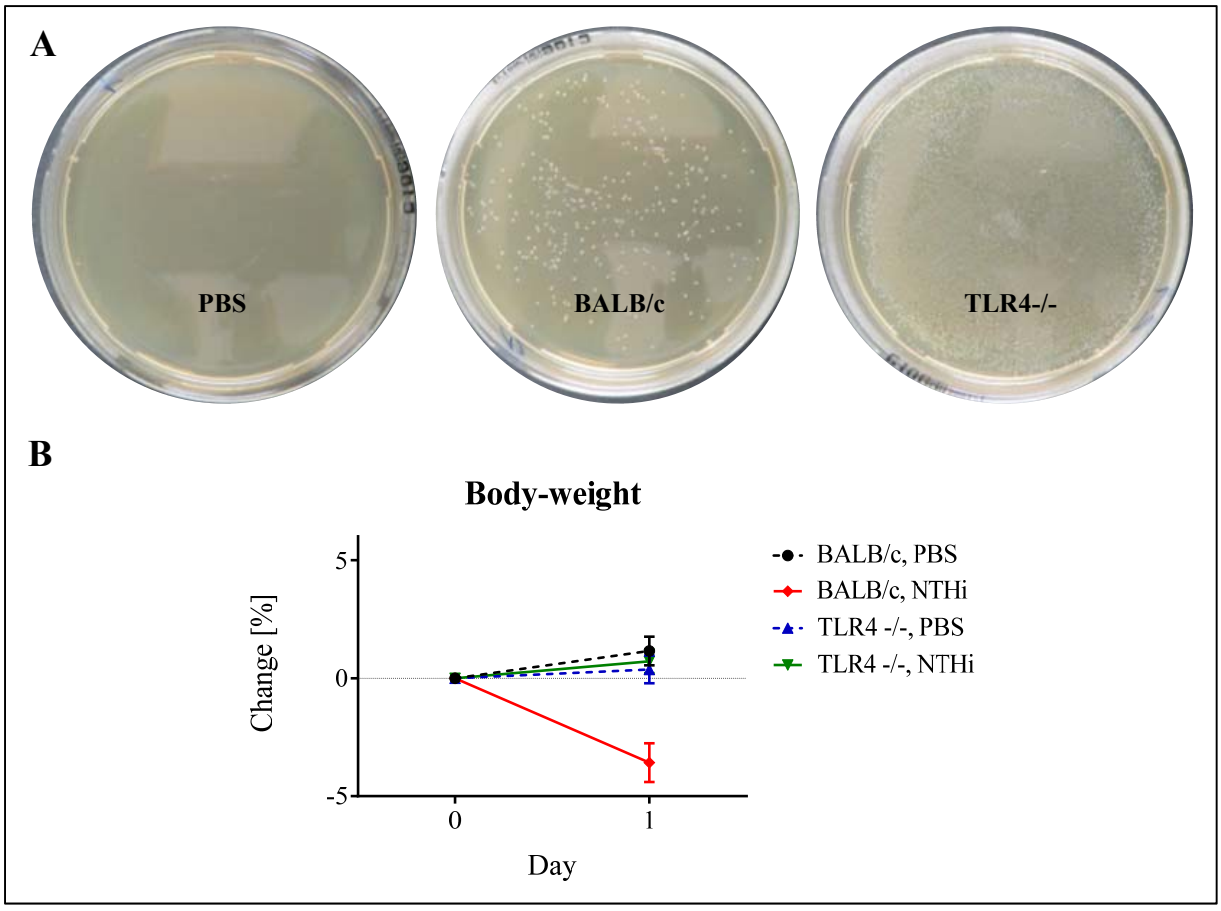

Figure 35: Infection of BALB/c or TLR4-/- mice with NTHi
Mice were infected with $5x10^6$ CFU NTHi. (A) Representative examples of plated BAL fluids are displayed. (B) Body-weight loss is shown as % change.

3.4.4 Dexamethasone fails to reduce pulmonary inflammation and increases the bacterial burden

The effect of Dexamethasone was investigated in CS-exposed and NTHi-infected mice. The experimental scheme is illustrated in **Figure 36A**. As shown in **Figure 36B**, drug administration resulted in a dose-dependent aggravation of the body-weight loss. A dose-dependent increase in NTHi load in BAL fluid was observed (**Figure 36C**). Dexamethasone treatment had no effect on total cell and neutrophil cell count but reduced macrophage numbers (**Figure 36E**). Regarding cytokine levels in lung homogenate, Dexamethasone reduced IFN-γ and IL-6 (**Figure 36F**). **Figure 36D** illustrates that CS/NTHi challenge of mice reduced lung compliance. Dexamethasone administration further decreased compliance values.

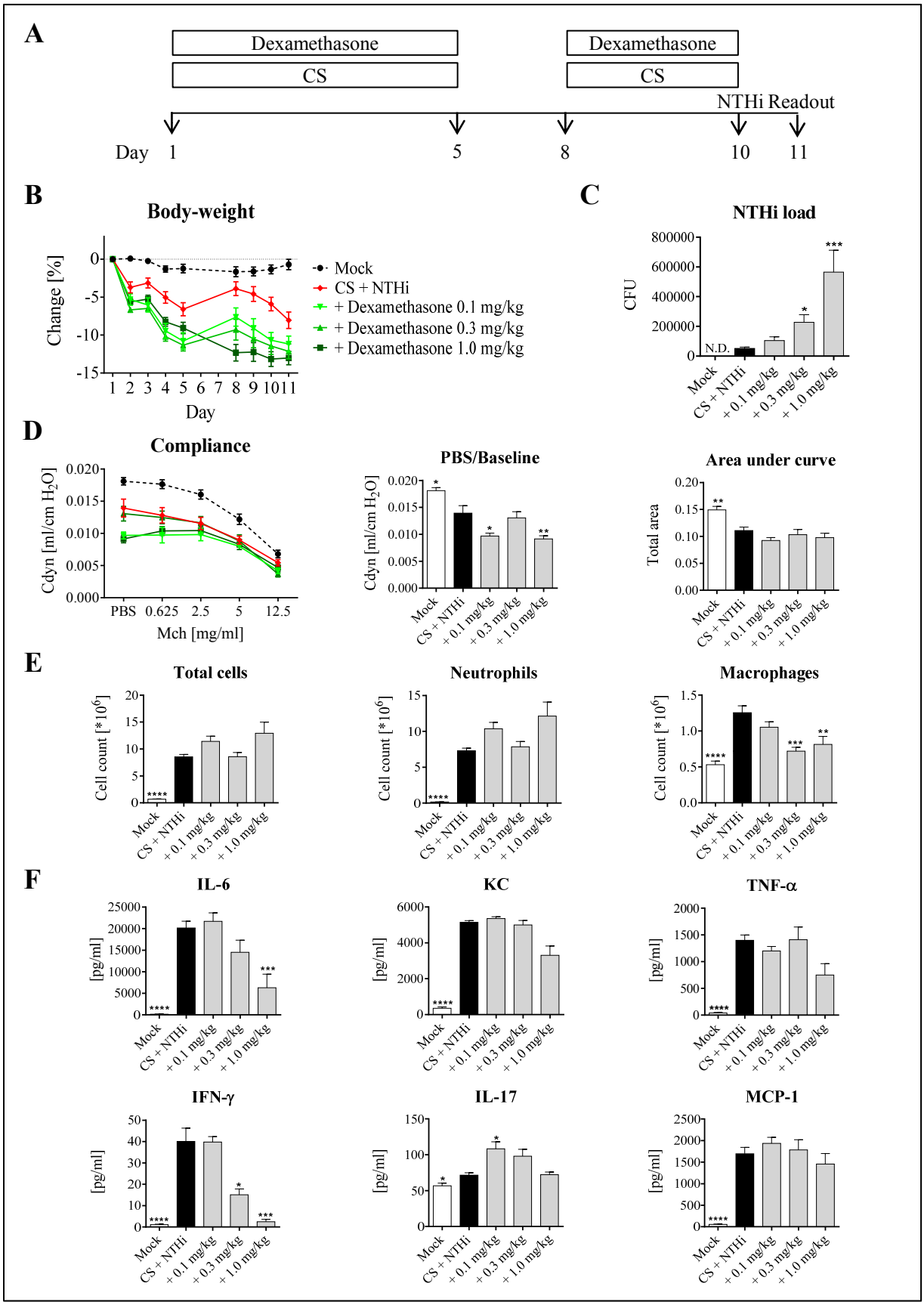

Figure 36: Treatment of CS-exposed and NTHi-infected mice with Dexamethasone
(A) Mice were challenged with CS and NTHi. They were treated in a preventive manner with Dexamethasone. (B) Body-weight loss as % change. (C) NTHi load in BAL fluid. (D) Compliance values after administration of raising methacholine (Mch) concentrations. (E) Total cell, neutrophil, macrophage numbers in BAL fluid and (F) cytokine levels in lung homogenate. Mean values ± SEM of n = 6-8 mice are shown. ****p < 0.0001, ***p < 0.001, **p < 0.01, *p < 0.05 represent significant differences compared to the CS/NTHi group.

3.4.5 Effects of Roflumilast treatment on inflammation in CS/NTHi-challenged mice

The effect of Roflumilast treatment was tested in CS/NTHi-challenged mice according to **Figure 37A**. Treatment with the drug slightly aggravated the loss of body-weight when using 30 mg/kg (**Figure 37B**). Roflumilast did not affect the bacterial load in BAL fluid (**Figure 37C**). Treatment of the animals increased compliance values, as illustrated in **Figure 37D**.

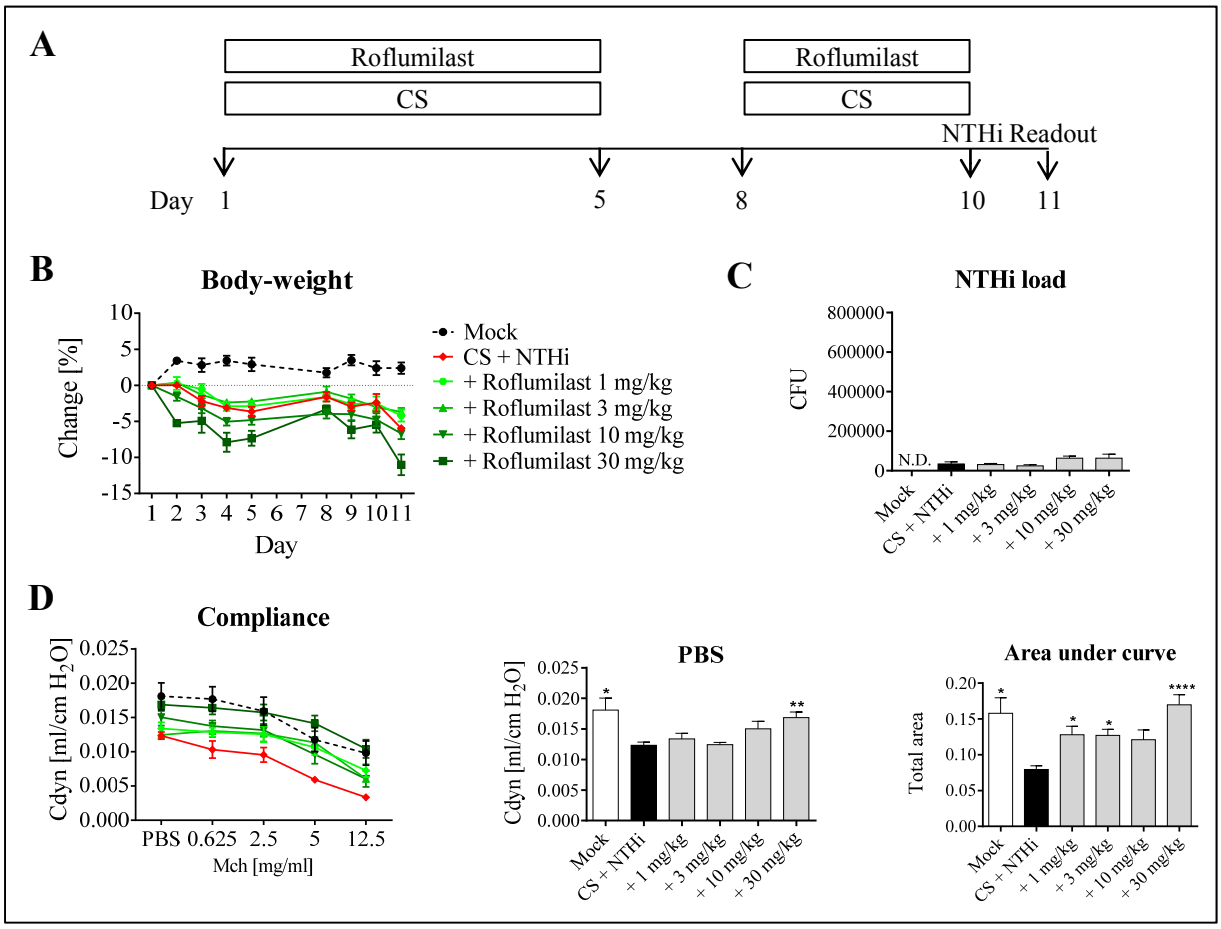

Figure 37: Treatment of CS-exposed and NTHi-infected mice with Roflumilast
(A) Mice were challenged with CS and NTHi. They were treated in a preventive manner with Roflumilast. (B) Body-weight loss as % change. (C) NTHi load in BAL fluid. (D) Compliance values after administration of raising methacholine (Mch) concentrations. Mean values ± SEM of n = 6-8 mice are shown. ****p < 0.0001, ***p < 0.001, **p < 0.01, *p < 0.05 represent significant differences compared to the CS/NTHi group.

Roflumilast failed to reduce total cells or neutrophils counts, respectively. However, it reduced macrophage numbers (**Figure 38A**). Cytokine levels in lung homogenate are shown in **Figure 38B**. Roflumilast failed to reduce any of them when using 1, 3 or 10 mg/kg, respectively. Upon administration of 30 mg/kg, levels of IFN-γ, MCP-1, TNF-α and KC were reduced significantly.

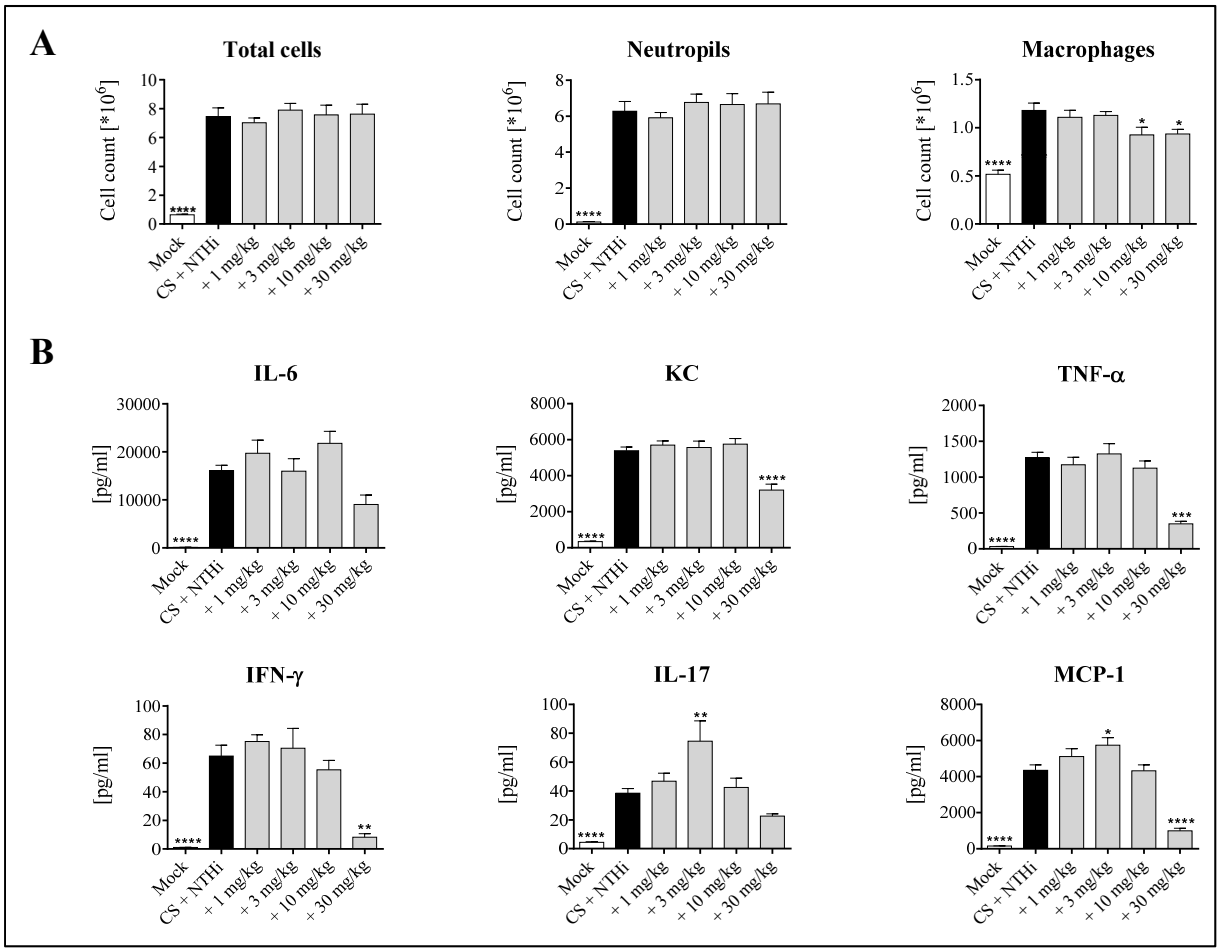

Figure 38: Treatment of CS-exposed and NTHi-infected mice with Roflumilast
Mice were challenged with CS and NTHi. They were treated in a preventive manner with Roflumilast. (A) Total cell, neutrophil and macrophage numbers in BAL fluid and (B) cytokine levels in lung homogenate. Mean values ± SEM of n = 6-8 mice are shown. ****p < 0.0001, ***p < 0.001, **p < 0.01, *p < 0.05 represent significant differences compared to the CS/NTHi group.

3.4.6 Azithromycin eliminates replication competent NTHi from BAL fluid of CS/NTHi-challenged mice

The effect of the macrolide antibiotic Azithromycin was examined in CS-exposed and NTHi-infected mice as shown in the experimental setup in **Figure 39A**. **Figure 39B** shows that none of the administered drug doses influenced the model-induced loss of body-weight. Azithromycin treatment resulted in a dose-dependent elimination of replication competent NTHi in BAL fluid as shown in **Figure 39C**. Drug administration had no effect on cell influx in the lungs of the animals, cytokine levels in lung homogenate or compliance (**Figure 39D-F**).

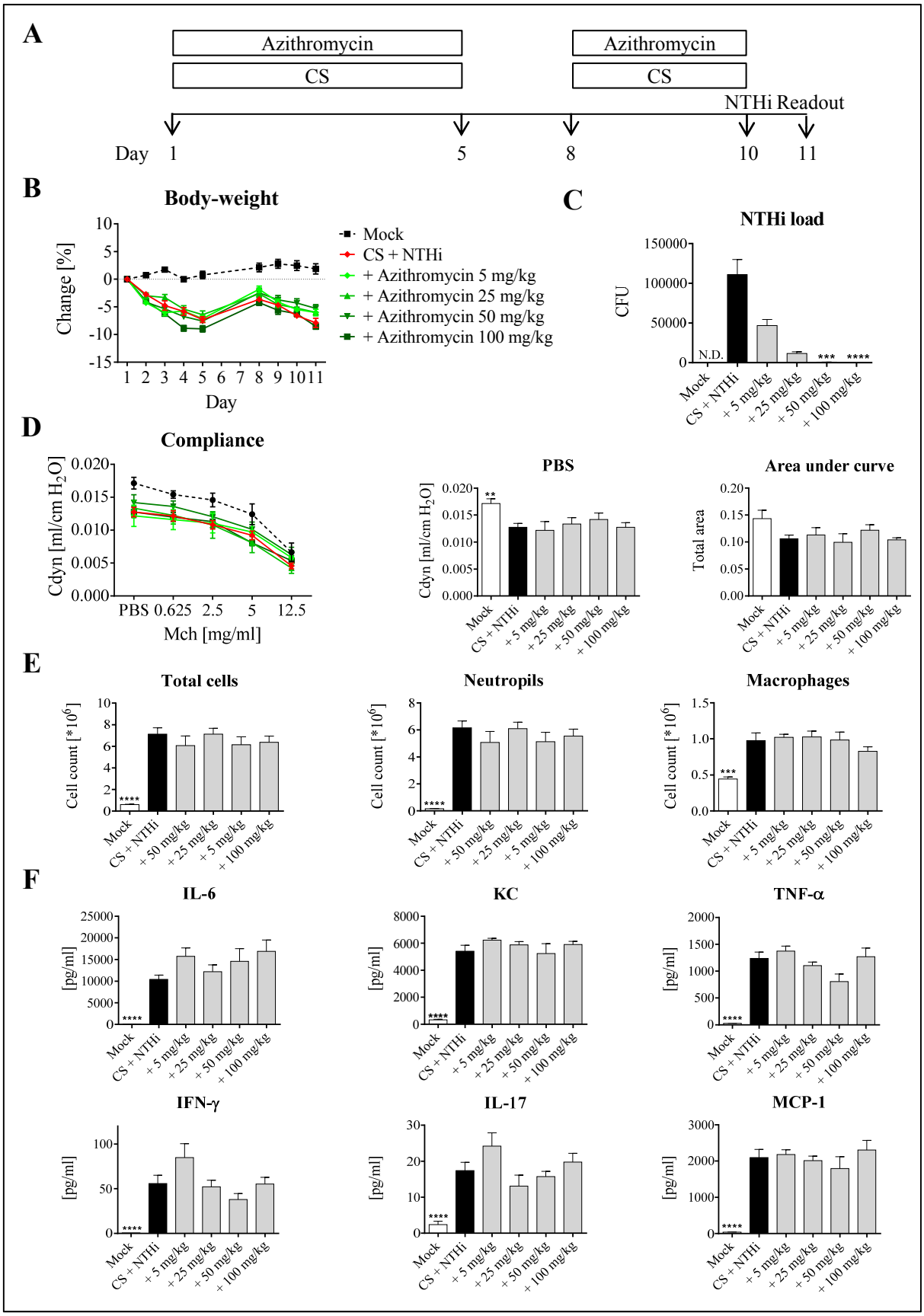

Figure 39: Treatment of CS-exposed and NTHi-infected mice with Azithromycin
(A) Mice were challenged with CS and NTHi. They were treated in a preventive manner with Azithromycin. (B) Body-weight loss as % change. (C) NTHi load in BAL fluid. (D) Compliance values after administration of raising methacholine (Mch) concentrations. (E) Total cell, neutrophil, macrophage counts in BAL fluid and (F) cytokine levels in lung homogenate. Mean values ± SEM of n = 6-8 mice are shown. ****p < 0.0001, ***p < 0.001, **p < 0.01, *p < 0.05 represent significant differences compared to the CS/NTHi group.

3.5 Cigarette smoke/H1N1/NTHi combination model establishment

Influenza infections of the airways can promote subsequent over-infection with NTHi thereby inducing a strong inflammatory response and exacerbations in COPD patients (section 1.1.6). Therefore, CS-exposed mice were infected with combined H1N1 and NTHi. The aim was to establish a model with depicts hallmarks of COPD exacerbation induced by CS, H1N1 and NTHi.

3.5.1 Combined H1N1/NTHi infection exacerbates pulmonary inflammation in CS-exposed mice

Mice were exposed to CS and infected with 3 IU H1N1 and $5x10^6$ CFU NTHi according to the experimental scheme in **Figure 40A**.

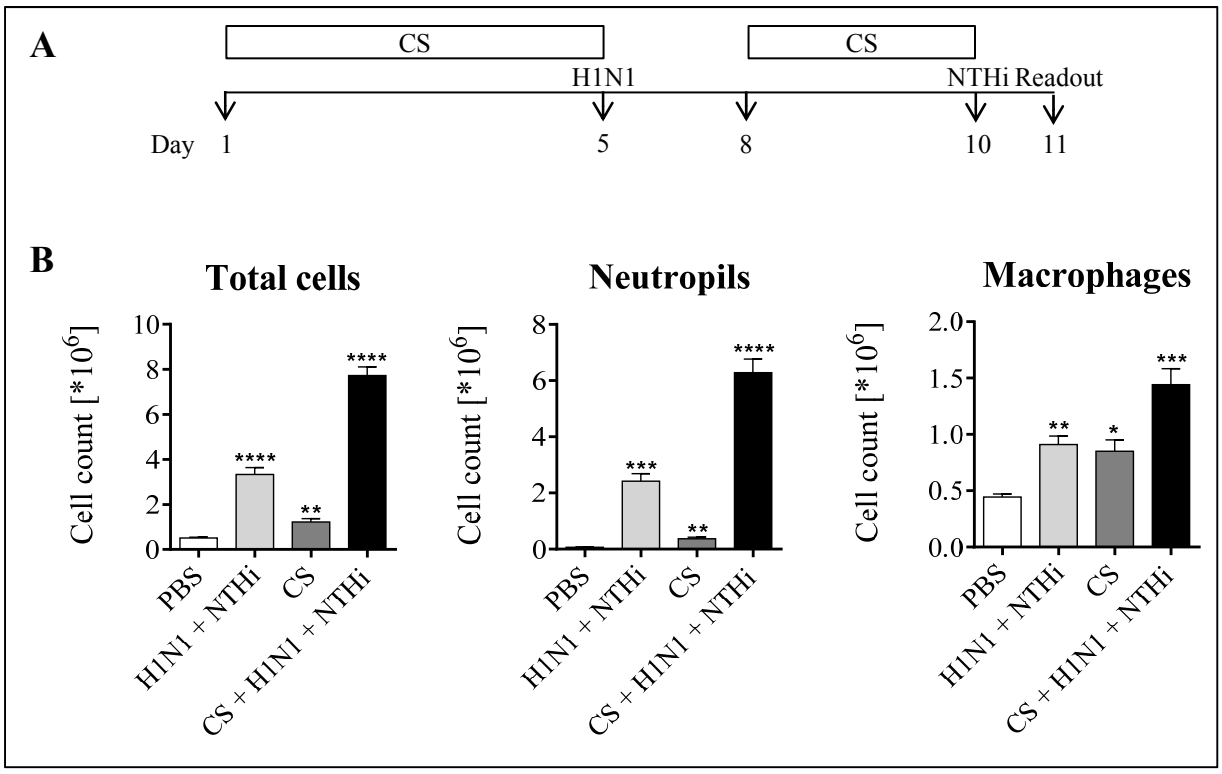

Figure 40: Combined H1N1/NTHi infection of CS-exposed mice
(A) Mice were exposed to CS for a total of 9 days (dark gray bars). Additional mice were infected with combined H1N1 and NTHi (light gray bars) or CS-exposed and infected with H1N1/NTHi (black bars). White bars show the results from PBS-treated control animals. (B) Total cell, neutrophil, and macrophage numbers in BAL fluid. Mean values ± SEM of n = 5-8 animals are shown. ****p < 0.0001, ***p < 0.001, **p < 0.01, and *p < 0.05 represent significant differences compared with the PBS group.

As shown in **Figure 40B**, CS-exposure of mice resulted in a moderate increase of total cells, neutrophils and macrophages in BAL fluid. Upon infection of the animals with combined H1N1 and NTHi a strong and significant influx of total cells, neutrophils and macrophages into the BAL fluid was detectable. Additional infection of CS-exposed mice with H1N1 and NTHi resulted in an exacerbated phenotype characterized by a strong influx of the mentioned

inflammatory cells. Notably, also individual infection with H1N1 or NTHi of (CS-exposed) mice induced a significant influx of inflammatory cells into the airways. However, cell counts were lower compared to the CS/H1N1/NTHi combination (data not shown).

MCP-1, IL-2 and KC cytokine levels in lung homogenate were slightly but significantly elevated in lung homogenate of CS-exposed mice (**Figure 41**). A strong increase of IFN-γ, RANTES, MCP-1, IL-2, TNF-α, IL-6, KC and IL-17 levels were detectable upon infection of mice with H1N1 and NTHi. Interestingly, cytokine levels did not further increase upon infection of CS-exposed mice.

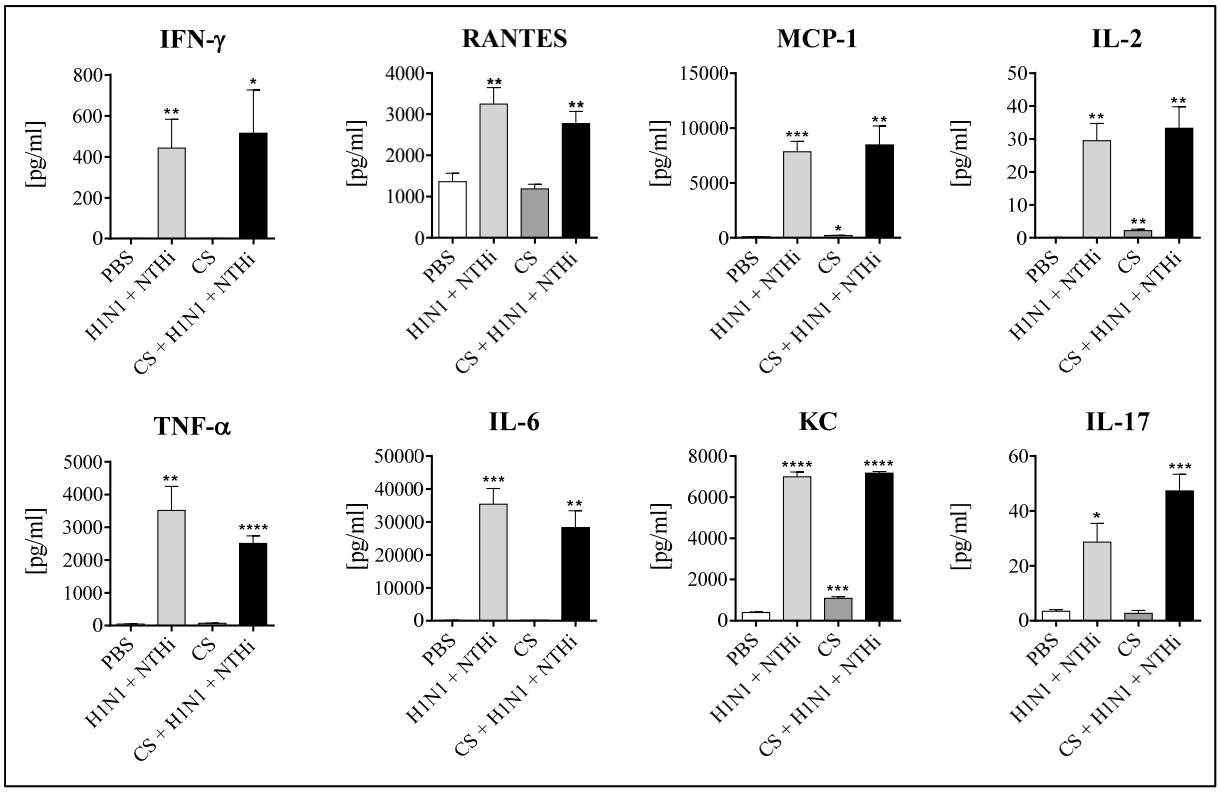

Figure 41: Combined H1N1/NTHi infection of CS-exposed mice
Mice were exposed to CS for a total of 9 days (dark gray bars). Additional mice were infected with combined H1N1 and NTHi (light gray bars) or CS-exposed and infected with H1N1/NTHi (black bars). White bars show the results from PBS-treated control animals. Cytokine levels in lung homogenate. Mean values ± SEM of n = 5-8 animals are shown. ****p < 0.0001, ***p < 0.001, **p < 0.01, and *p < 0.05 represent significant differences compared with the PBS group.

3.5.2 Effects of Dexamethasone, Roflumilast and Azithromycin CS-exposed and H1N1/NTHi-infected mice

Dexamethasone, Roflumilast and Azithromycin were tested in the CS/H1N1/NTHi combination model (**Figure 42A**). Roflumilast, and in particular Dexamethasone increased the loss of body-weight as observed in the CS/H1N1 or the CS/NTHi exacerbation models. In contrast, the development of body-weight was not influenced by Azithromycin administration (data not shown).

Again, Roflumilast had no effect on the bacterial load in BAL fluid, while Dexamethasone showed a tendency to increase the bacterial burden. Replication competent NTHi were eliminated in a dose-dependent manner upon Azithromycin administration (**Figure 42B**).

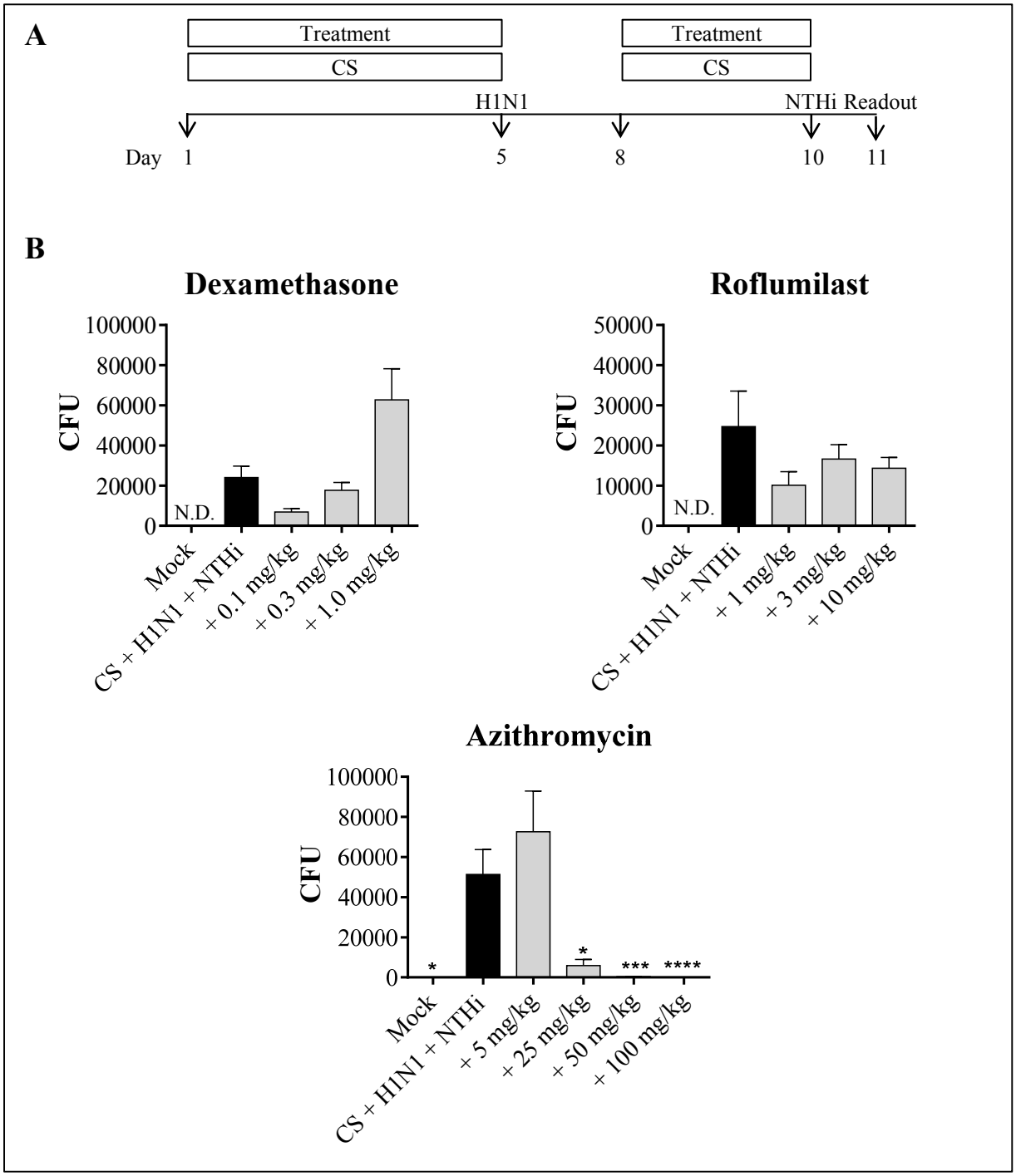

Figure 42: NTHi load in CS-exposed and H1N1/NTHi-infected mice after treatment with Dexamethasone, Roflumilast and Azithromycin

(A) Mice were challenged with CS and infected with H1N1 and NTHi. They were treated in a preventive manner with Dexamethasone, Roflumilast and Azithromycin. (B) NTHi load in BAL fluid. Mean values ± SEM of n = 6-8 mice are shown. ****p < 0.0001, ***p < 0.001, **p < 0.01, *p < 0.05 represent significant differences compared to the CS/H1N1/NTHi group.

When examining inflammatory cells in BAL fluid, significantly elevated counts of total cells and neutrophils were observed upon treatment with 1.0 mg/kg Dexamethasone (**Figure 43A**).

Notably, administration of Azithromycin reduced numbers of total cells, neutrophils and macrophages dose-dependently and significantly (**Figure 43C**). Roflumilast treatment had no effect on cell counts (**Figure 43B**).

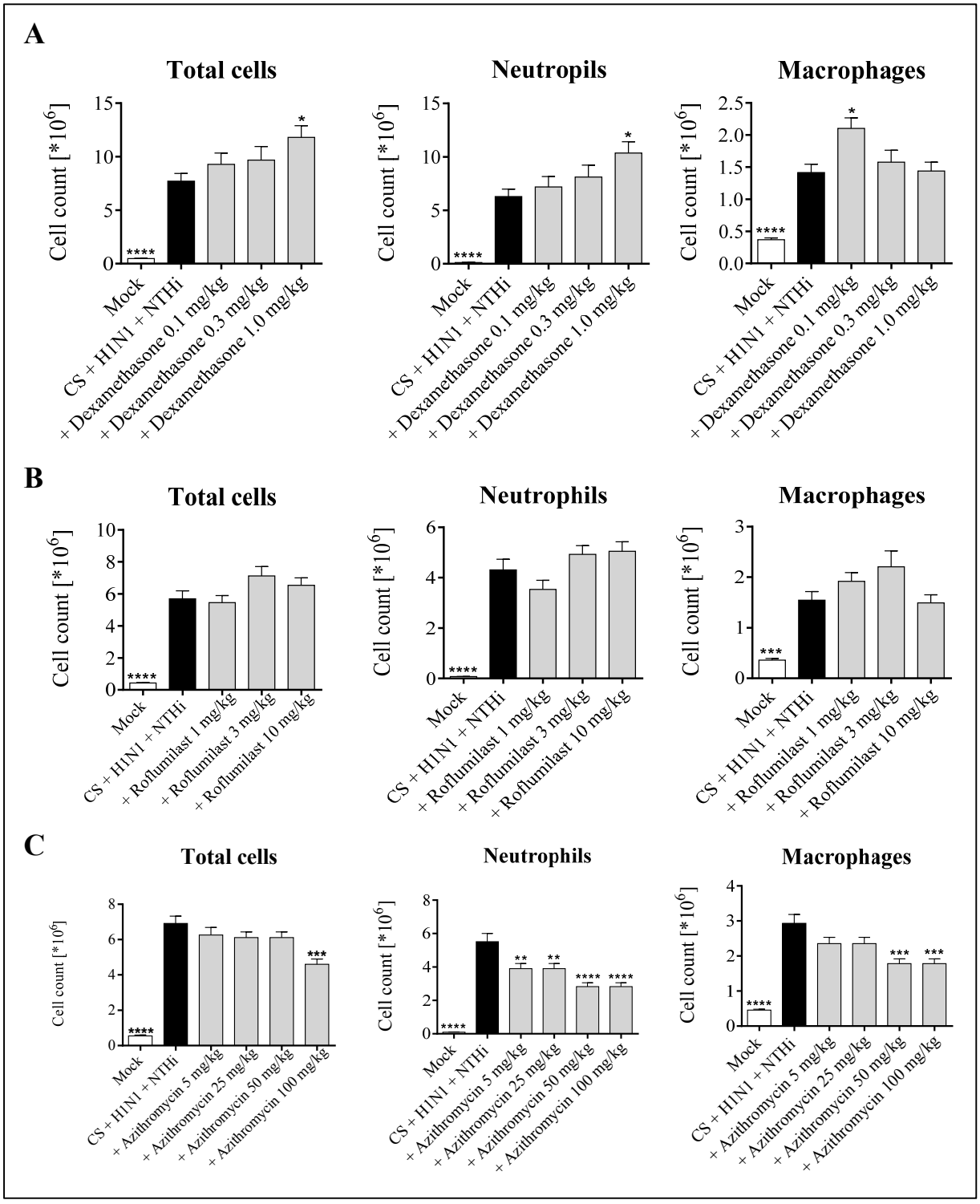

Figure 43: Cell counts in BAL fluid of CS-exposed and H1N1/NTHi-infected mice after treatment with Dexamethasone, Roflumilast and Azithromycin

Mice were challenged with CS and infected with H1N1 and NTHi. They were treated in a preventive manner with (A) Dexamethasone, (B) Roflumilast and (C) Azithromycin. Total cell, neutrophil, macrophage counts in BAL fluid. Mean values ± SEM of n = 6-8 mice are shown. ****$p < 0.0001$, ***$p < 0.001$, **$p < 0.01$, *$p < 0.05$ represent significant differences compared to the CS/H1N1/NTHi group.

Consistent with the observed anti-inflammatory effects regarding cell counts, Azithromycin treatment of CS-exposed and H1N1/NTHi-infected mice reduced levels of TNF-α and KC in lung homogenate (**Figure 44C**). Neither Dexamethasone nor Roflumilast reduced levels of those cytokines (data not shown).

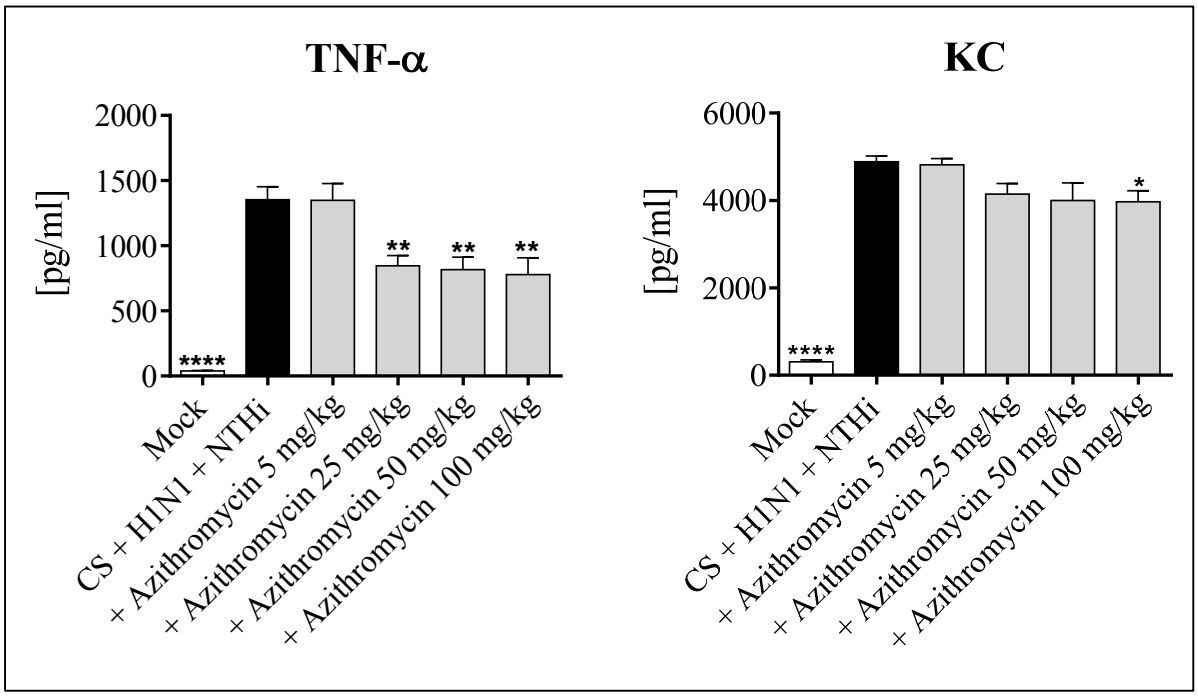

Figure 44: Cytokine levels in lung homogenate of CS-exposed and H1N1/NTHi-infected mice after treatment with Azithromycin

Mice were challenged with CS and infected with H1N1 and NTHi. They were treated in a preventive manner with Azithromycin. Cytokine levels in lung homogenate. Mean values ± SEM of n = 6-8 mice are shown. ****$p < 0.0001$, ***$p < 0.001$, **$p < 0.01$, *$p < 0.05$ represent significant differences compared to the CS/NTHi group.

4 Discussion

Viral- and bacterial-induced exacerbations of COPD account for an increased morbidity and mortality in COPD patients. Moreover, they constitute an enormous burden for healthcare systems (section 1.1.1). Pre-clinical mouse models of COPD are crucial to gain insights into disease mechanisms and for the development of novel therapies in the fight against the disease (section 1.2).

In the last years, several groups exposed mice to CS or infected them with viruses to model aspects of human lung inflammation and COPD. However, only few studies were conducted combining CS-exposure and virus infection to mimic aspects of COPD exacerbations. One prominent study describing a COPD exacerbation model was conducted by Stämpfli et al. [205]. They exposed C57BL/6 mice to CS for 4 days and additionally infected them with H1N1. Thereby, they were able to model aspects of an exacerbated lung inflammation, for example exacerbated counts of inflammatory cells in BAL fluid. Furthermore, Han et al. investigated the influence of CS on pdmH1N1- and H9N2-induced lung inflammation in C57B6/N mice [219]. Interestingly, they found that CS attenuated virus-induced lung inflammation and combination of the stimuli did not result in an exacerbated phenotype. Further evidence that CS might have anti-inflammatory effects under distinct circumstances comes from a recently published study by Tilp et al. [220]. In their experiments they tested the effects of CS in an asthma mouse model. CS-exposure reduced eosinophil numbers, IL-4 and IL-5 levels in the lungs and improved lung function. Consequently, it is crucial to choose an appropriate experimental setup when aiming at modeling an exacerbated COPD phenotype in mice. Besides H1N1, also murine CS/RSV models were studied previously [221, 222]. It was shown that RSV has the ability to aggravate CS-induced pulmonary inflammation and tissue. Thus, CS/RSV models might be valuable for COPD research. None of the published studies dealing with CS/virus models contains profound pre-clinical data regarding the effects of corticosteroids, PDE-4 inhibitors and muscarinic receptor antagonist on inflammatory parameters, viral load and lung function.

In the current study, published by Bucher et al., mice were exposed to CS and additionally infected with H1N1 or RSV to mimic aspects of a viral-induced exacerbations [206]. In this study, an exacerbated phenotype was obtained, including increased cytokine levels of IL-6, KC, TNF-α and deteriorated lung function. Several clinically relevant treatment options such as the long-acting muscarinic receptor antagonist Tiotropium, the corticosteroids Fluticasone propionate and Dexamethasone, and the PDE-4-inhibitor Roflumilast were tested in the

established CS/virus models as benchmarks. In addition, a novel therapeutic approach using anti-IL-1α, anti-IL-1β and anti-IL-1R1 Abs was investigated. In the following, the results are discussed in the light of current scientific and clinical findings.

COPD patients suffer from bronchoconstriction which contributes to a reduction in lung function especially during episodes of virus-induced exacerbations [178, 179]. Treatment with Tiotropium was shown to improve lung function, quality of life and to reduce the frequency and severity of exacerbations in COPD patients. It is currently a standard treatment for COPD [175, 181, 223, 224]. Tiotropium blocks M3 muscarinic receptors on smooth muscle cells thereby preventing bronchoconstriction explaining the positive effects on lung function and quality of life observed in patients [180]. However, how Tiotropium reduces the severity and the frequency of exacerbations is not completely understood. Interestingly, recent studies suggest that Tiotropium also has additional anti-inflammatory effects, possibly contributing to the efficacy seen in patients suffering from exacerbations [184]. For example, Wollin et al. found that Tiotropium significantly reduced IL-6, TNF-α, MCP-1, MIP-1α, KC levels and neutrophil cell counts in BAL fluid of CS-exposed mice [185]. Furthermore, Tiotropium also reduced inflammation and remodeling in several models of asthma [186-190]. In addition, some *in vitro* studies also attest anti-inflammatory properties to Tiotropium [191-194]. Therefore, the positive effects of Tiotropium on exacerbations in COPD patients may be due to the direct reduction in bronchoconstriction by smooth muscle cells induced by the infectious agent, the anti-inflammatory properties, or a combination of both.

In this study it was investigated whether Tiotropium has anti-inflammatory and bronchoprotective effects in mice, where inflammation and bronchoconstriction is triggered by a combination of CS-exposure and H1N1, or CS and infection with RSV in novel models for COPD exacerbation.

Tiotropium suppressed the reduction in lung function induced by CS and the H1N1 infection, confirming its bronchoprotective effect. Furthermore, numbers of neutrophils and macrophages were also significantly reduced in the Tiotropium-treated mice. Both neutrophils and macrophages are increased in numbers in the lungs of patients with COPD, and in particular neutrophils are further increased during exacerbations [96]. It has been suggested that they may contribute to or cause the symptoms of exacerbations [225]. Thus, lowering the influx of these inflammatory cells to the lungs may contribute to the positive effect of Tiotropium on exacerbations. In addition, Tiotropium also dose-dependently decreased IL-6 and IFN-γ levels in the airways. Both inflammatory mediators are increased in COPD patients

and levels peak during exacerbations [36]. Previously, a clinical study linked significantly higher amounts of IL-6 in sputum of COPD patients to virus-induced exacerbations and airway obstruction [226]. Moreover, in murine studies IFN-γ was associated with the development of emphysema, a further hallmark of severe COPD in patients [227]. Consistent with the findings of this study, Wollin et al. showed that nebulized Tiotropium significantly reduced total cells, neutrophils and cytokines such as IL-6 in the lungs of CS-exposed mice [185]. Comparable effects were also observed in this study where levels of total cells, neutrophils and cytokines in the lungs were much higher, indicating an anti-inflammatory effect of Tiotropium also in an exacerbated disease condition. These results suggest that in addition to reducing the numbers of neutrophils, Tiotropium may reduce the frequency and severity of exacerbations by lowering the production of IL-6 and IFN-γ in the lungs of patients.

Currently, it is a matter of speculation through which downstream mechanisms exactly Tiotropium mediates the anti-inflammatory effects which were detected in the established exacerbation models. In this study Tiotropium down-regulated the mRNA expression of ChAT, and NANS in the lungs of CS/H1N1-challenged mice. ChAT catalyzes the synthesis of acetylcholine and both are ubiquitously expressed throughout the airways and furthermore are involved in inflammatory processes and remodelling partly independent of M3 receptor signalling [213-215, 228]. Therefore, a reduction of ChAT expression leading to a reduction in acetylcholine, due to Tiotropium treatment, might explain in part some of the observed anti-inflammatory features. In addition, NANS expression, up-regulated in the lung of CS/H1N1-challenged mice, was significantly reduced in the Tiotropium-treated mice. NANS is an important enzyme for the biosynthesis of sialic acid, a receptor for influenza virus [216, 217]. Therefore, reduced NANS expression could result in a reduction of sialic acid thereby attenuating viral entry. This in turn could result in less replication, a reduced viral load, and thereby less inflammation. Supporting this view is the finding that the H1N1 load was significantly reduced in the CS/H1N1 model upon treatment with Tiotropium. The finding that Tiotropium might directly reduce viral load is supported by *in vitro* studies [229]. Further studies, evaluating through which mechanism Tiotropium reduces inflammation during viral exacerbations are warranted. The results of this study suggest that Tiotropium may have this effect by either reducing inflammation directly and/or by reducing viral entry/load leading to less inflammation.

The effects of Fluticasone propionate on CS/H1N1-induced inflammation were also investigated. In contrast to Tiotropium, Fluticasone increased the amount of IL-6, KC, TNF-α and IFN-γ in the airways, failed to reduce total neutrophil or macrophage numbers in the lung, worsened lung function and increased body-weight loss in mice exposed to CS and infected with H1N1. The amplified inflammation might be responsible for the increased decline in lung function observed in this study. In addition, an increased destruction of epithelia was observed in the airways upon treatment of CS-exposed and H1N1-infected mice with Fluticasone. In support of these findings are the results of a recent study linking Fluticasone treatment to the induction of epithelial injury and altered epithelial barrier function [230]. The altered epithelial barrier upon treatment with Fluticasone might also explain in part the increased viral load as it may facilitate viral distribution in the tissue. These findings suggest that ICS treatment in particular with Fluticasone, the major ICS being used to treat COPD, might increase the viral burden and the amount of inflammatory cytokines in patients. Moreover, it might explain the increased risk for pneumonia in COPD patients upon ICS treatment [174, 231] and supports the finding that many COPD patients do not benefit from ICS treatment [232, 233].

It remains to be elucidated whether other ICS, e.g. Budesonide, Mometasone, Ciclesonide or Fluticasone fuorate have the same effects as Fluticasone propionate. Interestingly, the increase in viral load both in the CS/H1N1-infected mice and the NCI-H292 cells were also observed when applying Dexamethasone, strongly suggesting that the increase in the viral load is not Fluticasone-specific but due to the general mode of action of steroids. In contrast to Fluticasone, Dexamethasone-treated mice exhibited a reduction of some pro-inflammatory cytokines in the lungs. Dexamethasone treatment also did not worsen or reduce lung function but similar to Fluticasone increased body-weight loss.

A further therapy available to COPD patients is the treatment with Roflumilast [176, 177]. Roflumilast was tested in the CS/H1N1 model and found to reduce macrophage numbers, IL-6 and KC in the lungs but not to have a significant effect on neutrophil numbers or lung function. Viral load in the animals and in NCI-H292 cells and loss of body-weight was also not affected by Roflumilast. These results illustrate the anti-inflammatory properties of Roflumilast on some COPD associated inflammatory parameters such as IL-6 and the murine CXCL8 homologues KC. The reduction of inflammation might explain the reduced rate of exacerbations in some patients treated with the drug [234]. However, the tolerability of Roflumilast is limited [177].

Exacerbations in COPD patients are caused by different viruses [105]. For this reason, the effects of different drugs were tested in an additional model of COPD exacerbation using a different virus. For this purpose, a RSV infection and CS-exposure mouse model of COPD exacerbation was developed. A RSV re-infection protocol was used, because this yielded a more robust exacerbation phenotype compared to a single infection. Furthermore, humans are often re-infected with RSV, because similar to mice humans do not generate a protective memory response against RSV [210, 211]. Compared to the CS/H1N1 exacerbation model the inflammatory response in the CS/RSV model was weaker and no impairment of lung function was measurable. Nevertheless, Tiotropium again reduced the pro-inflammatory mediators IL-6, IFN-γ, and TNF-α and neutrophil numbers in the lung significantly, without affecting the loss in body-weight or the viral load in the lung. In contrast, Fluticasone increased the amount of KC and the amount of virus in the lungs, and increased body-weight loss but had no effect on neutrophil numbers. Although Roflumilast showed some suppressive effects in the CS/H1N1 model, no anti-inflammatory effects were detected in the CS/RSV model. Roflumilast treatment also did not impact the viral load but lead to a slight increase in the loss of body-weight. Taken together, again, Tiotropium was superior in inhibiting inflammatory responses induced by CS and RSV compared to Fluticasone and Roflumilast. Fluticasone, similar to the CS/H1N1 experiments, increased the RSV load in the lung, an effect also observed in cell culture using bronchial epithelial cells infected with RSV and treated with Fluticasone. Neither Tiotropium nor Roflumilast had any effect on the RSV load in the NCI-H292 cells.

In conclusion, Tiotropium had anti-inflammatory effects on both CS/H1N1- and CS/RSV-induced inflammation in mice without increasing viral load or inducing body-weight loss. These findings are in line with previous reports showing anti-inflammatory effects of Tiotropium *in vivo* and *in vitro* and show that M3 muscarinic receptor signaling contributes to inflammation [183, 185, 235]. Surprisingly, the observed anti-inflammatory effects were superior to Roflumilast and Fluticasone. Fluticasone was not only inferior to Tiotropium but also increased viral load and body-weight loss in both CS/H1N1 and CS/RSV exacerbation models. The data of this study supports the view that the positive effect of Tiotropium on exacerbation rates can be partly attributed to its anti-inflammatory activity.

High exacerbation frequency has been associated with chronic systemic inflammation and mortality in patients with COPD [87]. The pro-inflammatory IL-1 family members IL-1α and IL-1β are increased in patients with stable COPD and during exacerbations [85, 86, 236-238].

Previous *in vitro* studies with human primary cells suggest a plethora of roles of IL-1 family members in the inflammatory process [90]. However, the functional relevance of IL-1α and IL-1β for the pathology of COPD remains to be determined.

In this study, the relevance of IL-1α and IL-1β was explored *in vivo* in the CS/H1N1 model. Individual neutralization of IL-1α in CS/H1N1-challenged mice had significant suppressive effects on inflammatory cell influx and KC levels into the lungs. In contrast, individual neutralization of IL-1β did not provide significant reduction of inflammatory cells or cytokines/chemokines. Previously, the IL-1 pathway was investigated in CS models. Therefore, the effects of individual IL-1α or IL-1β neutralization were also explored in a murine one-week CS model. As in the CS/H1N1 model, a predominant role of IL-1α was found compared to neutralization of IL-1β, which failed to exert significant anti-inflammatory effects. In line with the *in vivo* results, treatment of H1N1-infected primary human bronchial epithelial cells with anti-IL-1α Abs resulted in significantly reduced levels of IL-6 and TNF-α whereas anti-IL-1β Abs had no effect on released cytokines. These findings extend previous results reported in a related *in vitro* setting where the IL-1R1 antagonist Anakinra was shown to suppress rhinovirus-induced cytokine release from human primary epithelial cells [239].

In an additional *in vivo* study, concomitant neutralization of IL-1α and IL-1β revealed the strongest anti-inflammatory effects that almost fully blocked CS/H1N1-driven airway inflammation. Inhibition of the IL-1R1 provided pronounced effects. However, the effects were inferior compared to individual inhibition of its soluble ligands, IL-1α and IL-1β.

Taken together, this work supports and extends previous findings that IL-1α might be a key player driving CS and CS/virus-induced airway inflammation [85, 240] but also notes that concomitant blockade of IL-1β provides additional benefit. It also confirms and extends previous reports that blocking IL-1R1 is an efficient anti-inflammatory intervention in mouse CS and CS/virus models [85, 86, 241, 242]. In addition, the results from this study indicate that combined neutralization of IL-1α and IL-1β by Abs is superior to blockade of the IL-1R1. In order to exclude that potential pharmacokinetic (PK) liabilities of the IL-1R1 Ab (potential target mediated drug dispositioning, sink effects) could account for the inferior activity, plasma obtained at the end of the CS experiment from mice treated with the IL-1α Ab or IL-1β Ab versus mice treated with the IL-1R1 Ab was tested on activated bEnd.3 cells (data not shown). Similar or even superior potency of the IL-1R1 Ab plasma to suppress recombinant mouse IL-1α- or IL-1β-induced KC release in bEnd.3 cells was found compared to plasmas of the anti-IL-1α- or anti-IL-1β Ab treatment groups, respectively. It remains to be

clarified whether differences in affinity, target distribution, or other yet to be defined parameters might account for the weaker activity of IL-1R1 Abs compared to treatment with combined IL-1α/IL-1β Abs.

The superior efficacy of combined IL-1α/IL-1β neutralization was also reflected by the loss of body-weight in this work. While single treatment with anti-IL-1α or anti-IL-1β Abs failed to reduce the model-induced loss of body-weight, combined neutralization of IL-1α/IL-1β had significant positive effects which were superior when compared to the effects of IL-1R1 blockade. It may be that the observed suppressive effects of the IL-1 pathway inhibitors on body-weight loss are the consequence of reduced inflammation and/or may be based on direct effects on lipid/energy metabolism as described elsewhere [243, 244].

Besides significantly reducing inflammation and the loss of body-weight, combined neutralization of IL-1α/IL-1β by Abs also suppressed CS/H1N1-induced ICAM-1 expression. ICAM-1 was previously linked to the pathogenesis of COPD and the development of emphysema in patients [245, 246]. An explanation might be the fact that ICAM-1 contributes to the recruitment of neutrophils to the site of inflammation. As stated before, neutrophils play a central role in the inflammatory process of COPD, and NE was linked to the development of emphysema, a hallmark of COPD, previously [42, 247].

Notably, none of the Ab treatments resulted in increased viral loads in lung homogenate. In contrast, a reduced viral load was observed in the lungs of anti-IL-1α/IL-1β Ab-treated mice. One explanation might be that the epithelial barrier is possibly less affected in less inflamed lung tissue. In turn, this would hamper distribution of viral pathogens in the lung. However, the specific pathogen-free housing conditions and setup of these studies do not allow assessing the general infection risk after IL-1 antagonization that has been discussed in clinical studies [248, 249].

Both an anti-IL-1β Ab (Canakinumab) and an anti-IL-1R1 (MEDI-8968) Ab were recently tested in Phase II studies in patients with COPD [91, 92]. No clinically meaningful improvement in any lung function parameter was achieved by Canakinumab, although doses were used that provided efficacy in other inflammatory diseases. Therefore, it can be postulated that inhibition of IL-1β alone is not sufficient to provide clinical efficacy in COPD. The pre-clinical data generated in the present study supports this assumption. The apparently negative outcome of the anti-human anti-IL-1R1 Ab MEDI-8968 is unexpected based on the pre-clinical data of this study and published IL-1R1-/- data, which suggest a crucial role of IL-1R1 and IL-1α/IL-1β signaling for CS- and CS/virus-induced lung inflammation [85, 86,

241, 242]. One might speculate that translation of mouse models to the human COPD patient is not predictive. However, there are several lines of evidence which indicate that the IL-1 pathway is active in patients with COPD and one cannot exclude the possibilities of caveats in the clinical study such as potential PK issues of IL-1R1 Abs (as reported for another clinical IL-1R1 Ab by Cohen et al. [250]), lack of lung exposure, and/or suboptimal selection of the study patient population that might have contributed to the negative outcome. Further investigations will be required to resolve these issues and to reveal the contribution of IL-1α and IL-1β in patients with COPD. The data from this study suggest that combined inhibition of IL-1α and IL-1β with individual Abs might be a preferable approach. Moreover, targeting of additional potentially redundant IL-1 family members might be required to achieve further improved anti-inflammatory effects. For instance, additional targeting of IL-18 might provide greater anti-inflammatory efficacy as demonstrated for some readouts such as chemokines from this study. In addition, there is emerging evidence that novel IL-1 family members such as IL-33 and IL-36 might also contribute to COPD pathology [251-253].

In conclusion, this work supports the view that the IL-1 pathway might be an attractive therapeutic target for the development of novel therapeutics for patients with COPD. In particular, the results of this study suggest that combined inhibition of both IL-1α and IL-1β might be superior in reducing inflammation and exacerbations in COPD patients compared to blockade of the IL-1R1.

Besides viral infections of the respiratory tract, also bacterial infections, for example with NTHi are expected to be important triggers of exacerbations in COPD patients (section 1.1.6). Previously, several murine CS/(HK-)NTHi models have been published. For example, Lugade et al. investigated the effects of CS after chronic NTHi infection and found that CS has suppressive effects on the adaptive immune response to NTHi, possibly explaining recurrent infections in patients [254]. Gaschler et. al exposed C57BL/ and BALB/c mice to CS over a period of 8 weeks following intranasal challenge with NTHi thereby exacerbating the inflammatory response [255, 256]. To model aspects of a bacterial-induced COPD exacerbations in this study, mice were exposed to CS for 8 days and infected with NTHi. Dexamethasone, Roflumilast and Azithromycin were tested as benchmarks in the established model.

As already stated, NTHi has the ability to amplify inflammation in the lower airways thereby triggering exacerbations of COPD (section 1.1.6). In this work, infection of CS-exposed mice exacerbated pulmonary inflammation, characterized by a strong influx of total cells,

macrophages and neutrophils into the lungs. In particular neutrophils are thought to be major contributors to COPD pathology and clinical studies found numbers of neutrophils elevated during exacerbations [39, 40]. Furthermore, IFN-γ was exacerbated in the lungs of CS/NTHi-challenged mice. The cytokine was associated with the development of emphysema in murine studies, a hallmark of severe COPD in patients [227]. Expression of IFN-y and other pro-inflammatory cytokines such as TNF-α, IL-1β, IL-6 and IL-17 is induced by NF-κB activation, which in turn is triggered by TLR4, in the case of NTHi due to activation by LOS [157, 163]. The contribution of TLR4 activation by NTHi to lung inflammation in mice using a TLR4 deficient strain was investigated. Upon infection, TLR4 deficient animals illustrated significantly reduced inflammatory cells and cytokines in the lungs. However, a significant inflammation was still present, providing an indication that the NTHi-induced inflammation is partly mediated by NTHi LOS and TLR4 activation. This finding is further supported by an additional experiment in which different infection doses of NTHi and HK-NTHi were tested. In this experiment, using an NTHi infection dose of $5x10^4$ CFU induced significant increased numbers of inflammatory cells and cytokines in the lungs of mice whereas the same infection dose of HK-NTHi did not (data not shown). Other bacterial components such as the NTHi outer membrane proteins (OMPs) might have the ability to trigger inflammatory responses in the airways, independent from TLR4 signaling. Supporting studies were conducted by Berenson et al., who found that the OMP P6 of NTHi induces macrophage inflammatory events, including CXCL8 and TNF-α release [257]. Another OMP, P2, is recognized by TLR2 [258].

A major problem in COPD medication is the lack of efficient anti-inflammatory treatments. As stated before, corticosteroids are often used to dampen Th2-driven inflammation in asthma patients. Unfortunately, these drugs fail to reduce neutrophil-driven inflammation in COPD patients [232, 259]. As observed in the established CS/virus models, Dexamethasone treatment did not reduce inflammatory cells in our CS/NTHi model and moreover failed to improve compliance values. In contrast, an increased loss of body-weight and an increased NTHi load in BAL fluid was observed. The finding that Dexamethasone treatment increased the NTHi load in our model might reflect clinical observations that link corticosteroid treatment of patients with an increased risk of pneumonia [172, 174].

Another approach to reduce inflammation in the lungs of patients with severe COPD and frequent exacerbations is the use of the PDE-4 inhibitor Roflumilast [176, 177]. We observed that the drug had no effect in our established CS/NTHi model when using 1, 3 or 10 mg/kg,

respectively. These or even lower doses had significant anti-inflammatory effects in other studies in which they were tested in CS or CS/virus models [185, 206]. In the current work, anti-inflammatory efficacy was detectable on cell numbers and cytokines only when using a high dose of 30 mg/kg. An explanation for this might be provided by a study of Susuki-Miyata et al. They showed that NTHi and Roflumilast synergize to induce PDE-4B2 expression *in vitro* and *in vivo* [260]. PDE-4B2 was linked to the induction of expression of chemokines such as CCL5, chemokine ligand 7 (CCL7, MCP-3) and CXCL10, which play an important role in the recruitment of inflammatory cells [261, 262]. Susuki-Miyata et al. demonstrated that Roflumilast is less effective in suppressing NTHi-induced CCL5, CCL7 and CXCL10 release in the presence of PDE-4B2 compared to PDE-4B2-depleted cells. These observations might explain the findings of this work that Roflumilast is less effective in our CS/NTHi model compared to other CS or CS/virus models. It further implicates that Roflumilast treatment might be less efficient in patients suffering from NTHi-induced inflammation.

The macrolide Azithromycin is used during exacerbations, and preventive application of the drug is regarded as a treatment option in patients with frequent exacerbations [195]. In the current work, Azithromycin treatment eliminated replication competent NTHi from BAL fluid of CS/NTHi-challenged mice. This finding might explain reduced exacerbation rates in clinics. Despite its described anti-inflammatory features, we did not observe anti-inflammatory effects of Azithromycin in our model [263]. This might be due to the very acute setup of the NTHi-induced inflammation in which a possible dampened inflammation due to NTHi elimination is not detectable as the readout is performed shortly after the infection.

Interestingly, anti-inflammatory effects of Azithromycin were observed in the established CS/H1N1/NTHi model. This novel and complex model of COPD exacerbation is described for the first time in the current work and depicts aspects of exacerbated lung inflammation such as cell counts of total cells, neutrophils and macrophages. It was established due to the fact that, besides virus infection or NTHi infection alone, simultaneous infection with virus/NTHi was found in COPD patients during exacerbations [169]. The finding that Azithromycin had anti-inflammatory effects and reduced numbers of total cells, neutrophils, macrophages as well as TNF-α and KC levels in the lungs of the CS/H1N1/NTHi-challenged mice but not in the CS/NTHi model indicates that Azithromycin might have anti-inflammatory effects in particular on viral-induced inflammation. Supporting findings were made by Beigelman et al., who described anti-inflammatory properties of Azithromycin in a

mouse model of viral bronchiolitis [264]. As already described for the CS/NTHi model Azithromycin treatment furthermore eliminated replication competent NTHi from BAL fluid of CS/H1N1/NTHi-challenged mice. Both Dexamethasone and Roflumilast treatment did not have any anti-inflammatory effects.

In conclusion, four pre-clinical mouse models were established in this work (CS/H1N1, CS/RSV, CS/NTHi, CS/H1N1/NTHi) depicting clinically relevant aspects of human COPD and viral- and bacterial-induced exacerbations. Benchmarking of the models with clinically relevant treatments corroborate previous findings and furthermore provide additional explanations for clinical observations. In particular, the finding that corticosteroid treatment did not have any overall positive effect and resulted in an increased viral- and bacterial-burden and an aggravated loss of body-weight in all the established models should raise concerns regarding corticosteroid treatment in the general COPD population. Moreover, the finding that Tiotropium had anti-inflammatory effects in CS/virus models in this work might help to understand the observed reduction in exacerbation frequency in COPD patients treated with the drug. The very impressive and clear results of the Ab studies targeting the IL-1 pathway prove that the established models might be a valuable tool for the development of novel therapies in the fight against COPD and its tremendous impact on human health and economies worldwide.

References

1. Vestbo, J., et al., *Global strategy for the diagnosis, management, and prevention of chronic obstructive pulmonary disease: GOLD executive summary.* Am J Respir Crit Care Med, 2013. **187**(4): p. 347-65.

2. Mathers, C.D. and D. Loncar, *Projections of global mortality and burden of disease from 2002 to 2030.* PLoS Med, 2006. **3**(11): p. e442.

3. Anzueto, A., *Impact of exacerbations on COPD.* Eur Respir Rev, 2010. **19**(116): p. 113-8.

4. Anzueto, A., I. Leimer, and S. Kesten, *Impact of frequency of COPD exacerbations on pulmonary function, health status and clinical outcomes.* Int J Chron Obstruct Pulmon Dis, 2009. **4**: p. 245-51.

5. Wedzicha, J.A., *Mechanisms of Chronic Obstructive Pulmonary Disease Exacerbations.* Ann Am Thorac Soc, 2015. **12 Suppl 2**: p. S157-S159.

6. van den Boom, G., et al., *Active detection of chronic obstructive pulmonary disease and asthma in the general population. Results and economic consequences of the DIMCA program.* Am J Respir Crit Care Med, 1998. **158**(6): p. 1730-8.

7. Aisanov, Z., et al., *Primary care physician perceptions on the diagnosis and management of chronic obstructive pulmonary disease in diverse regions of the world.* Int J Chron Obstruct Pulmon Dis, 2012. **7**: p. 271-82.

8. Buist, A.S., et al., *International variation in the prevalence of COPD (the BOLD Study): a population-based prevalence study.* Lancet, 2007. **370**(9589): p. 741-50.

9. Pauwels, R.A. and K.F. Rabe, *Burden and clinical features of chronic obstructive pulmonary disease (COPD).* Lancet, 2004. **364**(9434): p. 613-620.

10. Kaszuba, E., et al., *Heart failure and levels of other comorbidities in patients with chronic obstructive pulmonary disease in a Swedish population: a register-based study.* BMC Res Notes, 2016. **9**(1): p. 215.

11. Chaudhary, S.C., et al., *Prevalence of psychiatric comorbidities in chronic obstructive pulmonary disease patients.* Lung India, 2016. **33**(2): p. 174-8.

12. Dance, A., *Health impact: Breathless.* Nature, 2012. **489**(7417): p. S2-S3.

13. Lee, J., V. Taneja, and R. Vassallo, *Cigarette smoking and inflammation: cellular and molecular mechanisms.* J Dent Res, 2012. **91**(2): p. 142-9.

14. Kark, J.D., M. Lebiush, and L. Rannon, *Cigarette smoking as a risk factor for epidemic a(h1n1) influenza in young men.* N Engl J Med, 1982. **307**(17): p. 1042-6.

15. Garber, K., *Biochemistry: A radical treatment.* Nature, 2012. **489**(7417): p. S4-S6.

16. Rutgers, S.R., et al., *Ongoing airway inflammation in patients with COPD who Do not currently smoke.* Chest, 2000. **117**(5 Suppl 1): p. 262S.

17. Bhome, A.B., *COPD in India: Iceberg or volcano?* J Thorac Dis, 2012. **4**(3): p. 298-309.

18. Hughes, V., *Public health: Where there's smoke.* Nature, 2012. **489**(7417): p. S18-S20.

19. ATS, *American Thoracic Society. What constitutes an adverse health effect of air pollution? Official statement of the American Thoracic Society.* Am J Respir Crit Care Med, 2000. **161**(2 Pt 1): p. 665-73.

20. Amoli, K., *Bronchopulmonary disease in Iranian housewives chronically exposed to indoor smoke.* Eur Respir J, 1998. **11**(3): p. 659-663.

21. Pandey, M.R., *Domestic smoke pollution and chronic bronchitis in a rural community of the Hill Region of Nepal.* Thorax, 1984. **39**(5): p. 337-339.

22. Kauffmann, F., et al., *Occupational exposure and 12-year spirometric changes among Paris area workers.* Br J Ind Med, 1982. **39**(3): p. 221-232.

23. Vogelzang, P.F., et al., *Endotoxin exposure as a major determinant of lung function decline in pig farmers.* Am J Respir Crit Care Med, 1998. **157**(1): p. 15-18.

24. Silverman, E.K., *Perspective: How can genetics help?* Nature, 2012. **489**(7417): p. S7-S7.

25. Fregonese, L. and J. Stolk, *Hereditary alpha-1-antitrypsin deficiency and its clinical consequences.* Orphanet J Rare Dis, 2008. **3**: p. 16.

26. Silverman, E.K. and R.A. Sandhaus, *Clinical practice. Alpha1-antitrypsin deficiency.* N Engl J Med, 2009. **360**(26): p. 2749-57.

27. Cao, J., et al., *Three-dimensional regulation of transcription.* Protein Cell, 2015. **6**(4): p. 241-53.

28. Severin, P.M., et al., *Effects of cytosine hydroxymethylation on DNA strand separation.* Biophys J, 2013. **104**(1): p. 208-15.

29. Patil, V.K., et al., *Interaction of prenatal maternal smoking, interleukin 13 genetic variants and DNA methylation influencing airflow and airway reactivity.* Clin Epigenetics, 2013. **5**(1): p. 22.

30. Meek, P.M., et al., *Epigenetic change (GATA-4 gene methylation) is associated with health status in chronic obstructive pulmonary disease.* Biol Res Nurs, 2015. **17**(2): p. 191-8.

31. Zong, D.D., R.Y. Ouyang, and P. Chen, *Epigenetic mechanisms in chronic obstructive pulmonary disease.* Eur Rev Med Pharmacol Sci, 2015. **19**(5): p. 844-56.

32. Qiu, W., et al., *Variable DNA methylation is associated with chronic obstructive pulmonary disease and lung function.* Am J Respir Crit Care Med, 2012. **185**(4): p. 373-81.

33. Monick, M.M., et al., *Coordinated changes in AHRR methylation in lymphoblasts and pulmonary macrophages from smokers.* Am J Med Genet B Neuropsychiatr Genet, 2012. **159B**(2): p. 141-51.

34. Wan, E.S., et al., *Cigarette smoking behaviors and time since quitting are associated with differential DNA methylation across the human genome.* Hum Mol Genet, 2012. **21**(13): p. 3073-82.

35. Barnes, P.J., *Immunology of asthma and chronic obstructive pulmonary disease.* Nat Rev Immunol, 2008. **8**(3): p. 183-192.

36. Barnes, P.J., *The cytokine network in asthma and chronic obstructive pulmonary disease.* J Clin Inv, 2008. **118**(11): p. 3546.

37. Sethi, S., et al., *Inflammation in COPD: implications for management.* Am J Med, 2012. **125**(12): p. 1162-70.

38. Barnes, P.J., *Alveolar macrophages as orchestrators of COPD.* COPD, 2004. **1**(1): p. 59-70.

39. Hoenderdos, K. and A. Condliffe, *The Neutrophil in Chronic Obstructive Pulmonary Disease.* Am J Respir Cell and Mol Biol, 2013. **48**(5): p. 531-539.

40. Bathoorn, E., et al., *Airways inflammation and treatment during acute exacerbations of COPD.* Int J Chron Obstruct Pulmon Dis, 2008. **3**(2): p. 217-29.

41. Stockley, R.A., *Neutrophils and protease/antiprotease imbalance.* Am J Respir Crit Care Med, 1999. **160**(5 Pt 2): p. S49-52.

42. Abboud, R.T. and S. Vimalanathan, *Pathogenesis of COPD. Part I. The role of protease-antiprotease imbalance in emphysema.* Int J Tuberc Lung Dis, 2008. **12**(4): p. 361-7.

43. Russell, R.E., et al., *Alveolar macrophage-mediated elastolysis: roles of matrix metalloproteinases, cysteine, and serine proteases.* Am J Physiol Lung Cell Mol Physiol, 2002. **283**(4): p. L867-73.

44. Nurwidya, F., T. Damayanti, and F. Yunus, *The Role of Innate and Adaptive Immune Cells in the Immunopathogenesis of Chronic Obstructive Pulmonary Disease.* Tuberc Respir Dis (Seoul), 2016. **79**(1): p. 5-13.

45. Barczyk, A., et al., *Cytokine production by bronchoalveolar lavage T lymphocytes in chronic obstructive pulmonary disease.* J Allergy Clin Immunol, 2006. **117**(6): p. 1484-1492.

46. Ostler, T., W. Davidson, and S. Ehl, *Virus clearance and immunopathology by CD8(+) T cells during infection with respiratory syncytial virus are mediated by IFN-gamma.* Eur J Immunol, 2002. **32**(8): p. 2117-23.

47. de Boer, W.I., et al., *Monocyte chemoattractant protein 1, interleukin 8, and chronic airways inflammation in COPD.* J Pathol, 2000. **190**(5): p. 619-626.

48. Traves, S.L., et al., *Increased levels of the chemokines GROalpha and MCP-1 in sputum samples from patients with COPD.* Thorax, 2002. **57**(7): p. 590-595.

49. Costa, C., et al., *CXCR3 and CCR5 chemokines in induced sputum from patients with COPD.* Chest, 2008. **133**(1): p. 26-33.

50. Saetta, M., et al., *Increased expression of the chemokine receptor CXCR3 and its ligand CXCL10 in peripheral airways of smokers with chronic obstructive pulmonary disease.* Am J Respir Crit Care Med, 2002. **165**(10): p. 1404-1409.

51. Smyth, L.J., et al., *CD8 chemokine receptors in chronic obstructive pulmonary disease.* Clin Exp Immunol, 2008. **154**(1): p. 56-63.

52. Culpitt, S.V., et al., *Impaired inhibition by dexamethasone of cytokine release by alveolar macrophages from patients with chronic obstructive pulmonary disease.* Am J Respir Crit Care Med, 2003. **167**(1): p. 24-31.

53. Shao, M.X. and J.A. Nadel, *Neutrophil elastase induces MUC5AC mucin production in human airway epithelial cells via a cascade involving protein kinase C, reactive oxygen species, and TNF-alpha-converting enzyme.* J Immunol, 2005. **175**(6): p. 4009-4016.

54. de Boer, W.I., et al., *Transforming growth factor beta1 and recruitment of macrophages and mast cells in airways in chronic obstructive pulmonary disease.* Am J Respir Crit Care Med, 1998. **158**(6): p. 1951-1957.

55. Takizawa, H., et al., *Increased expression of transforming growth factor-beta1 in small airway epithelium from tobacco smokers and patients with chronic obstructive pulmonary disease (COPD).* Am J Respir Crit Care Med, 2001. **163**(6): p. 1476-1483.

56. Grumelli, S., et al., *An immune basis for lung parenchymal destruction in chronic obstructive pulmonary disease and emphysema.* PLoS Med, 2004. **1**(1): p. e8.

57. Di Stefano, A., et al., *STAT4 activation in smokers and patients with chronic obstructive pulmonary disease.* Eur Respir J, 2004. **24**(1): p. 78-85.

58. Trinchieri, G., S. Pflanz, and R.A. Kastelein, *The IL-12 family of heterodimeric cytokines: new players in the regulation of T cell responses.* Immunity, 2003. **19**(5): p. 641-644.

59. Wills-Karp, M., *Interleukin-13 in asthma pathogenesis.* Immunol. Rev, 2004. **202**: p. 175-190.

60. Kuperman, D.A., et al., *Direct effects of interleukin-13 on epithelial cells cause airway hyperreactivity and mucus overproduction in asthma.* Nat. Med, 2002. **8**(8): p. 885-889.

61. Dragon, S., et al., *IL-17 enhances IL-1beta-mediated CXCL-8 release from human airway smooth muscle cells.* Am J Physiol Lung Cell Mol Physiol, 2007. **292**(4): p. L1023-L1029.

62. Volpe, E., et al., *A critical function for transforming growth factor-beta, interleukin 23 and proinflammatory cytokines in driving and modulating human T(H)-17 responses.* Nat Immunol, 2008. **9**(6): p. 650-7.

63. Manel, N., D. Unutmaz, and D.R. Littman, *The differentiation of human T(H)-17 cells requires transforming growth factor-beta and induction of the nuclear receptor RORgammat.* Nat Immunol, 2008. **9**(6): p. 641-9.

64. Bhowmik, A., et al., *Relation of sputum inflammatory markers to symptoms and lung function changes in COPD exacerbations.* Thorax, 2000. **55**(2): p. 114-120.

65. Thomas, P.S., D.H. Yates, and P.J. Barnes, *Tumor necrosis factor-alpha increases airway responsiveness and sputum neutrophilia in normal human subjects.* Am J Respir Crit Care Med, 1995. **152**(1): p. 76-80.

66. Acuner Ozbabacan, S.E., et al., *The structural pathway of interleukin 1 (IL-1) initiated signaling reveals mechanisms of oncogenic mutations and SNPs in inflammation and cancer.* PLoS Comput Biol, 2014. **10**(2): p. e1003470.

67. Dinarello, C.A., *Immunological and inflammatory functions of the interleukin-1 family.* Annu Rev Immunol, 2009. **27**: p. 519-50.

68. Dinarello, C.A., *Anti-inflammatory Agents: Present and Future.* Cell, 2010. **140**(6): p. 935-50.

69. Gabay, C., C. Lamacchia, and G. Palmer, *IL-1 pathways in inflammation and human diseases.* Nat Rev Rheumatol, 2010. **6**(4): p. 232-41.

70. Sims, J.E. and D.E. Smith, *The IL-1 family: regulators of immunity.* Nat Rev Immunol, 2010. **10**(2): p. 89-102.

71. Dinarello, C.A., *Interleukin-1 in the pathogenesis and treatment of inflammatory diseases.* Blood, 2011. **117**(14): p. 3720-32.

72. Hacham, M., et al., *Different patterns of interleukin-1alpha and interleukin-1beta expression in organs of normal young and old mice.* Eur Cytokine Netw, 2002. **13**(1): p. 55-65.

73. Rider, P., et al., *IL-1alpha and IL-1beta recruit different myeloid cells and promote different stages of sterile inflammation.* J Immunol, 2011. **187**(9): p. 4835-43.

74. Gross, O., et al., *Inflammasome activators induce interleukin-1alpha secretion via distinct pathways with differential requirement for the protease function of caspase-1.* Immunity, 2012. **36**(3): p. 388-400.

75. Apte, R.N. and E. Voronov, *Is interleukin-1 a good or bad 'guy' in tumor immunobiology and immunotherapy?* Immunol Rev, 2008. **222**: p. 222-41.

76. Lukens, J.R., J.M. Gross, and T.D. Kanneganti, *IL-1 family cytokines trigger sterile inflammatory disease.* Front Immunol, 2012. **3**: p. 315.

77. van de Veerdonk, F.L. and M.G. Netea, *New Insights in the Immunobiology of IL-1 Family Members.* Front Immunol, 2013. **4**: p. 167.

78. Dinarello, C.A., *A signal for the caspase-1 inflammasome free of TLR.* Immunity, 2007. **26**(4): p. 383-5.

79. Brikos, C., et al., *Mass spectrometric analysis of the endogenous type I interleukin-1 (IL-1) receptor signaling complex formed after IL-1 binding identifies IL-1RAcP, MyD88, and IRAK-4 as the stable components.* Mol Cell Proteomics, 2007. **6**(9): p. 1551-9.

80. Huang, J., et al., *Recruitment of IRAK to the interleukin 1 receptor complex requires interleukin 1 receptor accessory protein.* Proc Natl Acad Sci U S A, 1997. **94**(24): p. 12829-32.

81. Cao, Z., W.J. Henzel, and X. Gao, *IRAK: a kinase associated with the interleukin-1 receptor.* Science, 1996. **271**(5252): p. 1128-31.

82. Wald, D., et al., *SIGIRR, a negative regulator of Toll-like receptor-interleukin 1 receptor signaling.* Nat Immunol, 2003. **4**(9): p. 920-7.

83. Garlanda, C., et al., *Intestinal inflammation in mice deficient in Tir8, an inhibitory member of the IL-1 receptor family.* Proc Natl Acad Sci U S A, 2004. **101**(10): p. 3522-6.

84. Dinarello, C.A. and J.W. van der Meer, *Treating inflammation by blocking interleukin-1 in humans.* Semin Immunol, 2013. **25**(6): p. 469-84.

85. Botelho, F.M., et al., *IL-1alpha/IL-1R1 expression in chronic obstructive pulmonary disease and mechanistic relevance to smoke-induced neutrophilia in mice.* PLoS One, 2011. **6**(12): p. e28457.

86. Pauwels, N.S., et al., *Role of IL-1alpha and the Nlrp3/caspase-1/IL-1beta axis in cigarette smoke-induced pulmonary inflammation and COPD.* Eur Respir J, 2011. **38**(5): p. 1019-1028.

87. Agusti, A., et al., *Persistent systemic inflammation is associated with poor clinical outcomes in COPD: a novel phenotype.* PLoS One, 2012. **7**(5): p. e37483.

88. Hurst, J.R., et al., *Systemic and upper and lower airway inflammation at exacerbation of chronic obstructive pulmonary disease.* Am J Respir Crit Care Med, 2006. **173**(1): p. 71-78.

89. Samara, K.D., et al., *Somatic DNA alterations in lung epithelial barrier cells in COPD patients.* Pulm Pharmacol Ther, 2010. **23**(3): p. 208-14.

90. Garlanda, C., C.A. Dinarello, and A. Mantovani, *The interleukin-1 family: back to the future.* Immunity, 2013. **39**(6): p. 1003-1018.

91. Rogliani, P., et al., *Canakinumab for the treatment of chronic obstructive pulmonary disease.* Pulm Pharmacol Ther, 2015. **31**: p. 15-27.

92. Sethi, S., et al., *A Phase 2 Study Of Medi8968, An Anti-Interleukin-1 Receptor I (il-1ri) Monoclonal Antibody, In Adults With Moderate-To-Very Severe Chronic Obstructive Pulmonary Disease (COPD).* Am J Respir Crit Care Med, 2015. **191**: p. A3964.

93. Rodriguez-Roisin, R., *Toward a consensus definition for COPD exacerbations.* Chest, 2000. **117**(5 Suppl 2): p. 398S-401S.

94. Burge, S. and J.A. Wedzicha, *COPD exacerbations: definitions and classifications.* Eur Respir J Suppl, 2003. **41**: p. 46s-53s.

95. Seemungal, T.A., et al., *Time course and recovery of exacerbations in patients with chronic obstructive pulmonary disease.* Am J Respir Crit Care Med, 2000. **161**(5): p. 1608-1613.

96. Wedzicha, J.A. and T.A. Seemungal, *COPD exacerbations: defining their cause and prevention.* Lancet, 2007. **370**(9589): p. 786-796.

97. Mannino, D.M., et al., *The natural history of chronic obstructive pulmonary disease.* Eur Respir J, 2006. **27**(3): p. 627-43.

98. Donaldson, G.C., et al., *Relationship between exacerbation frequency and lung function decline in chronic obstructive pulmonary disease.* Thorax, 2002. **57**(10): p. 847-52.

99. Pasquale, M.K., et al., *Impact of exacerbations on health care cost and resource utilization in chronic obstructive pulmonary disease patients with chronic bronchitis from a predominantly Medicare population.* Int J Chron Obstruct Pulmon Dis, 2012. **7**: p. 757-64.

100. Dalal, A.A., et al., *Costs of COPD exacerbations in the emergency department and inpatient setting.* Respir Med, 2011. **105**(3): p. 454-60.

101. Yu, A.P., et al., *Incremental third-party costs associated with COPD exacerbations: a retrospective claims analysis.* J Med Econ, 2011. **14**(3): p. 315-23.

102. Di Stefano, A., et al., *Severity of airflow limitation is associated with severity of airway inflammation in smokers.* Am J Respir Crit Care Med, 1998. **158**(4): p. 1277-85.

103. Marashian, S.M., et al., *Role of Innate Lymphoid Cells in Lung Disease.* Iran J Allergy Asthma Immunol, 2015. **14**(4): p. 346-60.

104. Silver, J.S., et al., *Inflammatory triggers associated with exacerbations of COPD orchestrate plasticity of group 2 innate lymphoid cells in the lungs.* Nat Immunol, 2016. **17**(6): p. 626-35.

105. Sapey, E. and R.A. Stockley, *COPD exacerbations - 2: Aetiology.* Thorax, 2006. **61**(3): p. 250-258.

106. Drost, E.M., et al., *Oxidative stress and airway inflammation in severe exacerbations of COPD.* Thorax, 2005. **60**(4): p. 293-300.

107. Saetta, M., et al., *Airway eosinophilia in chronic bronchitis during exacerbations.* Am J Respir Crit Care Med, 1994. **150**(6 Pt 1): p. 1646-1652.

108. Qiu, Y., et al., *Biopsy neutrophilia, neutrophil chemokine and receptor gene expression in severe exacerbations of chronic obstructive pulmonary disease.* Am J Respir Crit Care Med, 2003. **168**(8): p. 968-975.

109. Hansel, T.T. and P.J. Barnes, *New drugs for exacerbations of chronic obstructive pulmonary disease.* Lancet, 2009. **374**(9691): p. 744-55.

110. Dewar, M. and R.W. Curry, Jr., *Chronic obstructive pulmonary disease: diagnostic considerations.* Am Fam Physician, 2006. **73**(4): p. 669-76.

111. Anderson, H.R., et al., *Air pollution and daily admissions for chronic obstructive pulmonary disease in 6 European cities: results from the APHEA project.* Eur Respir J, 1997. **10**(5): p. 1064-1071.

112. Dockery, D.W., et al., *An association between air pollution and mortality in six U.S. cities.* N Engl J Med, 1993. **329**(24): p. 1753-1759.

113. MacNee, W. and K. Donaldson, *Exacerbations of COPD: environmental mechanisms.* Chest, 2000. **117**(5 Suppl 2): p. 390S-397S.

114. Mallia, P. and S.L. Johnston, *How viral infections cause exacerbation of airway diseases.* Chest, 2006. **130**(4): p. 1203-1210.

115. Proud, D. and C.W. Chow, *Role of viral infections in asthma and chronic obstructive pulmonary disease.* Am J Respir Cell Mol Biol, 2006. **35**(5): p. 513-518.

116. Varkey, J.B. and B. Varkey, *Viral infections in patients with chronic obstructive pulmonary disease.* Curr Opin Pulm Med, 2008. **14**(2): p. 89-94.

117. Seemungal, T., et al., *Respiratory viruses, symptoms, and inflammatory markers in acute exacerbations and stable chronic obstructive pulmonary disease.* Am J Respir Crit Care Med, 2001. **164**(9): p. 1618-1623.

118. Varkey, J.B., A.B. Varkey, and B. Varkey, *Prophylactic vaccinations in chronic obstructive pulmonary disease: current status.* Curr Opin Pulm Med, 2009. **15**(2): p. 90-9.

119. McHardy, V.U., et al., *A study of infective and other factors in exacerbations of chronic bronchitis.* Br J Dis Chest, 1980. **74**(3): p. 228-238.

120. De, S.G., et al., *Importance of viral and bacterial infections in chronic obstructive pulmonary disease exacerbations.* J Clin Virol, 2009. **46**(2): p. 129-133.

121. Sethi, S., *Infectious etiology of acute exacerbations of chronic bronchitis.* Chest, 2000. **117**(5 Suppl 2): p. 380S-385S.

122. Wilkinson, T.M., et al., *Effect of interactions between lower airway bacterial and rhinoviral infection in exacerbations of COPD.* Chest, 2006. **129**(2): p. 317-324.

123. Anthonisen, N.R., et al., *Antibiotic therapy in exacerbations of chronic obstructive pulmonary disease.* Ann Intern Med, 1987. **106**(2): p. 196-204.

124. Hale, B.G., R.A. Albrecht, and A. Garcia-Sastre, *Innate immune evasion strategies of influenza viruses.* Future Microbiol, 2010. **5**(1): p. 23-41.

125. Salomon, R. and R.G. Webster, *The influenza virus enigma.* Cell, 2009. **136**(3): p. 402-10.

126. Nayak, D.P., et al., *Influenza virus morphogenesis and budding.* Virus Res, 2009. **143**(2): p. 147-61.

127. Gonzalez, P.A., et al., *Respiratory syncytial virus infection and immunity.* Rev Med Virol, 2012. **22**(4): p. 230-44.

128. Staat, M.A., *Respiratory syncytial virus infections in children.* Semin Respir Infect, 2002. **17**(1): p. 15-20.

129. Welliver, R.C., *Review of epidemiology and clinical risk factors for severe respiratory syncytial virus (RSV) infection.* J Pediatr, 2003. **143**(5 Suppl): p. S112-7.

130. Storey, S., *Respiratory syncytial virus market.* Nat Rev Drug Discov, 2010. **9**(1): p. 15-6.

131. Falsey, A.R. and E.E. Walsh, *Respiratory syncytial virus infection in adults.* Clin Microbiol Rev, 2000. **13**(3): p. 371-84.

132. Falsey, A.R., et al., *Respiratory syncytial virus infection in elderly and high-risk adults.* N Engl J Med, 2005. **352**(17): p. 1749-59.

133. Tripp, R.A., C. Oshansky, and R. Alvarez, *Cytokines and respiratory syncytial virus infection.* Proc Am Thorac Soc, 2005. **2**(2): p. 147-9.

134. Hegele, R.G., et al., *Mechanisms of airway narrowing and hyperresponsiveness in viral respiratory tract infections.* Am J Respir Crit Care Med, 1995. **151**(5): p. 1659-64; discussion 1664-5.

135. Kim, J., et al., *Role of NF-kappa B in cytokine production induced from human airway epithelial cells by rhinovirus infection.* J Immunol, 2000. **165**(6): p. 3384-92.

136. Biagioli, M.C., et al., *The role of oxidative stress in rhinovirus induced elaboration of IL-8 by respiratory epithelial cells.* Free Radic Biol Med, 1999. **26**(3-4): p. 454-62.

137. Subauste, M.C., et al., *Infection of a human respiratory epithelial cell line with rhinovirus. Induction of cytokine release and modulation of susceptibility to infection by cytokine exposure.* J Clin Invest, 1995. **96**(1): p. 549-57.

138. Schroth, M.K., et al., *Rhinovirus replication causes RANTES production in primary bronchial epithelial cells.* Am J Respir Cell Mol Biol, 1999. **20**(6): p. 1220-8.

139. Randall, R.E. and S. Goodbourn, *Interferons and viruses: an interplay between induction, signalling, antiviral responses and virus countermeasures.* J Gen Virol, 2008. **89**(Pt 1): p. 1-47.

140. Ramaswamy, M., et al., *Specific inhibition of type I interferon signal transduction by respiratory syncytial virus.* Am J Respir Cell Mol Biol, 2004. **30**(6): p. 893-900.

141. Chelbi-Alix, M.K. and J. Wietzerbin, *Interferon, a growing cytokine family: 50 years of interferon research.* Biochimie, 2007. **89**(6-7): p. 713-8.

142. Turner, S.J., et al., *Disregulated influenza A virus-specific CD8+ T cell homeostasis in the absence of IFN-gamma signaling.* J Immunol, 2007. **178**(12): p. 7616-22.

143. Garcia-Sastre, A., et al., *Influenza A virus lacking the NS1 gene replicates in interferon-deficient systems.* Virology, 1998. **252**(2): p. 324-30.

144. Garcia-Sastre, A., et al., *The role of interferon in influenza virus tissue tropism.* J Virol, 1998. **72**(11): p. 8550-8.

145. Szretter, K.J., et al., *Early control of H5N1 influenza virus replication by the type I interferon response in mice.* J Virol, 2009. **83**(11): p. 5825-34.

146. Kugel, D., et al., *Intranasal administration of alpha interferon reduces seasonal influenza A virus morbidity in ferrets.* J Virol, 2009. **83**(8): p. 3843-51.

147. Pichlmair, A., et al., *RIG-I-mediated antiviral responses to single-stranded RNA bearing 5'-phosphates.* Science, 2006. **314**(5801): p. 997-1001.

148. Mogensen, T.H., *Pathogen recognition and inflammatory signaling in innate immune defenses.* Clin Microbiol Rev, 2009. **22**(2): p. 240-73, Table of Contents.

149. Allen, I.C., et al., *The NLRP3 inflammasome mediates in vivo innate immunity to influenza A virus through recognition of viral RNA.* Immunity, 2009. **30**(4): p. 556-65.

150. Thomas, P.G., et al., *The intracellular sensor NLRP3 mediates key innate and healing responses to influenza A virus via the regulation of caspase-1.* Immunity, 2009. **30**(4): p. 566-75.

151. Glaab, T., et al., *Invasive and noninvasive methods for studying pulmonary function in mice.* Respir Res, 2007. **8**: p. 63.

152. Nie, Z., et al., *Role of TNF-alpha in virus-induced airway hyperresponsiveness and neuronal M(2) muscarinic receptor dysfunction.* Br J Pharmacol, 2011. **164**(2b): p. 444-52.

153. Jacoby, D.B. and A.D. Fryer, *Interaction of viral infections with muscarinic receptors.* Clin Exp Allergy, 1999. **29 Suppl 2**: p. 59-64.

154. Fryer, A.D. and J. Maclagan, *Muscarinic inhibitory receptors in pulmonary parasympathetic nerves in the guinea-pig.* Br J Pharmacol, 1984. **83**(4): p. 973-8.

155. Fryer, A.D. and D.B. Jacoby, *Parainfluenza virus infection damages inhibitory M2 muscarinic receptors on pulmonary parasympathetic nerves in the guinea-pig.* Br J Pharmacol, 1991. **102**(1): p. 267-71.

156. Monick, M.M., et al., *Respiratory syncytial virus up-regulates TLR4 and sensitizes airway epithelial cells to endotoxin.* J Biol Chem, 2003. **278**(52): p. 53035-44.

157. King, P.T. and R. Sharma, *The Lung Immune Response to Nontypeable Haemophilus influenzae (Lung Immunity to NTHi).* J Immunol Res, 2015. **2015**: p. 706376.

158. Zwahlen, A., et al., *The molecular basis of pathogenicity in Haemophilus influenzae: comparative virulence of genetically-related capsular transformants and correlation with changes at the capsulation locus cap.* Microb Pathog, 1989. **7**(3): p. 225-35.

159. Kadlec, K., et al., *Molecular basis of sulfonamide and trimethoprim resistance in fish-pathogenic Aeromonas isolates.* Appl Environ Microbiol, 2011. **77**(20): p. 7147-50.

160. Novotny, L.A. and L.O. Bakaletz, *Intercellular adhesion molecule 1 serves as a primary cognate receptor for the Type IV pilus of nontypeable Haemophilus influenzae.* Cell Microbiol, 2016.

161. Avadhanula, V., et al., *Nontypeable Haemophilus influenzae adheres to intercellular adhesion molecule 1 (ICAM-1) on respiratory epithelial cells and upregulates ICAM-1 expression.* Infect Immun, 2006. **74**(2): p. 830-8.

162. Othumpangat, S., et al., *ICAM-1 regulates the survival of influenza virus in lung epithelial cells during the early stages of infection.* Virology, 2016. **487**: p. 85-94.

163. King, P., *Haemophilus influenzae and the lung (Haemophilus and the lung).* Clin Transl Med, 2012. **1**(1): p. 10.

164. Jono, H., et al., *Transforming growth factor-beta -Smad signaling pathway cooperates with NF-kappa B to mediate nontypeable Haemophilus influenzae-induced MUC2 mucin transcription.* J Biol Chem, 2002. **277**(47): p. 45547-57.

165. Khair, O.A., R.J. Davies, and J.L. Devalia, *Bacterial-induced release of inflammatory mediators by bronchial epithelial cells.* Eur Respir J, 1996. **9**(9): p. 1913-22.

166. Mikami, F., et al., *Epidermal growth factor receptor acts as a negative regulator for bacterium nontypeable Haemophilus influenzae-induced Toll-like receptor 2 expression via an Src-dependent p38 mitogen-activated protein kinase signaling pathway.* J Biol Chem, 2005. **280**(43): p. 36185-94.

167. Ueki, I.F., et al., *Respiratory virus-induced EGFR activation suppresses IRF1-dependent interferon lambda and antiviral defense in airway epithelium.* J Exp Med, 2013. **210**(10): p. 1929-36.

168. Monick, M.M., et al., *Activation of the epidermal growth factor receptor by respiratory syncytial virus results in increased inflammation and delayed apoptosis.* J Biol Chem, 2005. **280**(3): p. 2147-58.

169. Bandi, V., et al., *Infectious exacerbations of chronic obstructive pulmonary disease associated with respiratory viruses and non-typeable Haemophilus influenzae.* FEMS Immunol Med Microbiol, 2003. **37**(1): p. 69-75.

170. Barnes, P.J., *New treatments for COPD.* Nat Rev Drug Discov, 2002. **1**(6): p. 437-446.

171. Li, H., et al., *A step-wise application of methylprednisolone versus dexamethasone in the treatment of acute exacerbations of COPD.* Respirology, 2003. **8**(2): p. 199-204.

172. Park, H.Y., S.F. Man, and D.D. Sin, *Inhaled corticosteroids for chronic obstructive pulmonary disease.* BMJ, 2012. **345**: p. e6843.

173. Rich, A., *Corticosteroids and chronic obstructive pulmonary disease in the nursing home.* J Am Med. Dir. Assoc, 2005. **6**(3 Suppl): p. S68-S74.

174. Calverley, P.M., et al., *Salmeterol and fluticasone propionate and survival in chronic obstructive pulmonary disease.* N Engl J Med, 2007. **356**(8): p. 775-789.

175. Magnussen, H., et al., *Withdrawal of inhaled glucocorticoids and exacerbations of COPD.* N Engl J Med, 2014. **371**(14): p. 1285-1294.

176. Rabe, K.F., *Update on roflumilast, a phosphodiesterase 4 inhibitor for the treatment of chronic obstructive pulmonary disease.* Br J Pharmacol, 2011. **163**(1): p. 53-67.

177. Oba, Y. and N.A. Lone, *Efficacy and safety of roflumilast in patients with chronic obstructive pulmonary disease: a systematic review and meta-analysis.* Ther Adv Respir Dis, 2013. **7**(1): p. 13-24.

178. Rodriguez-Roisin, R., *COPD exacerbations.5: management.* Thorax, 2006. **61**(6): p. 535-544.

179. Rabe, K.F., et al., *Global strategy for the diagnosis, management, and prevention of chronic obstructive pulmonary disease GOLD executive summary.* Am J Respir Crit Care Med, 2007. **176**(6): p. 532-555.

180. Disse, B., et al., *Tiotropium (Spiriva): mechanistical considerations and clinical profile in obstructive lung disease.* Life Sci, 1999. **64**(6-7): p. 457-464.

181. Tashkin, D.P., et al., *A 4-year trial of tiotropium in chronic obstructive pulmonary disease.* N Engl J Med, 2008. **359**(15): p. 1543-1554.

182. Vogelmeier, C., et al., *Tiotropium versus salmeterol for the prevention of exacerbations of COPD.* N Engl J Med, 2011. **364**(12): p. 1093-1103.

183. Arai, N., et al., *Inhibition of neutrophil elastase-induced goblet cell metaplasia by tiotropium in mice.* Eur Respir J, 2010. **35**(5): p. 1164-1171.

184. Cui, Y., et al., *Tiotropium reduction of lung inflammation in a model of chronic gastro-oesophageal reflux.* Eur Respir J, 2010. **35**(6): p. 1370-1376.

185. Wollin, L. and M.P. Pieper, *Tiotropium bromide exerts anti-inflammatory activity in a cigarette smoke mouse model of COPD.* Pulm Pharmacol Ther, 2010. **23**(4): p. 345-354.

186. Bosnjak, B., et al., *Tiotropium bromide inhibits relapsing allergic asthma in BALB/c mice.* Pulm Pharmacol Ther, 2014. **27**(1): p. 44-51.

187. Buels, K.S., D.B. Jacoby, and A.D. Fryer, *Non-bronchodilating mechanisms of tiotropium prevent airway hyperreactivity in a guinea-pig model of allergic asthma.* Br J Pharmacol, 2012. **165**(5): p. 1501-1514.

188. Ohta, S., et al., *Effect of tiotropium bromide on airway inflammation and remodelling in a mouse model of asthma.* Clin Exp Allergy, 2010. **40**(8): p. 1266-1275.

189. Bos, I.S., et al., *Inhibition of allergen-induced airway remodelling by tiotropium and budesonide: a comparison.* Eur Respir J, 2007. **30**(4): p. 653-661.

190. Gosens, R., et al., *Protective effects of tiotropium bromide in the progression of airway smooth muscle remodeling.* Am J Respir Crit Care Med, 2005. **171**(10): p. 1096-1102.

191. Asano, K., et al., *Suppressive activity of tiotropium bromide on matrix metalloproteinase production from lung fibroblasts in vitro.* Int J Chron Obstruct Pulmon Dis, 2008. **3**(4): p. 781-789.

192. Bateman, E.D., et al., *Alternative mechanisms for tiotropium.* Pulm Pharmacol Ther, 2009. **22**(6): p. 533-542.

193. Buhling, F., et al., *Tiotropium suppresses acetylcholine-induced release of chemotactic mediators in vitro.* Respir Med, 2007. **101**(11): p. 2386-2394.

194. Suzaki, I., et al., *Suppression of IL-8 production from airway cells by tiotropium bromide in vitro.* Int J Chron Obstruct Pulmon Dis, 2011. **6**: p. 439-448.

195. Euba, B., et al., *Relationship between azithromycin susceptibility and administration efficacy for nontypeable Haemophilus influenzae respiratory infection.* Antimicrob Agents Chemother, 2015. **59**(5): p. 2700-12.

196. Retsema, J., et al., *Spectrum and mode of action of azithromycin (CP-62,993), a new 15-membered-ring macrolide with improved potency against gram-negative organisms.* Antimicrob Agents Chemother, 1987. **31**(12): p. 1939-47.

197. Taylor, S.P., E. Sellers, and B.T. Taylor, *Azithromycin for the Prevention of COPD Exacerbations: The Good, Bad, and Ugly.* Am J Med, 2015. **128**(12): p. 1362 e1-6.

198. Vlahos, R. and S. Bozinovski, *Recent advances in pre-clinical mouse models of COPD.* Clin Sci (Lond), 2014. **126**(4): p. 253-65.

199. Vlahos, R., et al., *Modelling COPD in mice.* Pulm Pharmacol Ther, 2006. **19**(1): p. 12-7.

200. Dawkins, P.A. and R.A. Stockley, *Animal models of chronic obstructive pulmonary disease.* Thorax, 2001. **56**(12): p. 972-977.

201. Mahadeva, R. and S.D. Shapiro, *Chronic obstructive pulmonary disease * 3: Experimental animal models of pulmonary emphysema.* Thorax, 2002. **57**(10): p. 908-14.

202. Shapiro, S.D., *Animal models for COPD.* Chest, 2000. **117**(5 Suppl 1): p. 223S-227S.

203. Rinaldi, M., et al., *Long-term nose-only cigarette smoke exposure induces emphysema and mild skeletal muscle dysfunction in mice.* Dis Model Mech, 2012. **5**(3): p. 333-341.

204. D'Armiento, J., et al., *Collagenase expression in the lungs of transgenic mice causes pulmonary emphysema.* Cell, 1992. **71**(6): p. 955-961.

205. Bauer, C.M., et al., *Treating viral exacerbations of chronic obstructive pulmonary disease: insights from a mouse model of cigarette smoke and H1N1 influenza infection.* PLoS One, 2010. **5**(10): p. e13251.

206. Bucher, H., et al., *Tiotropium Attenuates Virus-Induced Pulmonary Inflammation in Cigarette Smoke-Exposed Mice.* J Pharmacol Exp Ther, 2016. **357**(3): p. 606-18.

207. Hamelmann, E., et al., *Noninvasive measurement of airway responsiveness in allergic mice using barometric plethysmography.* Am J Respir Crit Care Med, 1997. **156**(3 Pt 1): p. 766-775.

208. Mitzner, W. and C. Tankersley, *Noninvasive measurement of airway responsiveness in allergic mice using barometric plethysmography.* Am J Respir Crit Care Med, 1998. **158**(1): p. 340-1.

209. Vanoirbeek, J.A., et al., *Noninvasive and invasive pulmonary function in mouse models of obstructive and restrictive respiratory diseases.* Am J Respir Cell Mol Biol, 2010. **42**(1): p. 96-104.

210. Singleton, R., et al., *Inability to evoke a long-lasting protective immune response to respiratory syncytial virus infection in mice correlates with ineffective nasal antibody responses.* J Virol, 2003. **77**(21): p. 11303-11311.

211. Collins, P.L. and B.S. Graham, *Viral and host factors in human respiratory syncytial virus pathogenesis.* J Virol, 2008. **82**(5): p. 2040-2055.

212. van der Velden, V.H., *Glucocorticoids: mechanisms of action and anti-inflammatory potential in asthma.* Mediators Inflamm, 1998. **7**(4): p. 229-237.

213. Kolahian, S. and R. Gosens, *Cholinergic regulation of airway inflammation and remodelling.* J Allergy, 2012. **2012**: p. 681258.

214. Gosens, R., et al., *Muscarinic receptor signaling in the pathophysiology of asthma and COPD.* Respir Res, 2006. **7**: p. 73.

215. Racke, K. and S. Matthiesen, *The airway cholinergic system: physiology and pharmacology.* Pulm Pharmacol Ther, 2004. **17**(4): p. 181-98.

216. Sauter, N.K., et al., *Binding of influenza virus hemagglutinin to analogs of its cell-surface receptor, sialic acid: analysis by proton nuclear magnetic resonance spectroscopy and X-ray crystallography.* Biochemistry, 1992. **31**(40): p. 9609-21.

217. Lawrence, S.M., et al., *Cloning and expression of the human N-acetylneuraminic acid phosphate synthase gene with 2-keto-3-deoxy-D-glycero- D-galacto-nononic acid biosynthetic ability.* J Biol Chem, 2000. **275**(23): p. 17869-77.

218. Pezzulo, A.A., et al., *The air-liquid interface and use of primary cell cultures are important to recapitulate the transcriptional profile of in vivo airway epithelia.* Am J Physiol Lung Cell Mol Physiol, 2011. **300**(1): p. L25-31.

219. Han, Y., et al., *Influenza virus-induced lung inflammation was modulated by cigarette smoke exposure in mice.* PLoS One, 2014. **9**(1): p. e86166.

220. Tilp, C., et al., *Effects of conventional tobacco smoke and nicotine-free cigarette smoke on airway inflammation, airway remodelling and lung function in a triple allergen model of severe asthma.* Clin Exp Allergy, 2016. **46**(7): p. 957-72.

221. Mebratu, Y.A., et al., *Inflammation and emphysema in cigarette smoke-exposed mice when instilled with poly (I:C) or infected with influenza A or respiratory syncytial viruses.* Respir Res, 2016. **17**(1): p. 75.

222. Foronjy, R.F., et al., *Respiratory syncytial virus infections enhance cigarette smoke induced COPD in mice.* PLoS One, 2014. **9**(2): p. e90567.

223. Mamary, A.J. and G.J. Criner, *Tiotropium bromide for chronic obstructive pulmonary disease.* Expert Rev Respir Med, 2009. **3**(3): p. 211-220.

224. Keam, S.J. and G.M. Keating, *Tiotropium bromide. A review of its use as maintenance therapy in patients with COPD.* Treat Respir Med, 2004. **3**(4): p. 247-268.

225. Papi, A., et al., *Pathophysiology of exacerbations of chronic obstructive pulmonary disease.* Proc Am Thorac Soc, 2006. **3**(3): p. 245-251.

226. Rohde, G., et al., *Inflammatory response in acute viral exacerbations of COPD.* Infection, 2008. **36**(5): p. 427-433.

227. Kang, M.J., et al., *IFN-gamma-dependent DNA injury and/or apoptosis are critical in cigarette smoke-induced murine emphysema.* Proc Am Thorac Soc, 2006. **3**(6): p. 517-518.

228. Racke, K., U.R. Juergens, and S. Matthiesen, *Control by cholinergic mechanisms.* Eur J Pharmacol, 2006. **533**(1-3): p. 57-68.

229. Iesato, K., et al., *Tiotropium bromide attenuates respiratory syncytial virus replication in epithelial cells.* Respiration, 2008. **76**(4): p. 434-441.

230. MacRedmond, R.E., et al., *Fluticasone Induces Epithelial Injury and Alters Barrier Function in Normal Subjects.* J Steroids Horm Sci, 2014. **5**(2).

231. Singh, S., A.V. Amin, and Y.K. Loke, *Long-term use of inhaled corticosteroids and the risk of pneumonia in chronic obstructive pulmonary disease: a meta-analysis.* Arch Intern Med, 2009. **169**(3): p. 219-229.

232. Barnes, P.J., *Corticosteroid resistance in airway disease.* Proc Am Thorac Soc, 2004. **1**(3): p. 264-268.

233. Barnes, P.J., *Corticosteroid resistance in patients with asthma and chronic obstructive pulmonary disease.* J Allergy Clin Immunol, 2013. **131**(3): p. 636-645.

234. Rennard, S.I., et al., *Reduction of exacerbations by the PDE4 inhibitor roflumilast - the importance of defining different subsets of patients with COPD.* Respir Res, 2011. **12**: p. 18.

235. Karakiulakis, G. and M. Roth, *Muscarinic receptors and their antagonists in COPD: anti-inflammatory and antiremodeling effects.* Mediators Inflamm, 2012. **2012**: p. 409580.

236. Bafadhel, M., et al., *Acute exacerbations of chronic obstructive pulmonary disease: identification of biologic clusters and their biomarkers.* Am J Respir Crit Care Med, 2011. **184**(6): p. 662-671.

237. Gessner, C., et al., *Exhaled breath condensate cytokine patterns in chronic obstructive pulmonary disease.* Respir Med, 2005. **99**(10): p. 1229-1240.

238. Sapey, E., et al., *Imbalances between interleukin-1 and tumor necrosis factor agonists and antagonists in stable COPD.* J Clin. Immunol, 2009. **29**(4): p. 508-516.

239. Piper, S.C., et al., *The role of interleukin-1 and interleukin-18 in pro-inflammatory and anti-viral responses to rhinovirus in primary bronchial epithelial cells.* PLoS One, 2013. **8**(5): p. e63365.

240. Botelho, F.M., et al., *Cigarette smoke-induced accumulation of lung dendritic cells is interleukin-1alpha-dependent in mice.* Respir Res, 2012. **13**: p. 81.

241. Churg, A., et al., *The role of interleukin-1beta in murine cigarette smoke-induced emphysema and small airway remodeling.* Am J Respir Cell Mol Biol, 2009. **40**(4): p. 482-490.

242. Doz, E., et al., *Cigarette smoke-induced pulmonary inflammation is TLR4/MyD88 and IL-1R1/MyD88 signaling dependent.* J Immunol, 2008. **180**(2): p. 1169-1178.

243. Matsuki, T., et al., *IL-1 plays an important role in lipid metabolism by regulating insulin levels under physiological conditions.* J Exp Med, 2003. **198**(6): p. 877-888.

244. Stienstra, R., et al., *Inflammasome is a central player in the induction of obesity and insulin resistance.* Proc Natl Acad Sci U S A, 2011. **108**(37): p. 15324-15329.

245. Zandvoort, A., et al., *High ICAM-1 gene expression in pulmonary fibroblasts of COPD patients: a reflection of an enhanced immunological function.* Eur Respir J, 2006. **28**(1): p. 113-22.

246. Aaron, C.P., et al., *Intercellular adhesion molecule 1 and progression of percent emphysema: the MESA Lung Study.* Respir Med, 2015. **109**(2): p. 255-64.

247. Bochner, B.S., et al., *Adhesion of human basophils, eosinophils, and neutrophils to interleukin 1-activated human vascular endothelial cells: contributions of endothelial cell adhesion molecules.* J Exp Med, 1991. **173**(6): p. 1553-7.

248. Hoy, S.M., *Canakinumab: a review of its use in the management of systemic juvenile idiopathic arthritis.* BioDrugs, 2015. **29**(2): p. 133-142.

249. Fleischmann, R.M., et al., *Safety of extended treatment with anakinra in patients with rheumatoid arthritis.* Ann Rheum Dis, 2006. **65**(8): p. 1006-1012.

250. Cohen, S.B., et al., *A randomized, double-blind study of AMG 108 (a fully human monoclonal antibody to IL-1R1) in patients with osteoarthritis of the knee.* Arthritis Res Ther, 2011. **13**(4): p. R125.

251. Byers, D.E., et al., *Long-term IL-33-producing epithelial progenitor cells in chronic obstructive lung disease.* J Clin Invest, 2013. **123**(9): p. 3967-3982.

252. Kearley, J., et al., *Cigarette smoke silences innate lymphoid cell function and facilitates an exacerbated type I interleukin-33-dependent response to infection.* Immunity, 2015. **42**(3): p. 566-579.

253. Ramadas, R.A., et al., *IL-36alpha exerts pro-inflammatory effects in the lungs of mice.* PLoS. One, 2012. **7**(9): p. e45784.

254. Lugade, A.A., et al., *Cigarette smoke exposure exacerbates lung inflammation and compromises immunity to bacterial infection.* J Immunol, 2014. **192**(11): p. 5226-5235.

255. Gaschler, G.J., et al., *Bacteria challenge in smoke-exposed mice exacerbates inflammation and skews the inflammatory profile.* Am J Respir Crit Care Med, 2009. **179**(8): p. 666-75.

256. Gaschler, G.J., et al., *Mechanisms of clearance of nontypeable Haemophilus influenzae from cigarette smoke-exposed mouse lungs.* Eur Respir J, 2010. **36**(5): p. 1131-42.

257. Berenson, C.S., et al., *Outer membrane protein P6 of nontypeable Haemophilus influenzae is a potent and selective inducer of human macrophage proinflammatory cytokines.* Infect Immun, 2005. **73**(5): p. 2728-35.

258. Finney, L.J., et al., *Lower airway colonization and inflammatory response in COPD: a focus on Haemophilus influenzae.* Int J Chron Obstruct Pulmon Dis, 2014. **9**: p. 1119-1132.

259. Barnes, P.J., *Corticosteroid resistance in patients with asthma and chronic obstructive pulmonary disease.* J Allergy Clin Immunol, 2013. **131**(3): p. 636-45.

260. Susuki-Miyata, S., et al., *Cross-talk between PKA-Cbeta and p65 mediates synergistic induction of PDE4B by roflumilast and NTHi.* Proc Natl Acad Sci U S A, 2015. **112**(14): p. E1800-9.

261. Michalec, L., et al., *CCL7 and CXCL10 orchestrate oxidative stress-induced neutrophilic lung inflammation.* J Immunol, 2002. **168**(2): p. 846-52.

262. Di Stefano, A., et al., *Association of increased CCL5 and CXCL7 chemokine expression with neutrophil activation in severe stable COPD.* Thorax, 2009. **64**(11): p. 968-75.

263. Steel, H.C., et al., *Pathogen- and host-directed anti-inflammatory activities of macrolide antibiotics.* Mediators Inflamm, 2012. **2012**: p. 584262.

264. Beigelman, A., et al., *Azithromycin attenuates airway inflammation in a mouse model of viral bronchiolitis.* Respir Res, 2010. **11**: p. 90.

Acknowledgements

Several people made this work possible and contributed to its outcome.

First and foremost, I would like to thank Prof. Dr. Klaus Erb, Dr. Birgit Jung, Dr. Henri Doods, Dr. Cara Williams and Prof. Dr. Thomas Rudel for giving me the opportunity to conduct my doctoral thesis work at Boehringer Ingelheim Pharma GmbH & Co. KG in collaboration with the University of Wuerzburg. In particular, I acknowledge Prof. Dr. Klaus Erb, Dr. Birgit Jung and Prof. Dr. Thomas Rudel for their supervision and support. Their expertise and guidance substantially contributed to the outcome of this work.

Special thanks to Dr. Daniel Peter and his team (Michèl Przibilla, Jochen Blender, Carmen Lerner, Melanie Groner, Silvia Frey), to Mathilde Borsch and to Helene Lichius for the good teamwork in BSL2 laboratories and the excellent support. Regarding cell culture, I would like to thank Kerstin Butscher for her help and useful suggestions.

Many thanks to Dr. Matthias Duechs and Dr. Cornelia Tilp for their help and support regarding BSL2, scientific and personal issues and for being very important companions throughout my time at Boehringer Ingelheim.

I am very grateful for the help and enlightening discussions concerning qPCR with Dr. Benjamin Strobel. Furthermore, I acknowledge Prof. Dr. Joachim Reidl and Dr. Sabine Lichtenegger for providing nontypeable *Haemophilus influenzae* and corresponding support. In addition, I would like to thank Dr. Klaus Fuchs and Dr. Mareike Wittenbrink for providing antibodies and support regarding anti-IL-1β and anti-IL-18 antibodies.

I would like to thank Dr. Birgit Stierstorfer and Dr. Gerald Birk for their support with histology and the insightful explanations concerning pathological effects in histological stainings.

Finally, I would like to thank my doctoral student colleagues Samuel Mang, Nicolas Pairet and Franziska Herrmann as well as Dr. Eva Wex for being such good companions contributing to an excellent atmosphere not only at work.

I am very grateful for the good and insightful time I had throughout my doctoral thesis project in the department of immunology and respiratory diseases research and I thank the whole team very much.

Publications

Journal articles

07/2016 **Effects of conventional tobacco smoke and nicotine-free cigarette smoke on airway inflammation, airway remodelling and lung function in a triple allergen model of severe asthma**

Tilp C.; Bucher H.; Haas H.; Duechs M. J.; Wex E.; Erb K. J.

Immunology & Respiratory Diseases Research, Boehringer Ingelheim Pharma GmbH & Co. KG, Birkendorfer Straße 65, 88400 Biberach an der Riss, Germany

Clin Exp Allergy. 2016 Jul;46(7):957-72

06/2016 **Development of a Scintillation Proximity Assay (SPA) Based, High Throughput Screening Feasible Method for the Identification of PDE12 Activity Modulators**

Mang S.; Bucher H.; Nickolaus P.

Immunology & Respiratory Diseases Research, Boehringer Ingelheim Pharma GmbH & Co. KG, Birkendorfer Straße 65, 88400 Biberach an der Riss, Germany

Curr Drug Discov Technol. 2016 Jun 22 [Epub ahead of print]

06/2016 **Tiotropium Attenuates Virus-Induced Pulmonary Inflammation in Cigarette Smoke-Exposed Mice**

Bucher H.; Duechs M. J.; Tilp C.; Jung B.; Erb K. J.

Immunology & Respiratory Diseases Research, Boehringer Ingelheim Pharma GmbH & Co. KG, Birkendorfer Straße 65, 88400 Biberach an der Riss, Germany

J Pharmacol Exp Ther. 2016 Jun;357(3):606-18

09/2015 **Modeling Pulmonary Disease Pathways Using Recombinant Adeno-Associated Virus 6.2**

Strobel B.[1]; Duechs M. J.[2]; Schmid R.[3]; Stierstorfer B. E.[1]; Bucher H.[2]; Quast K.[1]; Stiller D.[1]; Hildebrandt T.[1]; Mennerich D.[1]; Gantner F.[4]; Erb K. J.[2]; Kreuz S.[2]

[1]Target Discovery Research, [2]Respiratory Diseases Research, [3]Drug Metabolism and Pharmacokinetics, [4]Translational Medicine and Clinical Pharmacology, Boehringer Ingelheim Pharma GmbH & Co. KG, Birkendorfer Straße 65, 88400 Biberach an der Riss, Germany

Am J Respir Cell Mol Biol. 2015 Sep;53(3):291-302

Submitted

Neutralization of both IL-1α/IL-1β plays a major role in suppressing combined cigarette smoke/virus-induced pulmonary inflammation in mice

Bucher H.[1]; Keck M.[1]; Przibilla M.[1]; Lamb D.[1]; Wittenbrink M.[2]; Fuchs K.[2]; Jung B.[1]; Erb K. J.[2]; Peter D.[1]

[1]Immunology & Respiratory Diseases Research, [2]Immune-Modulation and Biotherapeutics Discovery, Boehringer Ingelheim Pharma GmbH & Co. KG, Birkendorfer Straße 65, 88400 Biberach an der Riss, Germany

In progress

Efficacy of Dexamethasone, Roflumilast and Azithromycin in a murine cigarette smoke/NTHi model

Bucher H.[1]; Jung B.[1]; Erb K. J.[2]

[1]Immunology & Respiratory Diseases Research, [2]Immune-Modulation and Biotherapeutics Discovery, Boehringer Ingelheim Pharma GmbH & Co. KG, Birkendorfer Straße 65, 88400 Biberach an der Riss, Germany

Conference presentations

09/2016

Efficacy of Dexamethasone, Roflumilast and Azithromycin in a novel cigarette smoke/NTHi model

Bucher H.; Jung B.; Erb K. J.

Congress of the European Respiratory Society (ERS), London, UK – Thematic Poster Session – Session 399/PA2620 (Microbiological issues and translational research in respiratory infections)

09/2016

Establishment of a murine asthma exacerbation model by combining OVA exposure with either RSV or influenza infection

Tilp C.; Bucher H.; Wex, E.; Erb K. J.

Congress of the European Respiratory Society (ERS), London, UK – Poster Discussion Session – Session 569/PA3636 (Immune response in the lung)

09/2016

Roflumilast but not Dexamethasone or Fluticasone reduces neutrophilic airway inflammation and hyperreactivity in a murine influenza-induced asthma exacerbation model

Tilp C.; Bucher H.; Wex, E.; Erb K. J.

Congress of the European Respiratory Society (ERS), London, UK – Poster Discussion Session – Session 699/PA4893 (Novel mechanisms and treatment modalities in asthma)

09/2015 **Effects of anti-IL-1α, anti-IL-1β, anti-IL-18 and anti-IL-1RI antibodies on combined smoke and virus-induced airway inflammation in mice**

Bucher H.[1]; Keck M.[1]; Przibilla M.[1]; Lamb D.[1]; Wyatt, D.[1]; Wittenbrink M.[2]; Fuchs K.[2]; Jung B.[1]; Erb K. J.[2]; Peter D.[1]

Congress of the European Respiratory Society (ERS), Amsterdam, The Netherlands – Poster Discussion Session – Session 393/P3577 (New models for treating airway diseases)

05/2015 **Tiotropium Attenuates Influenza Virus-Induced Pulmonary Inflammation in Smoke-Exposed Mice**

Bucher H.; Duechs M. J.; Tilp C.; Strobel B.; Wex E.; Jung B.; Erb K. J.

Congress of the American Thoracic Society (ATS), Denver, USA – Thematic Poster Session – Poster A5802, Poster Board P572 (D37-Help: Advances in COPD therapeutics)

03/2015 **Tiotropium Attenuates Influenza Virus-Induced Pulmonary Inflammation in Smoke-Exposed Mice**

Bucher H.; Duechs M. J.; Tilp C.; Strobel B.; Wex E.; Jung B.; Erb K. J.

DGfI Spring School on Immunology, Ettal, Germany

09/2014 **Tiotropium attenuates pulmonary inflammation in a novel mouse smoke RSV re-infection model**

Bucher H.; Strobel B.; Jung B.; Erb K. J.; Duechs M. J.

Congress of the European Respiratory Society (ERS), Munich, Germany – Poster Discussion Session – Session 514/P4944 (Pathogenesis and mechanisms of respiratory infections)

Erklärungen nach §4 Abs. 3 Satz 3, 5, 8 der Promotionsordnung der Fakultät für Biologie

Affidavit

I hereby declare that my thesis entitled: "Pre-clinical modeling of viral- and bacterial-induced exacerbations of chronic obstructive pulmonary disease" is the result of my own work. I did not receive any help or support from commercial consultants. All sources and/or materials applied are listed and specified in the thesis. Furthermore, I verify that the thesis has not been submitted as part of another examination process neither in identical nor in similar form.

Eidesstattliche Erklärung

Hiermit erkläre ich an Eides statt, die Dissertation: „Pre-clinical modeling of viral- and bacterial-induced exacerbations of chronic obstructive pulmonary disease" eigenständig, d.h. insbesondere selbständig und ohne Hilfe eines kommerziellen Promotionsberaters, angefertigt und keine anderen, als die von mir angegebenen Quellen und Hilfsmittel verwendet zu haben. Ich erkläre außerdem, dass die Dissertation weder in gleicher noch in ähnlicher Form bereits in einem anderen Prüfungsverfahren vorgelegen hat.

Würzburg, den ..... ……

(Name)